VIBRATIONAL STUDIES OF SOME INORGANIC SOLIDS

ProQuest LLC.
789 East Eisenhower Parkway
P.O. Box 1346
Ann Arbor, MI 48106 – 1346

A Thesis submitted to the
University of Glasgow
in fulfilment of the
requirements for the
Degree of Doctor of Philosophy
by

James T.R. Dunsmuir

Department of Chemistry,
University of Glasgow,
Glasgow, G12 8QQ.

October, 1972.

Summary

The solid state vibrational spectra of various inorganic halides and cyanides are discussed, and the advantages of single-crystal methods, particularly polarised far-i.r. reflectance spectroscopy, in determining the precise nature of solid state vibrational effects are illustrated.

Single-crystal data on halogenometallates containing isolated octahedral anions demonstrate the way in which the vibrations of these ions are split under the influence of the crystal field. The relationship between the spectra and structures of cross-linked octahedral anions is discussed, and the i.r. spectra of the main types of perovskite chloride ($AMCl_3$) structures are presented. The spectra of the $AHgX_3$ complexes are related to the presence of molecular HgX_2 units in a distorted octahedral environment.

The i.r. spectra of A_2MCl_4 and A_3MCl_5 crystals show most of the predicted internal modes of the approximately tetrahedral MCl_4^{2-} ions present in both. The observed splittings are used to estimate the magnitude of the static and dynamic field effects in these crystals, and to establish the relationship of the splitting of the fundamental modes of the tetrahedral anions to the degree of distortion in the various structures. The selection rules operating in the low temperature spectra of the $(NMe_4)_2MCl_4$ complexes are interpreted in terms of orientational disordering of the anions. The unusually high frequency of a lattice mode in the A_3MCl_5 complexes is attributed to the presence of free chloride ions in these structures.

A number of aquochlorometallates provide examples of interesting anions, and the spectra of some of these are investigated. A band due to the stretch of the long Cu-Cl bond in $K_2CuCl_4.2H_2O$ is identified, and the validity of this assignment is discussed. Far-i.r. results are also

given for $K_2FeCl_5.H_2O$ and some aquochloromanganates.

In order to explain peculiarities in the far-i.r. spectra of some ammonium halogenometallates, an attempt is made to determine the spectroscopic effects of hydrogen bonding on the fundamental and lattice vibrations of the ammonium ion. From the results obtained, a set of simple criteria for the routine detection of hydrogen bonding in these systems is proposed.

Results are presented for a number of cyanometallates, including $K_3Fe(CN)_6$. The frequencies of the bands observed in the complex low frequency region of the i.r. spectrum of this complex agree well with those calculated by a published normal coordinate analysis, and help to resolve an ambiguity in the vibrational assignments. The i.r. selection rules for the $\nu(CN)$ modes of hexacyanometallate ions doped in KCl crystals are used to determine the local environments of the doped ions in the lattice.

Acknowledgements

The author wishes to express his thanks to his supervisor, Dr. A.P. Lane, for his guidance and encouragement in this work. The author would also like to thank Mrs. F. Lawrie for her help with i.r. instrumentation, Dr. D.M. Adams of Leicester University for kindly providing the facilities for much of the Raman work, and the staff and research students of the Chemistry Department of Glasgow University for their assistance and helpful discussion. The financial support of the S.R.C. is gratefully acknowledged.

Contents

A list of references is given at the end of each chapter.

Chapter 1: Introduction

1.1: Aims of the Present Work

The increasing numbers of publications on single-crystal Raman spectra which have appeared in recent years following the development of laser sources, reflect a growing interest in solid state vibrational spectroscopy. Over the same period there has, by contrast, been very little work done on single-crystal i.r. spectroscopy, despite the availability of a range of suitable instrumentation. Although the i.r. characterisation of inorganic solids has been commonplace for a considerable time, it was only during the course of the present work that detailed studies of chemically interesting systems began to appear in significant numbers.[1]

The advantages of single-crystal techniques are obvious. By using polarised radiation, the vibrations involving a particular crystal-oriented Raman tensor component or i.r. transition moment vector can be selectively excited. This allows not only the observation, in most anisotropic materials, of a greater proportion of the fundamental modes than can be resolved in the "composite" powder spectra, but also the unambiguous assignment of each band to a symmetry type.

The uses of such specific vibrational data are manifold, and will be illustrated in the present work by studies of a variety of complex halides and pseudo-halides. These are for the most part investigated by far-i.r. reflectance measurements on single crystals, together with some Raman work, although in some cases conventional powder methods are found to be adequate. The far-i.r. region (defined here mainly for practical reasons as the region below 400 cm^{-1}), as well as covering the range of most M-X vibrations, is of particular interest in that it reveals low-energy features such as lattice modes which are peculiar to

the solid state.

The aim of this work is not primarily that of assignment of the bands observed to particular internal coordinates. Accepted "group frequencies" have generally been used for this purpose,[2] although polarisation data provide a powerful method of verifying or modifying these rather unreliable generalisations. In certain favourable cases, the possible symmetry coordinates are sufficiently restricted to permit almost ab initio assignments, but usually some assumptions are necessary.

Vibrational spectroscopy is not in general particularly well suited for the determination of crystal structures, but where sufficient spectral data are available, the highly specific selection rules operating can sometimes be used to differentiate between a few possible structures. This may lead to the detection of errors or the resolution of ambiguities in the X-ray diffraction results. However, spectroscopic methods do have an important contribution to make in the study of disordered systems, and examples will be discussed in which the i.r. spectra can be used to investigate orientational disordering of molecular or complex ionic units in crystalline materials.

The principal justification for the detailed examination of crystal spectra stems from the information they provide on the dynamic processes occurring in the solid state. Of particular interest here are the relationships between spectra and the structures of various coordinate groupings present in the crystals; the effects which anisotropic potential fields have on the vibrations of the polyatomic groups; and the way in which the vibrations of the individual groups couple to produce the crystal modes. Some attention will also be given to the nature of the lattice vibrations in certain systems.

1.2: Theory

Lattice dynamics: In a crystal made up of N unit cells each containing n atoms, there are a total of $3nN$ degrees of freedom, or $3nM-6$ non-zero solutions of the equations of motion. These vibrations or phonons may be regarded as standing waves in the crystal, derived by different phase combinations of displacements in each unit cell. For a macroscopic crystal, N is very large, and the range of phase combinations of any particular unit cell vibration becomes effectively continuous, forming $3n$ phonon "branches". The phase relationships are most conveniently expressed in reciprocal space by the phonon wave-vector k, defined as

$$k = 2\pi/\lambda \qquad 1.1$$

where λ is the phonon wavelength. Because of the particulate nature of crystals, k turns out to be a cyclic parameter, the values $0 \leqslant |k| \leqslant \pi/a$ (where a is the primitive translation of the lattice in the relevant direction) being representative of all possible wave-vectors. The values $k = \pm\frac{\pi}{a}$ mark the limits in reciprocal space of the region known as the first Brillouin zone.[3]

In principle, the frequencies of the various branches as a function of wave-vector can be computed by solving the secular determinants arising from the equations of motion. There are two types of solution: one in which $\nu \to 0$ as $k \to 0$, and another in which ν tends to some finite value as $k \to 0$. The former represents the dispersion curve of an acoustic branch, which at zero wave-vector (zero phase difference between unit cells) corresponds to a pure translation of the crystal. The second type of dispersion curve belongs to an optical branch. In order to conserve momentum in photon-phonon interactions, the first-order transitions observed by both i.r. and Raman spectroscopy are confined to the zone centre (i.e. $k \approx 0$) because of the comparatively very long wavelengths of excitation used in each case. Only optical modes are

therefore observed for crystals of normal unit cell dimensions (in the order of 10Å).

Group theory applied to crystal vibrations: Because of the restriction of first-order i.r. and Raman activity to zone centre modes, a full account of the spectra is given by consideration of the vibrations of a single unit cell. These are classified according to the symmetry of the crystal's factor group, which comprises all the symmetry elements of the primitive unit cell, and is isomorpnous with one of the crystallographic point groups.

The method of factor group analysis was was developed by Bhagavantam and Venkatarayudu[4] and later described by Mitra and Gielisse[5]. From an exact knowledge of the type of site occupied by each atom, this method permits the derivation of the irreducible representations for all of the unit cell modes. The computations required are rather tedious, but the proceedure has recently been greatly simplified by the introduction of a set of tables developed by Adams and Newton.[6] These give the irreducible representations for each set of Wyckoff[7] sites in all 230 space groups. Table 1.1 illustrates the use of these tables for the trigonal A_2MF_6 complexes, and provides a key to the symbols to be used throughout this work. The representations for each set of occupied sites (first three rows) and for the rotations of the polyatomic groups (R) are taken directly from the tables. Summation of the first three rows gives the symmetry classification of all the degrees of freedom of the primitive unit cell (N). The internal modes of the polyatomic groups (N_i) are derived by subtraction of R and ($T + T_a$), the latter comprising only the translational representations for discrete units (in this case the caesium cations and MF_6^{2-} anions). The acoustic modes (T_a) are determined by reference to the appropriate character table.[8]

Shortly after Adams and Newton published these tables, which also

Table 1.1: Example of the use of the tables of Adams and Newton[6] for the factor group analysis of the trigonal A_2MF_6 complexes.

Space group: D_{3d}^3 - No. 164 (Z = 1)

Point group: D_{3d}

	A_{1g}	A_{2g}	E_g	A_{1u}	A_{2u}	E_u	
M (1a)					1	1	(1)
A (2c)	1		1		1	1	(2)
F (6i)	2	1	3	1	2	3	(3)
(1)+(2)+(3) = N	3	1	4	1	4	5	(4)
(1)+(2) = T + T_a	1		1		2	2	(5)
T_a					1	1	(6)
(5)-(6) = T	1		1		1	1	(7)
R		1	1				(8)
(4)-(5)-(8) = N_i	2		2	1	2	3	(9)

Selection rules - Raman: A_{1g} x^2+y^2, z^2 I.r: A_{2u} z

E_g (x^2-y^2, xy), E_u (x,y)

(xz,yz)

N = total number of zone-centre (k = 0) modes

T_a = acoustic modes (translations)

T = translatory lattice modes

R = rotatory lattice modes (in complexes with structured cations and anions, these are denoted R_+ and R_- respectively)

N_i = internal modes of polyatomic groups

include a set of vector representations enabling a description of the crystal modes in terms of internal coordinates, Boyle[9] described an equally convenient "method of ascent in symmetry". This is in fact a refinement of proceedures which have been in use for some time.[10] Since the two methods appear to be equivalent in most respects, no further description of Boyle's method need be given here.

The recent developments in the group theoretical analysis of crystal vibrations have to some extent obscured the difference between the factor group method of Bhagavantam and Venkatarayudu[4] and the alternative site group approach originally proposed by Halford[11] to account for the modes of discrete polyatomic groups in crystals in terms of their site symmetry. It was later shown that this site group approximation could be modified to include the correlation of the vibrations of all polyatomic groups in the unit cell,[12] giving results equivalent to the factor group predictions for the internal modes. This method has the advantage of showing clearly the relations between the fundamental modes of the isolated polyatomic group and the crystal modes derived from them, as illustrated by the typical correlation diagram in Table 4.2. Conceptually, the various stages in this proceedure are analogous to the physical processes affecting splitting of the crystal modes. The potential energy of a harmonic oscillator may be represented by equation 1.2,[12] where V^{o} is the potential energy of the individual free molecule or

$$V = \sum_{j}(V_j^{o} + V_j) + \sum_{j}\sum_{i} V_{ij} + V_1 + V_{1j} \qquad 1.2$$

ion, and V_j is the perturbation due to the potential field of the crystal, which may give rise to site group or static field splitting of the degenerate vibrations of the free ion, as well as being responsible for the frequency shifts observed in going from liquids or gases to the condensed phase . The main contribution to the dynamic coupling

represented by the V_{ij} term comes from the interaction of modes of the same type in translationally non-equivalent ions within the unit cell, which takes the form of correlation field splitting in the crystal spectra. The last two terms are the potential energy of the lattice modes and the interaction of lattice and internal modes respectively.

Selection rules: At the foot of Table 1.1 are given the selection rules for Raman and i.r. activity, taken from the character table of the appropriate point group. These are in the form of the tensor components of the polarisability and the transition moment vectors of the active representations, expressed in terms of the crystallographic directions. Modes of a particular symmetry can therefore be selectively excited by suitable polarisation of the incident radiation (and of the scattered radiation for the Raman spectra). For instance, in the A_2MF_6 crystals, the Raman scattering observed with both incident and collected beam polarised parallel to the hexagonal (z) axis would involve only A_{1g} modes, and a similarly polarised i.r. beam would excite only A_{2u} modes.

I.r. reflectance spectra: These differ from absorption spectra in that the refractive index n as well as the extinction coefficient k plays an important part in determining the form of the bands. Taking the example of a system with a single harmonic oscillator with a dispersion frequency ν_0, the dispersion of the incident radiation obeys equation 1.3, where ϵ_0 and ϵ_∞ are the static and high frequency dielectric

$$\epsilon = \epsilon_\infty + (\epsilon_0 - \epsilon_\infty)/[1-(\nu/\nu_0)^2] \qquad 1.3$$

constants.[13] For i.r. excitation, the dispersion frequency of the vibration and the frequency of the transverse optic (TO) mode (ν_t) are the same. At normal incidence, the reflectivity R is given by

$$R = (n-1)^2/(n+1)^2 \qquad 1.4$$

The expressions 1.3 and 1.4 show that as the frequency increases towards ν_t, the dielectric constant and the refractive index $n = \epsilon^{\frac{1}{2}}$ also increase

until at ν_t they take infinite values and the crystal becomes totally reflecting. Immediately above ν_t, ϵ becomes negative and infinite, n is imaginary, and R = 1 until the frequency $\nu_l = (\epsilon_o/\epsilon_\infty)^{\frac{1}{2}}\nu_t$ is reached, above which ϵ is positive and n real, and the reflectivity drops. The frequency ν_l is in fact that of the longitudal optic (LO) mode.

The above treatment does not succeed in accurately describing the form of observed reflectivity bands. This can be remedied by introducing damping of the oscillator, so that expression 1.4 becomes

$$R = \frac{(n-1)^2 + k^2}{(n+1)^2 + k^2} \qquad 1.5$$

This has the effect of reducing the maximum reflectivity to fractional values, depending on the degree of damping. Reflectance bands can nevertheless still be regarded as regions of more or less high reflectivity between the limits ν_t and ν_l. The harmonic approximation has the advantage of offering a simple explanation of the complex nature of the spectra for systems with more than one oscillator of similar frequency.[14] For instance, the appearance of a weak oscillator lying between the TO and LO frequencies of a stronger oscillator as an inversion in the reflectance band of the latter can readily be understood in terms of the dispersion in the dielectric constant.

The foregoing discussion illustrates that for spectra containing broad bands, the oscillator frequencies are best determined by dispersion analysis of the reflectivity data. This can be done using expressions 1.6 and 1.7, where $r = R^{\frac{1}{2}}$ and θ is the phase difference between the incident and reflected radiation.[15] θ may be derived from the Kramers-Kronig relation 1.8.

$$n = (1-r^2)/(1+r^2-2r\cos\theta) \qquad 1.6$$

$$k = 2r\sin\theta/(1+r^2-2r\cos\theta) \qquad 1.7$$

$$\theta(\nu) = \frac{2\nu}{\pi} \int_{\infty}^{o} \frac{\ln r(\nu_o)}{\nu^2 - \nu_o^2} \, d\nu_o \qquad 1.8$$

The real and imaginary parts of the dielectric constant, ϵ' and ϵ'' are related to n and k by the expressions

$$\epsilon' = n^2 + k^2 \qquad 1.9$$

$$\epsilon'' = 2nk \qquad 1.10$$

From the variation of the parameters, the frequencies of the TO modes can be determined. For uniaxial crystals, the extraordinary and ordinary ray spectra (with the electric vector of the incident radiation respectively parallel and perpendicular to the unique axis) are analysed separately.

References

1 See, for example, D.M. Adams and D.C. Newton, J. Chem. Soc. (A), 1969, 2998.

2 See D.M. Adams, "Metal-Ligand and Related Vibrations", Arnold, London, 1967.

3 M. Born and K. Huang, "Dynamical Theory of Crystal Lattices", Oxford, 1954.

4 S. Bhagavantam and T. Venkatarayudu, "Theory of Groups and its Application to Physical Problems", Andhra University, Waltair, 1951.

5 S.S. Mitra and P.J. Gielisse, "Progress in Infra-red Spectroscopy", ed. H.A. Szymanski, Plenum Press, New York, 1964, Vol. 2, p. 47; S.S. Mitra, Solid State Phys., 1962, 13, 1.

6 D.M. Adams and D.C. Newton, "Tables for Factor Group and Point Group Analysis", Beckman-RIIC Ltd., Croydon, 1970; J. Chem. Soc. (A), 1970, 2822.

7 R.W.G. Wyckoff, "Crystal Structures", Interscience, New York, 2nd edn., 1965, Vol. 1.

8 E.B. Wilson, J.C. Decius and P.C. Cross, "Molecular Vibrations", McGraw-Hill, New York, 1955.

9 L.L. Boyle, Acta Cryst., 1972, A28, 172; Spectrochim Acta, 1972, 28A, 1347; ibid., p. 1355.

10 See, for example, M.H. Brooker and D.E. Irish, Canad. J. Chem., 1970, 48, 1183.

11 R.S. Halford, J. Chem. Phys., 1946, 14, 8.

12 D.F. Hornig, J.Chem. Phys., 1948, 16, 1063.

13 K. Huang, Proc. Roy. Soc., 1951, A208, 352.

14 C.M. Phillippi, Technical report, 1969, AFML-TR-68-317.

15 W.G. Spitzer, R.C. Miller, D.A. Kleinman and L.E. Howarth, Phys. Rev., 1962, 126, 1710; F. Stern, Solid State Phys., 1963, 15, 299; P.N. Schatz, S. Maeda and K. Kozima, J. Chem. Phys., 1963, 38, 2658.

Chapter 2: Complexes Containing Discrete or Cross-linked Octahedral Anions

2.1: Introduction

Octahedral coordination is commonly found among the halogenometallates. The structures of many $A_xM_yX_z$ complexes may be formally represented as cubic or hexagonal close packed arrays of A and X atoms, with M atoms occupying a proportion of those octahedral interstices surrounded by six X atoms. Depending on the exact arrangement of the occupied "holes", this can give rise to either discrete or cross-linked octahedral anions. Examples of the latter include face-sharing dimeric ions, infinite chain or sheet-like structures, or a complete three-dimensional network of linked anions.

The ability of the fluoride ion to stabilise higher coordination numbers makes hexa-coordination particularly common among the fluorometallates. Steric requirements in certain chlorides, notably complexes of the type A_2MCl_4, favour a tetrahedral arrangement of the MCl_4^{2-} ions, and in general this configuration becomes more important, but by no means universal, in the chemistry of the chlorometallates.

A large number of spectroscopic studies have been made of solids containing MX_6^{x-} ions,[1-3] but the majority of these have the highly symmetric K_2PtCl_6 structure.[4] This is particularly uninteresting from the point of view of solid state vibrational effects, since the point symmetry of the isolated ion, its site group and the crystal factor group are all isomorphous, and the selection rules of the isolated ion still apply. Among the structures of lower symmetry, few results have been interpreted in terms of factor group splitting.[2,3] Considerable attention has also been given to the spectra of the completely cross-linked cubic perovskite fluorides,[5-7] while other

bridged structures have been less thoroughly investigated, and are consequently imperfectly understood.

In this chapter, a few examples of isolated and partially cross-linked octahedral anions will be discussed, leaving the treatment of the perovskite-type structures to Chapter 3.

2.2: Complexes Containing Isolated Octahedral Anions

A_2MF_6 Complexes: The A_2MF_6 complexes (A = Rb, Cs; M = Ti, Zr, Hf; K_2TiF_6) adopt the trigonal β-$(NH_4)_2SiF_6$ structure with space group $P\bar{3}m1$ (D_{3d}^3) (Z = 1), and contain almost regular octahedral anions on D_{3d} sites.[8] These appear to be flattened somewhat along the trigonal axis in the zirconium and hafnium complexes and, if anything, slightly elongated in K_2TiF_6. Since the site symmetry is isomorphous with that of the unit cell, the site group approximation will apply in these systems. The effect of the reduction in symmetry on the normal modes of the anion is shown in Table 2.1. Apart from the removal of the restriction on the i.r. activity of one component of ν_6, the only change expected in the solid state spectrum is the splitting of each triply degenerate O_h mode into a non-degenerate and doubly degenerate component, reflecting the anisotropy of the potential field in the crystal. Factor group analysis also predicts a number of translatory and rotatory lattice modes given by representations 2.1 and 2.2 respectively.

$$\Gamma_{transl} = A_{1g} + E_g + A_{2u} + E_u \qquad 2.1$$

$$\Gamma_{rot} = A_{2g} + E_g \qquad 2.2$$

Lane and Sharp have previously observed most of the site group splitting of the O_h modes in the powder i.r. and Raman spectra of these complexes.[3] Naturally, this treatment did not allow the determination of the relative order of the A and E components, which is of some interest in assessing the influence of the static crystal field on the vibrations

Table 2.1: Vibrations of the MF_6^{2-} ions in the A_2MF_6 complexes.

		Free ion	Crystal
		O_h	D_{3d}
ν_1	ν(M-F)	A_{1g}	$\longrightarrow$ A_{1g}
ν_2	ν(M-F)	E_g	$\longrightarrow$ E_g
ν_3	ν(M-F)	F_{1u}	$\longrightarrow$ $A_{2u}+E_u$
ν_4	δ(M-F)	F_{1u}	
ν_5	δ(M-F)	F_{2g}	$\longrightarrow$ $A_{1g}+E_g$
ν_6	δ(M-F)	F_{2u}	$\longrightarrow$ $A_{1u}+E_u$

D_{3d} selection rules: Raman A_{1g} x^2+y^2, z^2 i.r: A_{2u} z

E_g (x^2-y^2, xy), E_u (x,y)

(xz,yz)

of the anion. The present work therefore re-examines the spectra of a few examples from this group by single crystal techniques in order to establish more fully the pattern of splitting of the O_h modes.

Results: The i.r. and Raman frequencies of the crystals examined are given in Table 2.2. Interpretation of the polarisation data in the Raman spectra was straightforward, the only point worthy of comment being the absence of the ν_2 band for all of the complexes, as found by the previous study. The frequencies of these have been calculated at about 450 cm^{-1} from combination bands.[3] For the polarised i.r. spectra, observation of the A_{2u} modes required reasonably large ac faces of the crystals, which were present only in Cs_2TiF_6 and Rb_2ZrF_6. The larger crystals of K_2TiF_6 and Cs_2HfF_6 grew as plates normal to the c axis, so that for these only the E_u spectrum could be recorded, and the A_{2u}

Table 2.2; Single-crystal i.r. and Raman frequencies (cm^{-1}) for some A_2MF_6 complexes.

K_2TiF_6	Cs_2TiF_6	Rb_2ZrF_6	Cs_2HfF_6		
618	604	589	592	A_{1g}	ν_1
-	-	-	-	E_g	ν_2
615	590	537	(493)[a]	E_u	ν_3
-	572	522		A_{2u}	
315	308	240	(217)	E_u	ν_4
(281)	276	192	(184)	A_{2u}	
308	290	258	257	A_{1g}	ν_5
300		244	267	E_g	
-	-	-	-	E_u	ν_6
138	90	90	83	E_g	lattice modes
82	72	74	69	E_g	
85	-	73	58	A_{1g}	
136	108	98	(87)	E_u	
(122)	80	92		A_{2u}	

[a] frequencies in parentheses are taken from i.r. transmission spectra.

frequencies had to be taken from the powder transmission spectra. This meant that the frequencies of the A_{2u} components of ν_3 could not be fixed with any accuracy in these cases. Even when A_{2u} spectra were available, the $\nu_3(A_{2u}-E_u)$ splitting was rather uncertain because of the breadth of the bands. No evidence for the $\nu_6(E_u)$ band reported by Lane and Sharp could be found for any of the complexes examined.

With the exception of the ν_2 and ν_6 modes, the vibrational spectrum of the A_2MF_6 systems is now fairly well established, all of the other bands having been observed for Rb_2ZrF_6. From the frequencies given in Table 2.2, the bending mode ν_4 would appear to be affected most by anisotropy of the potential field, with resultant $A_{2u}-E_u$ separations of 30-50 cm^{-1}. The splitting of ν_3 is less than 20 cm^{-1}, and about 10 cm^{-1} for ν_5. All of the complexes show a similar pattern, with $E_u > A_{2u}$ for ν_3 and ν_4 and $Ag > Eg$ for ν_5, which suggests that the trigonal distortion of the octahedral anion is in the same sense in each.

$\underline{K_4CdCl_6}$: The structure of K_4CdCl_6 bears some resemblance to that of the A_2MF_6 complexes, but the $CdCl_6^{4-}$ ions are twisted slightly about the C_3 axis, giving a pseudocubic rhombohedral unit cell with space group $R\bar{3}c$ (D_{3d}^6) ($Z = 2$) in which the anions are on C_{3i} (S_6) sites.[9] The correlation diagram for the vibrations of the O_h ions (Table 2.3) reveals the unusual situation of correlation coupling between crystal modes of the same symmetry. Also, the inactive $\nu_6(F_{2u})$ fundamental becomes formally i.r. active under the site symmetry of the anion. The translatory and rotatory lattice modes of the crystal derived by factor group analysis are given by the representations 2.3 and 2.4 respectively,

$$\Gamma_{trans} = A_{1g} + 3A_{2g} + 4E_g + 2A_{1u} + 3A_{2u} + 5E_u \qquad 2.3$$

$$\Gamma_{rot} = A_{1g} + A_{2g} + 2E_g \qquad 2.4$$

completing the vibrational predictions for this structure. The only i.r. investigation of this complex made so far extended down to 200 cm^{-1},

Table 2.3: Correlation diagram for the complex anions in K_4CdCl_6 (space group D_{3d}^6).

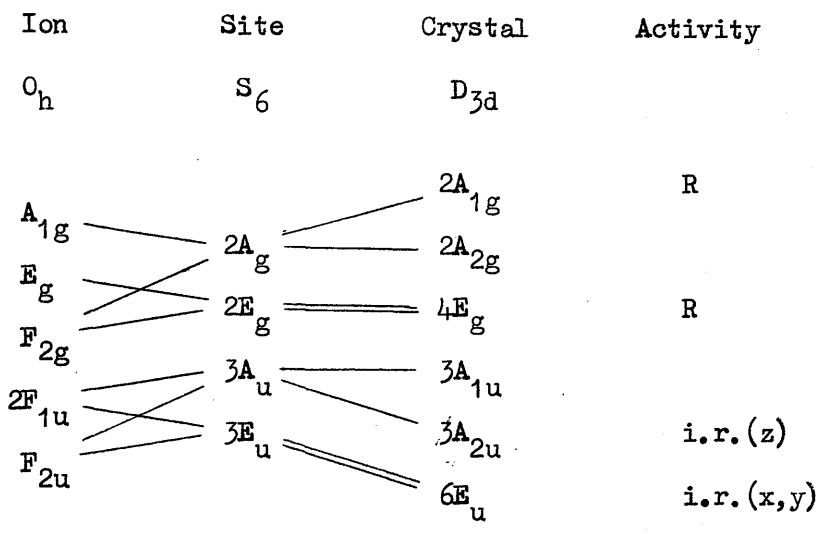

but failed to observe any bands.[10]

Results: The polarised i.r. reflectance spectra and Raman spectra of K_4CdCl_6 showed the bands listed in Table 2.4. Although attempts were made to obtain polarised Raman data, the extinctions of the observed lines were very poor, due presumably to the incorporation of gross defects in the crystals during rapid growth. The symmetry species given for the g modes in Table 2.4 are therefore largely intuitive, and the intensities are taken from the strongest lines observed among the set of spectra recorded.

Considering the Raman spectra first of all, one active component of ν_1, two of ν_2 and three of ν_5 are predicted. Assuming that the features below 110 cm^{-1} correspond to lattice modes, four bands due to the internal vibrations of the anions are observed, of which the highest may be assigned immediately to ν_1. The remaining three are in the ν_5

Table 2.4: I.r. and Raman frequencies (cm^{-1}) of K_4CdCl_6.

232	vs	A_{1g}	ν_1
210	ms	E_u	ν_3
180	vs,br	A_{2u}	
161	s	E_u	ν_3 or ν_4
157	s	A_{1g}	ν_5
148	w	E_u	ν_4 or ν_6
133	ms	E_g	ν_5
125	ms	E_g	
132	s	A_{2u}	ν_4
125	vs	E_u	
116	w	A_{2u}	ν_6
103	vw	E_u	ν_6 or lattice mode
103	m	A_{1g} or E_g	lattice modes
89	w	E_{2u}	
77	w	E_u	
68	w	A_{1g} or E_g	
60	s	A_{2u}	

Table 2.5: Far-i.r. reflectance frequencies (cm^{-1}) for $K_3TlCl_6.2H_2O$.

A_{2u}	E_u	
-	295	ν_3 ($TlCl_6^{3-}$)
247	230	H_2O translatory modes
218		
159	158	ν_4 ($TlCl_6^{3-}$)
128	142	
	115	
	72	lattice mode

bending region, and their spacing suggests that the lower two constitute the $Eg(\nu_5)$ correlation doublet. Again, no trace of the ν_2 bands could be resolved. Since these missing bands are expected just below ν_1, the observation of the predicted number of modes in the bending region confirms the assignment of the lattice modes.

The assignments of the three predicted A_{2u} internal modes in the i.r. spectrum are likewise fairly obvious, but the E_u spectrum poses a number of problems. This should comprise the three O_h modes ν_3, ν_4 and ν_6, each split into a correlation doublet. The bands at 210 and 125 cm^{-1} are evidently components of ν_3 and ν_4 respectively, but the strong 161 cm^{-1} band could be assigned to either of these. If it is taken to be the other component of ν_3, then the second ν_4 mode is placed at 148 cm^{-1}, while the alternative assignment puts ν_4 at 161 cm^{-1} and one of the ν_6 modes at 148 cm^{-1}. Whichever scheme is adopted, there are splittings of the O_h fundamentals of at least 36 cm^{-1}, apparently due to correlation coupling. Since this seems unreasonably large, it is perhaps more realistic to attribute the pattern of the E_u bands to some form of mixing of the stretching and bending modes. Because of these uncertainties, it is not possible to establish definitely the relation of the sequence of splitting in K_4CdCl_4 with that of the A_2MF_6 complexes, although the ν_3 and ν_5 frequencies of the chloride seem to indicate the same order in both.

$\underline{K_3TlCl_6.2H_2O}$: An early structure determination proposed space group $I4/mmm$ (D_{4h}^{17}) for this complex with a primitive unit cell containing seven octahedral $TlCl_6^{3-}$ ions on D_{4h}, D_{2h} and C_{2h} sites.[11] This leads to the prediction of seven A_{2u} internal modes (three components of ν_3 and ν_4, and one of ν_6) and twenty-one E_u internal modes (seven from each of ν_3, ν_4 and ν_6). The number of bands observed in the polarised i.r. spectra (Table 2.5) falls far short of this total, although if the ν_6

band in the A_{2u} spectrum (from the C_{2h} ion) is assumed to be weak, the correct number of A_{2u} bending modes are observed, which tend to confirm this rather unusual structure.

An interesting feature of the spectra is the presence of three bands at about 230 cm^{-1} due to the translatory modes of the non-coordinated "lattice" water molecules. These have approximately the same energy as the equivalent vibrations in ice.[12]

2.3: Complexes Containing Cross-linked Octahedra

K_2MgF_4-type Structures: A number of complex fluorides, including K_2CoF_4,[13] as well as a few chlorides such as Cs_2CdCl_4,[14] adopt the tetragonal K_2MgF_4 structure, with space group $I4/mmm$ (D_{4h}^{17}) ($Z = 2$)[15]. The divalent metal atoms are surrounded by six halagens. Four of these form bridging bonds, which generate infinite cross-linked layers perpendicular to the tetragonal axis, separated by the cations and non-bridging halogens; the terminal M-X bonds are colinear with the tetragonal axis. There is only one formula unit, and hence one layer, in each primitive unit cell (as opposed to the body-centred crystallographic cell). These layers represent a two-dimensional model of the completely cross-linked cubic perovskite structure (see Chapter 3).

The results of a factor group analysis of the K_2MgF_4 structure are given in Table 2.6. Three of the E_u modes are equivalent to the F_{1u} modes of the perovskites, while the B_{2u} mode has a counterpart in the inactive F_{2u} vibration. The vibrational spectra of these systems are obviously of considerable interest, but only one study has previously been reported,[16] in which three bands in the i.r. spectrum of K_2CoF_4 were vaguely attributed to vibrations of a tetrahedral ion and a librational mode of water. From a comparison of the frequencies with those of the present work, the sample purity was evidently even lower than the

Table 2.6: Factor group analysis of the K_2MgF_4 structure (D_{4h}^{17}).

	A_{1g}	A_{2g}	B_{1g}	B_{2g}	E_g	A_{1u}	A_{2u}	B_{1u}	B_{2u}	E_u
N	2				2		4		1	5
T	1				1		1			1
T_a							1			1
N_i	1				1		2		1	3
$\nu(M\text{-}X)_t$	1						1			
$\delta(M\text{-}X)_t$					1					1
$\nu(M\text{-}X)_b$										1
$\delta(M\text{-}X)_b$							1		1	1
I.r. activity							z			(x,y)

Table 2.7: I.r. reflectance bands (cm^{-1}) of Cs_2CdCl_4 single crystals.

A_{2u}	E_u	
	235	$\nu(Cd\text{-}Cl)_b$
220		$\nu(Cd\text{-}Cl)_t$
	130	$\delta(Cd\text{-}Cl)_t$
131	115	$\delta(Cd\text{-}Cl)_b$
80	92	lattice modes

authors suspected.

Results: The i.r. spectra of K_2CoF_4 and Cs_2CdCl_4 were examined in the range of the fundamental vibrations. The polarised reflectance spectra of single crystals of the cadmium salt, each containing the predicted number of bands, are shown in Fig. 2.1. The only ambiguity in the assignment of these concerns the two E_u bending modes. The form of the spectrum suggests the presence of a weak oscillator just above the strong 115 cm^{-1} band, giving an inversion in reflectivity at about 130 cm^{-1}. The assignments given for these in Table 2.7 are based on observations made for K_2CoF_4.

The only crystals of the fluoride available were thin (001) plates, from which only the E_u spectrum could be recorded by reflectance. This showed bands at 145, 240 and 437 cm^{-1} and was almost identical in form to the spectrum of the perovskite $KCoF_3$,[6] which has bands at 144, 238 and 438 cm^{-1}. It is therefore reasonable to assign the three observed bands to the bridging Co-F stretch and bend, and the lattice mode. The fourth mode, the terminal Co-F bend, was not observed. It is on the implied weakness of this mode that the assignment of the two E_u bending modes in Cs_2CdCl_4 is based. The powder transmission spectrum of K_2CoF_4 showed little change from that of the E_u reflectance spectrum, which is readily understood in terms of overlap of the A_{2u} bands by the presumably stronger E_u bands.

The similarity of the spectra of K_2CoF_4 and $KCoF_3$, and of their a_o unit cell dimensions (4.074Å and 4.071Å in K_2CoF_4 and $KCoF_3$ respectively[13,17]) indicates that the representation of the cross-linked layers in the A_2MX_4 complexes as "two-dimensional perovskites" may have more than merely a descriptive value. It would, in fact, be reasonable to assume that the forces acting within these layers are the same as in the corresponding three dimensional structures, so that the results of normal

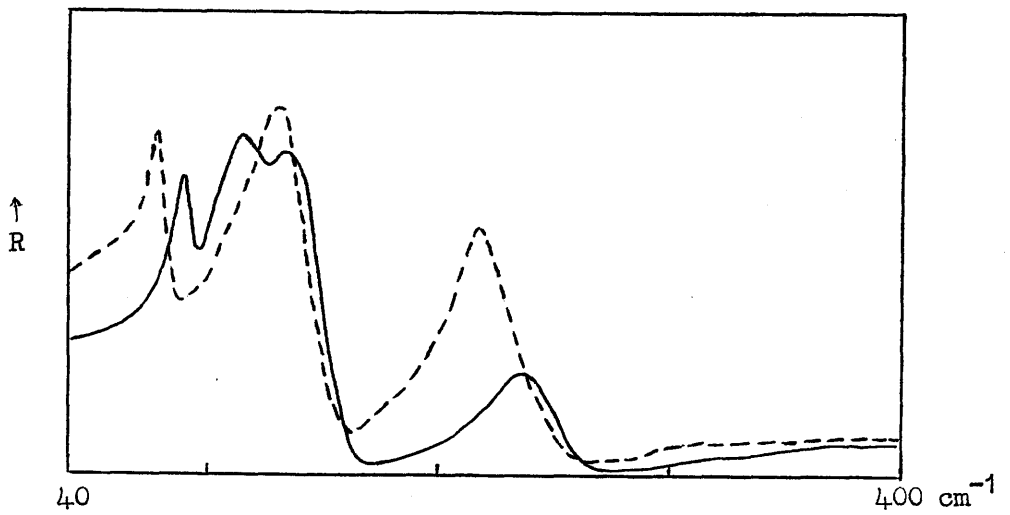

Figure 2.1: Single-crystal i.r. reflectance spectra of Cs_2CdCl_4; electric vector parallel (dashed line) and perpendicular (solid line) to c-axis.

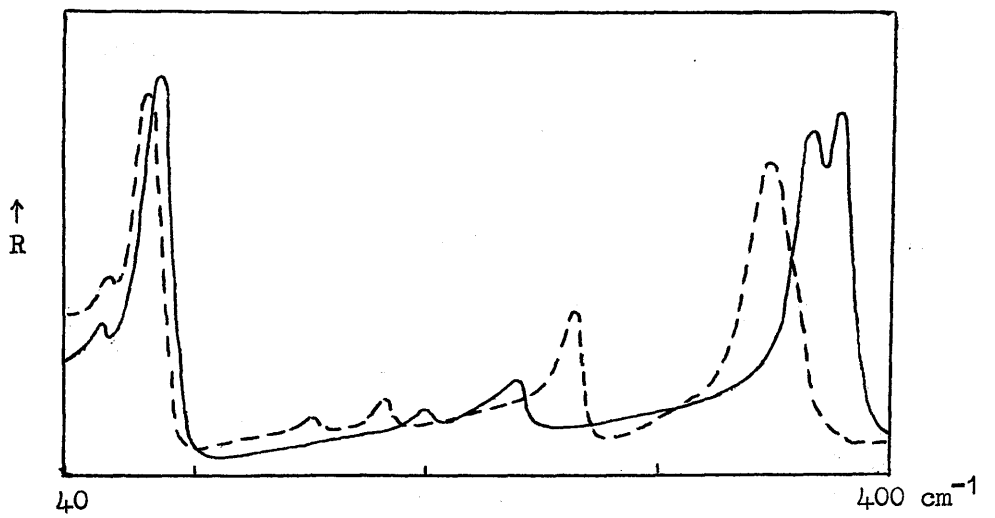

Figure 2.2: Single-crystal i.r. reflectance spectra of $Rb_3Cr_2Cl_9$ (solid line - $\vec{E} \perp c$; dashed line - $\vec{E} \parallel c$).

coordinate analyses[7] of the perovskites should remain valid for the E_u bridging modes in the A_2MX_4 complexes. This allows a more quantitative understanding of the vibrations of the layer structures.

Although the assignment of the A_{2u} modes of Cs_2CdCl_4 is fairly unambiguous, the result is at first sight somewhat surprising, since the terminal Cd-Cl stretching mode is placed below the E_u bridging stretch, which is the reverse of the order assumed in most systems.[18] However, this can be rationalised by considering the bond lengths. In the complexes for which sufficiently accurate data are available, [15, 19] the terminal and bridging bonds are of almost the same length, implying rather weak covalent interaction in the former. This probably applies also to Cs_2CdCl_4 and K_2CoF_4, and would explain the relatively low frequency of the terminal M-X stretching modes. The picture which emerges for this structure is therefore one of cross-linked layers with a similar bonding scheme to the AMX_3 complexes, with weakly bonded terminal halogens projecting above and below each layer. The frequencies of the two modes involving these non-bridging atoms are more compatible with the stretching and bending vibrations of weakly covalent bonds, rather than the lattice modes resulting from a pure ionic interaction.

Rb$_3$Cr$_2$Cl$_9$ and Cs$_3$Tl$_2$Cl$_9$: The $M_2Cl_9^{3-}$ ion, made up of two face-sharing octahedra, is structurally intermediate between the isolated octahedral MX_6^{x-} ion and the infinite chain like structures found in the hexagonal AMX_3 complexes. The alkali metal salts constitute a small range of closely related structures, which differ from one another only in the detailed packing arrangements, apart from $K_3W_2Cl_9$, which contains genuinely distorted $W_2Cl_9^{3-}$ ions. For example, $Cs_3Cr_2Cl_9$ and $Cs_3Tl_2Cl_9$ are reported to have bimolecular unit cells with space groups $P6_3/mmc$ (D_{6h}^4) and $R\bar{3}c$ (D_{3d}^6) respectively,[20, 21] while $Cs_3As_2Cl_9$ has space group P321 (D_3^2) ($Z = 1$).[22] A higher symmetry D_{3d}^3 structure has been proposed[23]

for $Cs_3Fe_2Cl_9$, but this places the atoms on sites incompatible with the D_{3h} symmetry of the isolated ion. The structure of $Rb_3Cr_2Cl_9$ has not been established, but since the potassium and caesium salts are isostructural,[24] it is likely that this too has the D^4_{6h} structure.

Table 2.8 gives the approximate forms of the normal vibrations of the $M_2Cl_9^{3-}$ ion, and the representations under which they appear in the various structural types. For the sake of clarity, the intermediate site group modes have been omitted; in the chromium salt the site symmetry is the same as that of the free anion in any case, while in the thallium and arsenic complexes, the centre of gravity of the anions lies on D_3 sites, so that the site group modes may be derived from the free ion modes merely by removal of the superscripted primes.

The powder i.r. and single crystal Raman spectra of $Cs_2Tl_2Cl_9$ have been reported by Beattie et al,[18] and their results can be satisfactorily interpreted according to the structure cited above.

Results: The bands observed in the i.r. reflectance spectra of $Rb_3Cr_2Cl_9$ and $Cs_3Tl_2Cl_9$ with the incident radiation polarised parallel and perpendicular to the hexagonal axes of the crystals are listed in Table 2.9. The spectra of the thallium complex were similar in form to those of the chromate shown in Fig. 2.2. The bands fall into several groups which can be assigned intuitively to the terminal or bridging vibrations. The bands observed for $K_3TlCl_6.2H_2O$ (Section 2.2) were taken into account in assigning the vibrations of $Cs_3Tl_2Cl_9$. The low intensity of the bands in the region 150–190 cm^{-1} in Fig. 2.2 is unexpected, and may be connected with the absence of the second E′ bridging mode in the x-polarisation.

The most striking feature of the spectra of $Rb_3Cr_2Cl_9$ is the presence of two terminal Cr-Cl stretching modes in the x-polarised spectrum. Since the higher of these is undoubtedly the weakly

Table 2.8: Approximate descriptions of the anion modes in the various $A_3M_2Cl_9$ structures.

	Free ion D_{3h}	$Cs_3Cr_2Cl_9$ (D_{6h}^4)	$Cs_3Tl_2Cl_9$ (D_{3d}^6)	$Cs_3As_2Cl_9$ (D_3^2)
$\nu(M\text{-}Cl)_t$, $\nu(M\text{-}Cl)_b$, $\delta(M\text{-}Cl)_t$, $\delta(M\text{-}Cl)_b$	A_1'	$A_{1g} + B_{2u}$	$A_{1g} + A_{2u}$	A_1
$(M\text{-}Cl_3)_t$ twist	A_2'	$A_{2g} + B_{1u}$	$A_{2g} + A_{2u}$	A_2
$\nu(M\text{-}Cl)_t$, $\delta(M\text{-}Cl)_t$, $\nu'(M\text{-}Cl)_b$[a], $\nu'(M\text{-}Cl)_b$, $(M\text{-}Cl_3)_t$ wag	E'	$E_{2g} + E_{1u}$	$E_g + E_u$	E
$(M\text{-}Cl_3)_t$ twist	A_1''	$B_{2g} + A_{1u}$	$A_{1g} + A_{1u}$	A_1
$\nu(M\text{-}Cl)_t$, $\delta(M\text{-}Cl)_t$, $\nu'(M\text{-}Cl)_b$	A_2''	$B_{1g} + A_{2u}$	$A_{2g} + A_{2u}$	A_2
$\nu(M\text{-}Cl)_t$, $\delta(M\text{-}Cl)_t$, $(M\text{-}Cl_3)_t$ wag, $\nu'(M\text{-}Cl)_b$	E''	$E_{1g} + E_{2u}$	$E_g + E_u$	E

[a] the $\nu'(M\text{-}Cl)_b$ modes involve both stretching and bending of the M-Cl-M bonds.

Table 2.9: Frequencies (cm^{-1}) of reflactance bands in the i.r. spectra of $Rb_3Cr_2Cl_9$ and $Cs_3Tl_2Cl_9$ crystals.

	$Rb_3Cr_2Cl_9$		$Cs_3Tl_2Cl_9$		
Polarisation:	z	x,y	z	x,y	
	355	375	281	277	$\nu(M\text{-}Cl)_t$
		364		268	
	263	237	213	216	bridge modes[a]
	185	195	186	180	$\delta(M\text{-}Cl)_t$
	152				$(M\text{-}Cl_3)$ twist
				141	$(M\text{-}Cl_3)_t$ wag
	80	84	101	116	lattice modes and bridge bends
	59	58		89	
			65	60	

[a] mainly M-Cl-M stretch

dipole active E'' mode of the anion causing an inversion in the stronger E' mode, the structure of the chromium salt cannot possibly be D^4_{6h}, which would allow only E' modes in this spectrum. This conclusion is supported by the observation of one more z-polarised band than is predicted for the D_{6h} structure. The alternative space group C^4_{6v} suggested[20] for $Cs_3Cr_2Cl_9$ would remove the anomaly of the E'' mode, but would also be expected to give doubling of the bands in the z-polarisation. However, all bands in the spectra can be assigned systematically on the basis of either the $Cs_3Tl_2Cl_9$ or $Cs_3As_2Cl_9$ structures, with due regard to the expected intensities of the various modes. In principle, at least, a choice between the D_{3d} and D_3 forms could be made with the help of accurate Raman spectra.

On the assumption that the rubidium and caesium salts are isostructural, these results cast serious doubts on the accuracy of the accepted structure of $Cs_3Cr_2Cl_9$, even though a fairly detailed X-ray study has recently proposed this same structure for a number of other complexes.[25] Although it would be unwise to overemphasise the significance of the spectroscopic results, diffraction methods often have difficulty in differentiating between closely similar structures, and the number of different $A_3M_2Cl_9$ structures may turn out to be fewer than proposed at present.

2.4: Experimental

Crystals of the A_2MF_6 complexes were prepared by evaporation or cooling of saturated solutions of the appropriate alkali metal fluoride and transition metal oxide in concentrated hydrofluoric acid. The crystals grew mainly as plates, with some rod-like prisms in the case of Rb_2ZrF_6 and Cs_2TiF_6. Twinning was prevalent among the prismatic crystals, and care had to be taken in selecting suitable faces for spectroscopic examination.

K_4CdCl_6 rapidly formed large but imperfect rhombohedral crystals on cooling of an aqueous solution containing a 6:1 molar ratio of $KCl:CdCl_2$. Some small faces parallel to the threefold axis were present, which were used as a guide in grinding faces of suitable size.

A large crystal of Cs_2CdCl_4 (m.p: 473°C) was grown from the melt by the Stockbarger method, starting from a mixture of the pure anhydrous chlorides. A phase transition[26] at 444°C did not prevent the growth of a good quality crystal. This could be cleaved with extreme ease along (001) planes, but careful grinding and polishing of a (100) face was required. Attempts to prepare K_2CoF_4 in a similar manner gave only small, flaky crystals. Growth from a KCl flux gave plates of

increased area, but the thickness was insufficient for recording the polarised reflectance spectrum.

Both $Cs_3Tl_2Cl_9$ and $K_3TlCl_6.2H_2O$ were prepared by slow evaporation of aqueous solutions of the constituent chlorides. The caesium salt grew as needle-like hexagonal prisms, and the hydrate as rectangular prisms. A large melt-grown crystal of $Rb_3Cr_2Cl_9$ with good $(1\bar{1}00)$ cleavage faces was supplied by J. D. Black of the Chemistry Department, Glasgow University.

References

1 See, for example, R.D. Peacock and D.W.A. Sharp, J. Chem. Soc., 1959, 2762; O.L. Keller, Inorg. Chem., 1963, 2, 783; I.R. Beattie, T. Gilson, K. Livingston, V. Fawcett, G.A. Ozin, J. Chem. Soc. (A), 1967, 712.

2 J.E. Griffiths and D.E. Irish, Inorg. Chem., 1964, 3, 1134; D.A. Brown, K.R. Dixon, C.M. Livingston, R.H. Nuttall and D.W.A. Sharp, J. Chem. Soc. (A), 1967, 100.

3 A.P. Lane and D.W.A. Sharp, J. Chem. Soc. (A), 1969, 2942.

4 F.J. Ewing and L. Pauling, Z. Krist., 1928, 68, 223.

5 G.R. Hunt, C.H. Perry and J. Ferguson, Phys. Rev., 1964, 134, 688; J.D. Axe and G.D. Petit, ibid., 1967, 157, 435; M. Balkanski, P. Moch and M.K. Teng, J. Chem. Phys., 1967, 46, 1619.

6. A.P. Lane, D.W.A. Sharp, J.M. Barraclough, D.H. Brown and D.A. Paterson, J. Chem. Soc. (A), 1971, 94.

7 I. Nakagawa, A. Tsuchida and T. Shimanouchi, J. Chem. Phys., 1967, 47, 982.

8 S. Siegel, Acta Cryst., 1952, 5, 683; B. Cox and A.G. Sharpe, J. Chem. Soc., 1953, 1783; H. Bode and G. Teufer, Z. anorg. Chem., 1956, 283, 18.

9 G. Bergerhoff and O. Schimitz-Dumont, Z. anorg. Chem., 1956, 284, 10.

10 G.E. Coates and D. Ridley, J. Chem. Soc., 1964, 166.

11 J.L. Hoard and L. Goldstein, J. Chem. Phys., 1935, 3, 645.

12 J.E. Bertie and E. Whalley, J. Chem. Phys., 1967, 46, 1271.

13 W. Rüdorff, J. Kändler, G. Lincke and D. Babel, Agew. Chem., 1959, 71, 672.

14 S. Siegel and E. Gebert, Acta Cryst., 1964, 17, 790.

15 B. Brehler and H.G.F. Winkler, Heidelberger Beitr. Mineral. Petrog., 1954, 4, 6.

16 J. Lecomte, C. Duval and C. Wadier, Compt. rend., 1959, 249, 1991.

17 K. Knox, Acta Cryst., 1961, 14, 583.

18 I.R. Beattie, T.R. Gilson and G.A. Ozin, J. Chem. Soc. (A), 1968, 2765.

19 W. Rüdorff, J. Kändler and D. Babel, Z. anorg. Chem., 1962, 317, 261.

20 G.J. Wessel and D.J.W. Ijdo, Acta Cryst., 1957, 10, 466.

21 H.M. Powell and A.F. Wells, J. Chem. Soc., 1935, 1008; J.L. Hoard and L. Goldstein, J. Chem. Phys., 1935, 3, 199.

22 J.L. Hoard and L. Goldstein, J. Chem. Phys., 1935, 3, 117.

23 H. Yamatera and K. Nakatsu, Bull. Chem. Soc. Japan, 1954, 27, 244.

24 C.M. Cook, J. Inorg. Nuclear Chem., 1963, 25, 123.

25 R. Saillant, R.B. Jackson, W.E. Streib, K. Folting and R.A.D. Wentworth, Inorg. Chem., 1971, 10, 1453.

26 H.J. Seifert and F.W. Koknat, Z. anorg. Chem., 1968, 357, 314.

Chapter 3: Perovskite-type AMX_3 Complexes

3.1: Introduction

A wide variety of oxides and halides of formula AMX_3 adopt structures made up of close-packed AX_3 layers in which near-neighbour A cations are avoided, with M ions in octahedral interstices surrounded by six X anions. These structures are stable only within certain limits of ionic radii concerned, as expressed by the Goldschmidt tolerance factor (t),[1] defined in equation 3.1. Perovskite-type structures are

$$t = (r_a + r_x) / \sqrt{2}(r_m + r_x) \qquad 3.1$$

found to be stable for tolerance factors in the range 0.8 to 1.0. The exact value of t within these limits appears to determine the particular structural modification to be adopted.

If the three possible phases of the close-packed AX_3 layers are denoted a,b and c, then various stacking arrangements giving rise to a series of related structures may be envisaged. The repeat sequence abcabc, for instance, gives exclusively cubic close-packing, as found in the cubic perovskite structure, while the sequence abab generates a hexagonal lattice with a two-layer repeat unit (denoted 2L). Various intermediate structures with differing ratios of cubic to hexagonal stacking are possible, but in fact only three others have so far been encountered among the AMX_3 complexes. The main features of these are listed in Table 3.1. No examples of the 4L structure have been established for the halides.

The general arrangement of the cross-linked octahedra surrounding each M atom for the various structures is shown in Fig. 3.1. In the 2L form, the octahedra form linear, face-sharing chains along the hexagonal axis, with no contact between chains. As the ratio of cubic stacking of the AX_3 layers increases on going to the 9L, 4L and 6L forms, the degree

of cross-linking of the chains by corner sharing becomes progressively greater, until in the cubic perovskite structure each octahedron shares corners with six others. Within the permitted range of tolerance factors the lower values usually favour cubic stacking of the AX_3 layers, while those near the upper limit are associated with a high proportion of hexagonal close-packing. Thus $CsMnCl_3$ has the 9L structure, while $RbMnCl_3$, for which t is smaller, adopts the 6L form, and $CsCoCl_3$, with a higher t value due to the decreased ionic radius of the divalent metal, has the 2L structure. The adherence to this empirical rule demonstrated by the type compounds given in Table 3.1 may result partly from a fortunate choice of examples. The concept of tolerance factors cannot be as rigorously applied to the chlorides as, for instance, in the case of the fluorides, because of the greater polarisability of the chloride ions.

For t values of about 0.8, a number of distorted orthorhombic and tetragonal structures exist for the $AMCl_3$ compounds,[8] presumably derived

Table 3.1: Perovskite structures.

Type compound	$CsPbCl_3$[a]	$RbMnCl_3$	$BaMnO_3$[a]	$CsMnCl_3$	$CsCoCl_3$
Space group	$Pm\bar{3}m$	$P6_3/mmc$	$P6_3/mmc$	$R\bar{3}m$	$P6_3/mmc$
	(O_h^1)	(D_{6h}^4)	(D_{6h}^4)	(D_{3d}^5)	(D_{6h}^4)
Z	1	6	4	3[b]	2
Stacking	abc	abcacb	abac	ababcbcac	ab
Notation	cubic	6L	4L	9L	2L
t value	0.82	0.89	-	0.95	0.98
References	2,8	4,6	5	3,4	7

[a] high temperature forms

[b] primitive unit cell

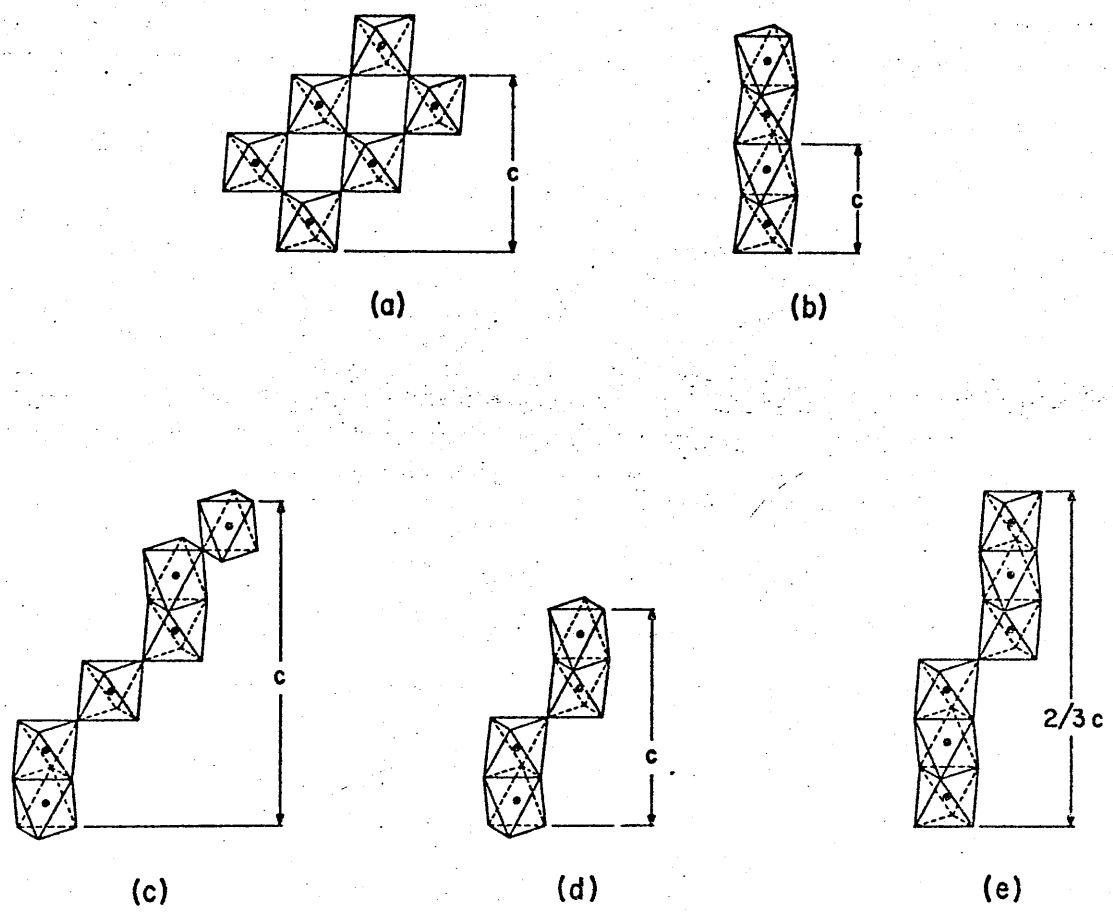

Figure 3.1: Cross-linking of the anion network in (a) cubic, (b) 2L, (c) 6L, (d) 4L and (e) 9L perovskite structures (projections normal to hexagonal axis).

from the cubic perovskite structure by distortion or twisting of the corner-sharing octahedra. Detailed structure determinations of these distorted forms have been confined to the analogous fluoride and oxide systems.[9, 10]

The differences in steric requirements and electrostatic energies between the various perovskite-type structures are relatively small,[11] and there are a number of examples of polymorphism under ambient conditions.[12] In a larger number of cases, small changes in pressure or even temperature[8] are sufficient to induce transformations to polymorphic forms. High pressure structural studies have been carried out on a number of fluorides and oxides,[11, 13] as well as on $CsMnCl_3$ and $RbMnCl_3$.[4] Both of these transform at moderately high pressures to the cubic structure, the change proceeding via the 6L form in the case of $CsMnCl_3$.

Apart from the obviously interrelated group of structural modifications described above, there are a number of similar structures which are distinguishable from these perovskites in some respect. The exact atomic arrangement in NMe_4MnCl_3, for instance, is distinct from that of any of the alkali metal complexes, although there are close similarities with the 2L form.[14] The structure of $CsCuCl_3$ likewise contains chains of face-sharing octahedra,[15] the symmetry being lowered in this case by the Jahn-Teller distortion of the copper ions. Certain $AHgX_3$ complexes are also classified as perovskites,[8,12,16,17] although this description takes no account of the nature of the bonding within the crystals. All of these systems constitute special cases, and will be treated separately.

The present work makes use of the structural variety of the AMX_3 compounds to investigate the effects of changes in structure on the vibrational spectra. There is in any case a need for vibrational data on the hexagonal modifications of the perovskite structure, which have

so far been largely neglected. These data are provided by a detailed examination of the i.r. and, in some cases, Raman spectra of examples from each structural type.

3.2: Representative Perovskite Structures

The i.r. spectra of the cubic perovskite oxides and fluorides have been exhaustively studied,[18] and normal coordinate analysis[19] has established the vibrational behaviour in these systems. Some distorted structures have also been examined,[20] but the successful interpretation of their spectra depends on the degree of similarity with those of the cubic forms. Prior to the commencement of the present work, the published vibrational data on the hexagonal tructures consisted of the single-crystal i.r. transmission (>200 cm^{-1})[21] and Raman[22] spectra of the 6L $RbNiF_3$. Since then, reports of the single-crystal i.r.[23] and Raman[24] spectra of $CsMnF_3$ (again 6L), the i.r. transmission spectra[25] of the polymorphic modifications of $CsNiF_3$ and $RbNiF_3$, and the powder Raman spectrum[26] of $CsNiCl_3$ have appeared.

In the present work, the i.r. and, in some cases, Raman spectra of a comprehensive range of AMX_3 structures, mostly chlorides, were examined. Polarised single-crystal data were obtained where possible. The results of this study are given below for each structural type.

Cubic perovskite structures: The simple cubic perovskites with space group $Pm\bar{3}m$ (O_h^1) (Z = 1) are much less common among the $AMCl_3$ complexes than for the corresponding fluorides or oxides.[9] A few examples are known, such as the high temperature form of $CsPbCl_3$[2] and one of the polymorphs of $CsCdCl_3$.[27] This structure has four triply degenerate modes of vibration given by representation 3.2. These comprise one

$$\Gamma = 3F_{1u} + F_{2u} \qquad 3.2$$

F_{1u} M-Cl stretch, F_{1u} and F_{2u} Cl-M-Cl bending modes and an F_{1u} lattice

mode. Only the F_{1u} vibrations are i.r. active, and there is no first-order Raman spectrum.

The cubic variety of $CsCdCl_3$ could only be prepared from solution as very small crystals, and some of the hexagonal form was always present. It was nevertheless possible to attribute two bands at 108 and 240 cm^{-1} in the i.r. transmission spectrum to the cubic form by comparison with the spectrum of the melt-grown 6L modification. These bands can be assigned to the bending and stretching vibrations of the cross-linked complex anions, which is consistent with similar assignments for Cs_2CdCl_4 as discussed in Chapter 2.3.

Above 47°C, $CsPbCl_3$ adopts the cubic perovskite structure. The high temperature i.r. reflectance spectrum showed only one very strong, broad band extending upwards from 40 cm^{-1} with a maximum at 150 cm^{-1} and a sharp cut-off at about 220 cm^{-1}. At room temperature, this compound is reported to have a tetragonal structure,[2,8] with space group P4mm (C^1_{4v}) (Z = 1). The exact atomic positions are not firmly established, but are thought to be similar to those of $PbTiO_3$,[10] derived by elongation of the cubic unit cell in one direction, with the lead atoms displaced out of the plane of the four equivalent chlorines. Such a structure should have the vibrational modes given by representation 3.3. The A_1 and E modes are both i.r. and Raman active, and include two Pb-Cl

$$\Gamma = 3A_1 + B_1 + 4E \qquad 3.3$$

stretching modes, while the B_1 vibration is active only in the Raman. The i.r. spectrum of the tetragonal structure is, in fact, virtually identical to that of the cubic form, but four bands were observed in the first-order Raman spectrum at 115, 169, 181 and 200 cm^{-1}. The last three of these fall in expected region for Pb-Cl stretching modes. The absence of corresponding resolved features in the i.r. spectrum suggests that the ferroelectric properties[28] of this phase may be

affecting its dielectric response to i.r. radiation. The appearance of three stretching bands in the Raman spectrum may be due to splitting of the longitudinal and transverse components of one of the modes by the electric field associated with the A_1 and E vibrations,[29] but might also indicate a more complicated structure with a larger unit cell for the low temperature form.

6L structure: There are two examples of chlorides adopting the 6L structure, namely $RbMnCl_3$[4,6] and the hexagonal form of $CsCdCl_3$.[30] The results of a factor group analysis of this structure are given in Table 3.2a. In arriving at the number of predicted lattice modes, it must be recognised that vibrations of the MCl_3 sub-lattice cannot constitute true lattice modes, and only the three translational degrees of freedom of the entire anionic network are used in combination with the displacements of the A cations.

The polarised i.r. reflectance spectra of $RbMnCl_3$ are shown in Fig. 3.2. Those of $CsCdCl_3$ were similar. The frequencies given in Table 3.3 for both compounds were obtained by a Kramers-Kronig (K-K) analysis of the reflectivity data. Of the fourteen predicted bands, ten could be observed for one or other of the compounds. The distribution of the bands is in good agreement with that recently reported[23] for $CsMnF_3$, and the i.r. spectrum of the 6L structure is therefore well established.

4L structure: The existence of 4L structures among the perovskite halides has not yet been domonstrated, but the unit cell parameters reported for $KNiCl_3$ suggest the presence of a four-layer repeat unit.[31] The i.r. transmission spectrum of this compound was recorded, but showed the same pattern of five bands as found for the 2L chlorides discussed below. It is therefore concluded that the published structural data are in error, and that $KNiCl_3$ in fact adopts the 2L structure.

Table 3.2: Factor group analyses of the 6L, 2L and 9L perovskite structures.

(a) 6L (D^4_{6h})

	A_{1g}	A_{2g}	B_{1g}	B_{2g}	E_{1g}	E_{2g}	A_{1u}	A_{2u}	B_{1u}	B_{2u}	E_{1u}	E_{2u}
N	5	2	6	1	6	8	1	7	2	6	9	7
T_a								1			1	
T	1		2		1	2		2		1	2	1
N_i	4	2	4	1	5	6	1	4	2	5	6	6

(b) 2L (D^4_{6h})

N	1	1	2		1	3		3	1	2	4	2
T_a								1			1	
T			1			1		1			1	
R		1										
N_i	1		1		1	2		1	1	2	2	2

D_{6h} selection rules - Raman: A_{1g} x^2+y^2, z^2 I.r: A_{2u} z

E_{1g} (xz,yz) E_{1u} (x,y)

E_{2g} (x^2-y^2, xy)

(c) 9L (D^5_{3d})

	A_{1g}	A_{2g}	E_g	A_{1u}	A_{2u}	E_u
N	4	1	5	2	8	10
T_a					1	1
T	1		1		2	2
N_i	3	1	4	2	5	7
I.r. activity					z	(x,y)

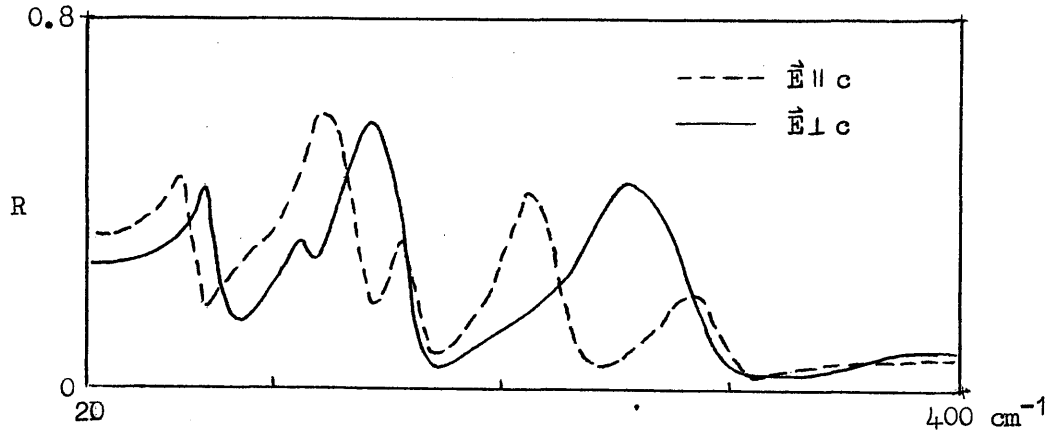

Figure 3.2: Single-crystal i.r. reflectance spectra of $RbMnCl_3$.

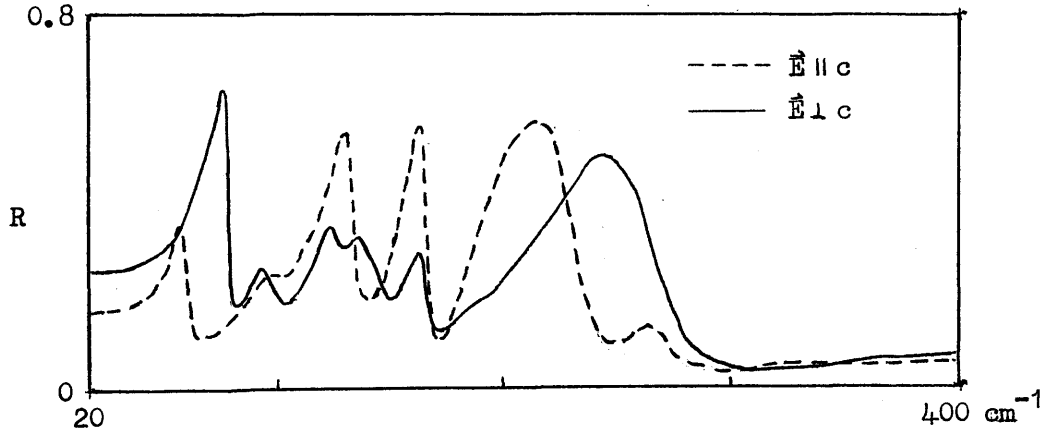

Figure 3.3: Single-crystal i.r. reflectance spectra of $CsMnCl_3$.

Table 3.3: Oscillator frequencies (cm^{-1}) derived from Kramers-Kronig analysis of the i.r. reflectance spectra of $RbMnCl_3$ and $CsCdCl_3$.

$RbMnCl_3$		$CsCdCl_3$	
A_{2u}	E_{1u}	A_{2u}	E_{1u}
249	280	240	269
	207	192	182
138	155	136	
118	118	107	95
72	62	71	64

Table 3.4: I.r. oscillator frequencies (cm^{-1}) of $CsMnCl_3$.

A_{2u}	E_u
264	234
199	158
158	135
124	118
93	89
55	70

9L structure: This structure is represented among the chlorides by $CsMnCl_3$, whose i.r. spectra are shown in Fig. 3.3. These contain six bands in each orientation, compared to the factor group predictions (Table 3.2c) of seven A_{2u} and nine E_u modes. The frequencies obtained by K-K analysis, given in Table 3.4, are consistent with the pattern calculated for the high pressure form of $CsNiF_3$ by Kohn and Nakagawa.[25]

2L structure: The completely hexagonal close-packed 2L structure is the form most commonly found for the $AMCl_3$ complexes where M is a first row transition metal.[9] Because of the comparative simplicity of this structure, the number of active modes predicted in Table 3.2b is fewer than for the 6L or 9L forms. Two examples, $CsCoCl_3$ and $RbCoCl_3$ were selected for a complete vibrational study by single-crystal i.r. and Raman techniques. The results, which are shown for the caesium complex in Figs. 3.4 and 3.5, allow the identification of all ten predicted i.r. and Raman active bands, and their assignment to either lattice (below 100 cm^{-1}) or internal modes. I.r. oscillator frequencies and Raman polarisation data are given for both compounds in Tables 3.5 and 3.6 respectively.

As well as these two detailed studies, the i.r. spectra of a number of other AMX_3 complexes were examined, and the observed frequencies of these are listed in Table 3.7. Because of the widths of some of the reflectance bands, these frequencies have for convenience been taken from powder transmission spectra, but assignments for all except the nickel complexes were based on polarised reflectance data. The i.r. transmission frequencies of the cobaltates are included for comparison. The close resemblance of the spectra of $KNiCl_3$ and $CsCdBr_3$ with those of the other halides of known 2L structure[7,32,33] suggests that both of these also contain only hexagonal close-packing of the AX_3 layers.

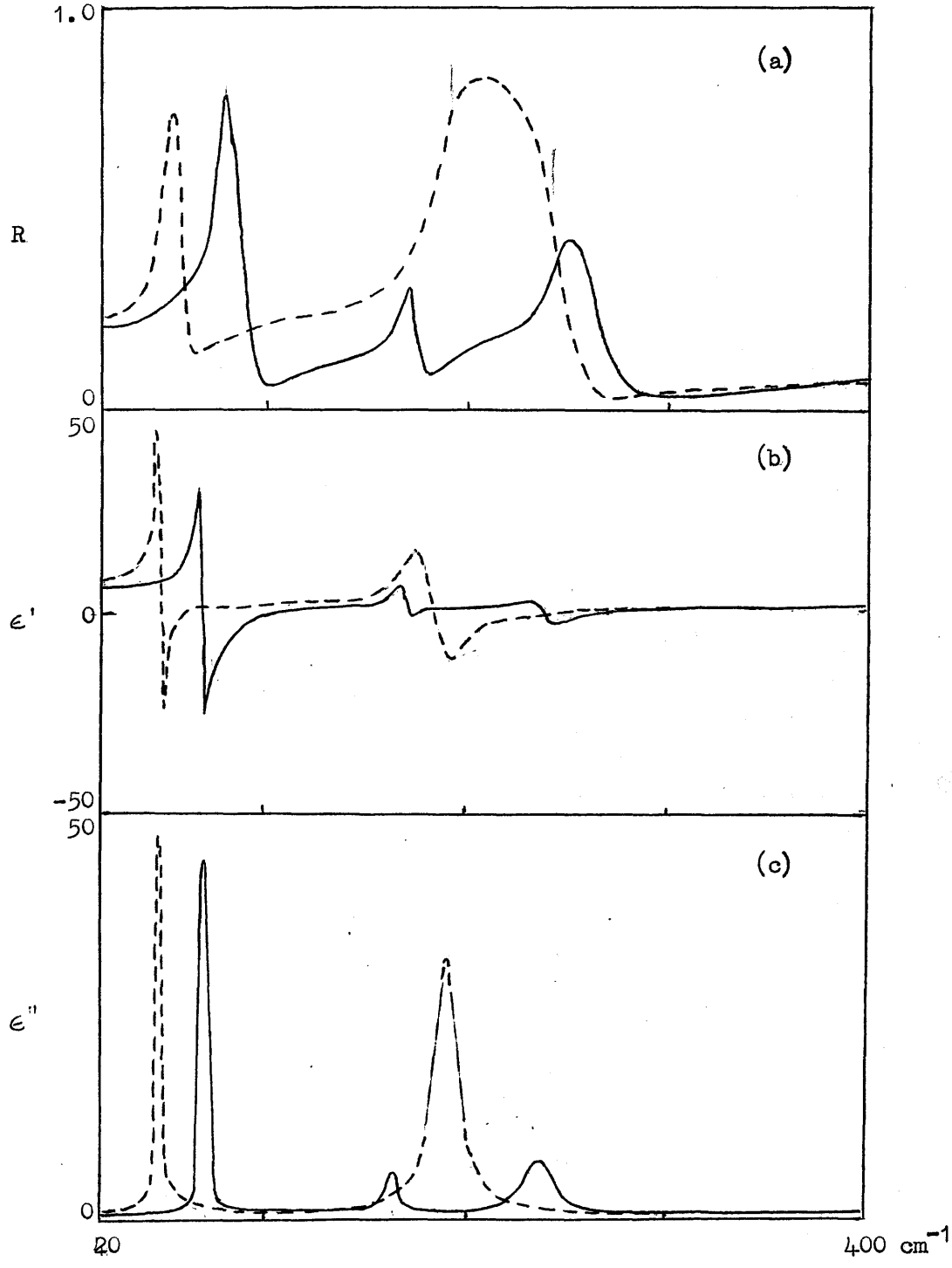

Figure 3.4 (a) Polarised single-crystal i.r. reflectance spectra of $CsCoCl_3$. (b) Real dielectric response. (c) Imaginary dielectric response; solid line, ordinary ray (E_{1u} modes) and dashed line, extraordinary ray (A_{2u} modes).

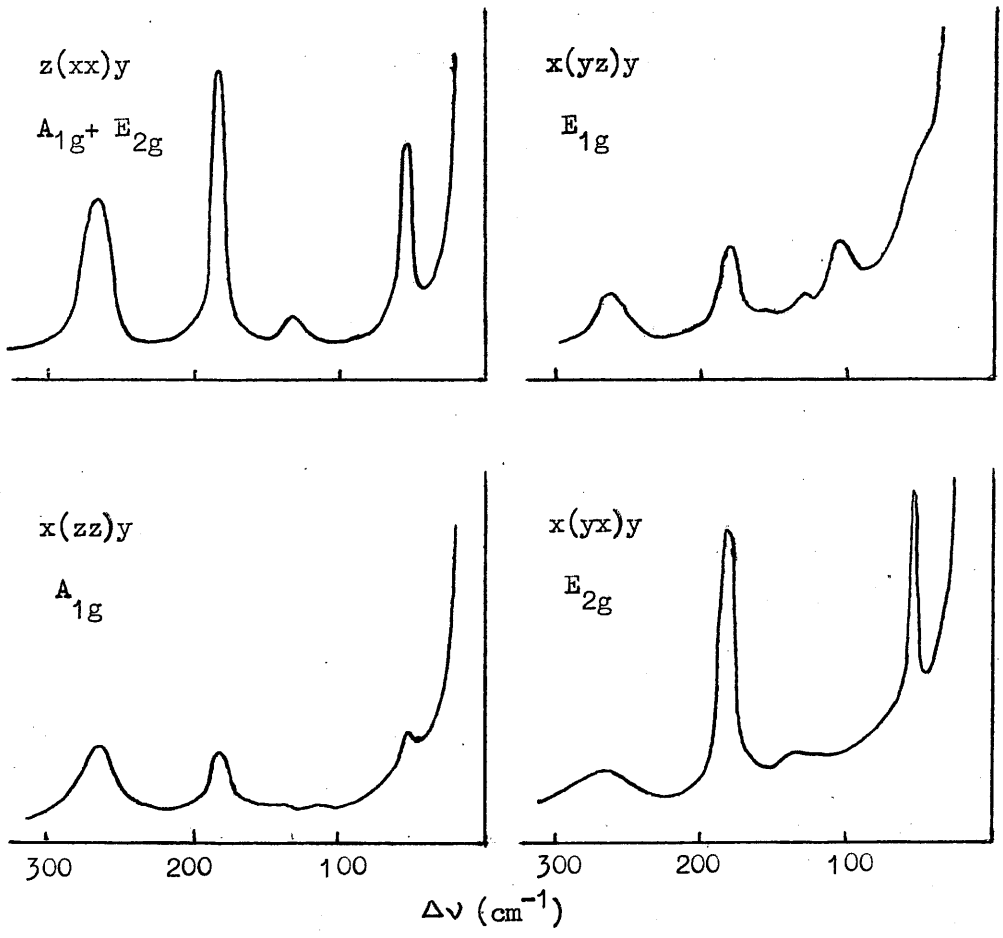

Figure 3.5: Single-crystal Raman spectra of $CsCoCl_3$.

Table 3.5: Oscillator frequencies (cm^{-1}) derived from a Kramers-Kronig analysis of the reflectance spectra of $CsCoCl_3$ and $RbCoCl_3$.

$CsCoCl_3$	$RbCoCl_3$	
238	240	E_{1u}
184	184	A_{2u}
168	167	E_{1u}
74	75	E_{1u}
50	50	A_{2u}

Table 3.6: Single-crystal Raman frequencies (cm^{-1}) and relative intensities for $CsCoCl_3$ and $RbCoCl_3$.

$\Delta\nu$ (cm^{-1})	z(xx)y	x(yz)y	x(zz)y	x(yx)y	
264	55	20	25	12	A_{1g}
(272)	(40)	(30)	(35)	(15)	
183	100	30	20	95	E_{2g}
(187)	(90)	(55)	(40)	(100)	
133	12	2	0	7	E_{2g}
(128)	(15)	(5)	(7)	(5)	
108	0	24	0	0	E_{1g}
(112)	(0)	(5)	(0)	(0)	
54	60	10	10	80	E_{2g}
([a])					

( ) - data for $RbCoCl_3$

[a] obscured by rising baseline

Table 3.7: I.r. transmission spectra of some powdered AMX_3 complexes (frequencies in cm^{-1}).

	A_{2u}	E_{1u}	E_{1u}	A_{2u}	E_{1u}
$CsNiF_3$	43	104	267	341	420[a]
$RbNiCl_3$	53	82	179	206	262[a]
$KNiCl_3$	67	103	180	209	260[a]
$CsCoCl_3$	51	76	166	198	247[b]
$RbCoCl_3$	49	78	167	201	250[b]
$CsFeCl_3$	51	78	159	194	256[b]
$RbFeCl_3$	49	78	159	196	254[b]
$CsCdBr_3$	36	56	103	126	154[b]
	lattice modes		internal modes		

[a] symmetry assignments by analogy

[b] symmetries from single-crystal spectra

Discussion

The main features of the i.r. spectra of the various perovskite-type structures can be rationalised in a general way by considering the nature of the possible vibrations for each of the MX_3 sub-lattices. In the cubic structure, for example, the two internal modes take the form of almost pure M-X stretching and X-M-X bending vibrations. These have obvious counterparts in the E_u internal modes of the 2L modification, which again fall clearly in the stretching and bending regions, although some degree of mixing, slight in this case, necessarily takes place. For the A_{2u} mode, on the other hand, the only available symmetry coordinate within the anionic chains involves relative displacements of the

M and X atoms parallel to the hexagonal axis. This involves a considerable degree of mixing of the internal coordinates, as is evident from its frequency in relation to the E_u modes.

In the 6L and 9L structures, the situation is further complicated by the non-equivalence of the X atoms on shared faces or shared corners of the M-filled octahedra. The resultant splitting of the two principal modes adequately accounts for the increased number of E_u bands in the 6L and 9L structures and their relationship to the stretching and bending modes of the 2L and cubic forms remains fairly clear. However, the major transformations of the A_{2u} spectra with change of structure can best be explained by widely differing symmetry restrictions on the forms of the normal vibrations concerned. This account of the effect of structure on the i.r. spectra of the chlorides differs little from that given by Kohn and Nakagawa.[25]

Two i.r. lattice bands, one in each polarisation, are observed for each of the hexagonal complexes examined. These occur below 85 cm^{-1} in the chlorides, with the exception of one band in $KNiCl_3$. It seems likely that the failure to observe the other two lattice modes of the 6L and 9L structures results from their low intensity rather than low frequency.

3.3: Related Structures

NMe_4MnCl_3: The structure of this complex is very similar to that of the 2L hexagonal perovskites, especially in respect of the arrangement of the anionic chains.[14] The presence of the structured cations, however, lowers the symmetry of the space group to either $P6_3/m$ (C_{6h}^2) or $P6_3$ (C_6^6). As in the 2L structure, there are two molecules per unit cell. The factor group predictions for the i.r. active vibrations of these two possibilities are given by representations 3.4 and 3.5 respectively.

$$\Gamma = 2A_u + 3E_{1u} \qquad 3.4$$

$$\Gamma = 5A_u + 5E_{1u} \qquad 3.5$$

The i.r. spectra were found to contain two A_u and three E_{1u} bands, so that they are entirely consistent with the centrosymmetric space group. In fact, the factor group predictions for this structure are effectively the same as those for the 2L perovskites as far as the i.r. and Raman active modes are concerned, despite the removal of the two-fold axes in the (001) planes. The form of the i.r. spectra turns out to be indistinguishable from that of the 2L $CsCoCl_3$ structure.

The observed frequencies given in Table 3.8 are in good agreement with those of an independent study by Adams and Smardzewski,[26] who also examined the single-crystal Raman spectra. Their Raman results confirm the similarity between the vibrational spectra of NMe_4MnCl_3 and $CsCoCl_3$.

The i.r. results for this pseudo-2L structure allows a direct comparison of the spectra of the three hexagonal perovskite modifications for the trichloromanganates. This illustrates clearly the points made at the end of Section 3.2.

<u>$CsCuCl_3$</u>: This compound crystallises in the space group $P6_122$ (D_6^2), with six formula units forming part of a single anionic chain in each unit cell.[15] The structure is again related to that of the 2L perovskites, with an increase in the repeat distance along the chain axis caused by the Jahn-Teller distortion of the octahedra surrounding each copper atom, resulting in four short (2.28 and 2.35Å) and two long (2.78Å) Cu-Cl distances. There are two ways of describing the complex anions in this structure. They may be regarded as chains of tetragonally elongated octahedra sharing opposite faces, to which the distortion imparts a slight helical twist with a six-layer interval of revolution. Alternatively, the original description of Wells[34] may be used, in which the long-bonded Cu-Cl interactions are ignored, and the anions are regarded

Table 3.8: I.r. reflectance bands (cm^{-1}) of NMe_4MnCl_3 single crystals.

228	E_{1u}	internal modes
180	A_u	
149	E_{1u}	
90	E_{1u}	lattice modes
52	A_u	

Table 3.9: I.r. reflectance bands (cm^{-1}) of $CsCuCl_3$ single crystals.

A_2	E_1	Approximate description
266	288	Cu-Cl stretching
	254	
181	188	Cu-Cl bending
	175	
147	159	
	112	
96	80	lattice modes
51	72	

as bridged chains of square planar $CuCl_4$ units sharing two adjacent corners spiralling along the chain axis. Whichever description is adopted, the predicted i.r. active modes of the structure are given by representation 3.6. Three modes of each symmetry are lattice vibrations,

$$\Gamma = 8A_2 + 14E_1 \qquad 3.6$$

including one A_2 rotatory mode of the chains.

The i.r. reflectance spectra of $CsCuCl_3$ (Fig. 3.6) show just over half of the predicted bands, and the frequencies of these are given in Table 3.9. There are some major discrepancies between these results and those of the recent work on this complex by Adams and Newton,[35] leading to a fundamental difference in interpretation. Using Wells' model of the structure these workers have shown that there should be one A_2 and two E_1 stretching modes of both the terminal and bridging Cu-Cl bonds of the square-planar ions, and have assigned two high frequency groups of bands to these vibrations. If it is accepted that the short Cu-Cl stretching modes occur above 200 cm^{-1}, then the results of the present work show only three such bands, i.e. half the predicted number. This could be due to vanishingly low intensities for some of the bands, or to very small energy differences between pairs of terminal and bridging stretches. Even if each of the three observed bands is regarded as predominantly a terminal or a bridging mode, any attempt to distinguish between these on the basis of frequency would be futile, since the spread of these bands is no greater than of the corresponding modes in the symmetrically bridged hexagonal perovskites. The present work therefore concludes that although the "octahedral ion" description of this structure is too complex to be of much use in describing the crystal vibrations, the square-planar model leads to an oversimplified and possibly misleading representation of the bonding scheme within the anionic chains.

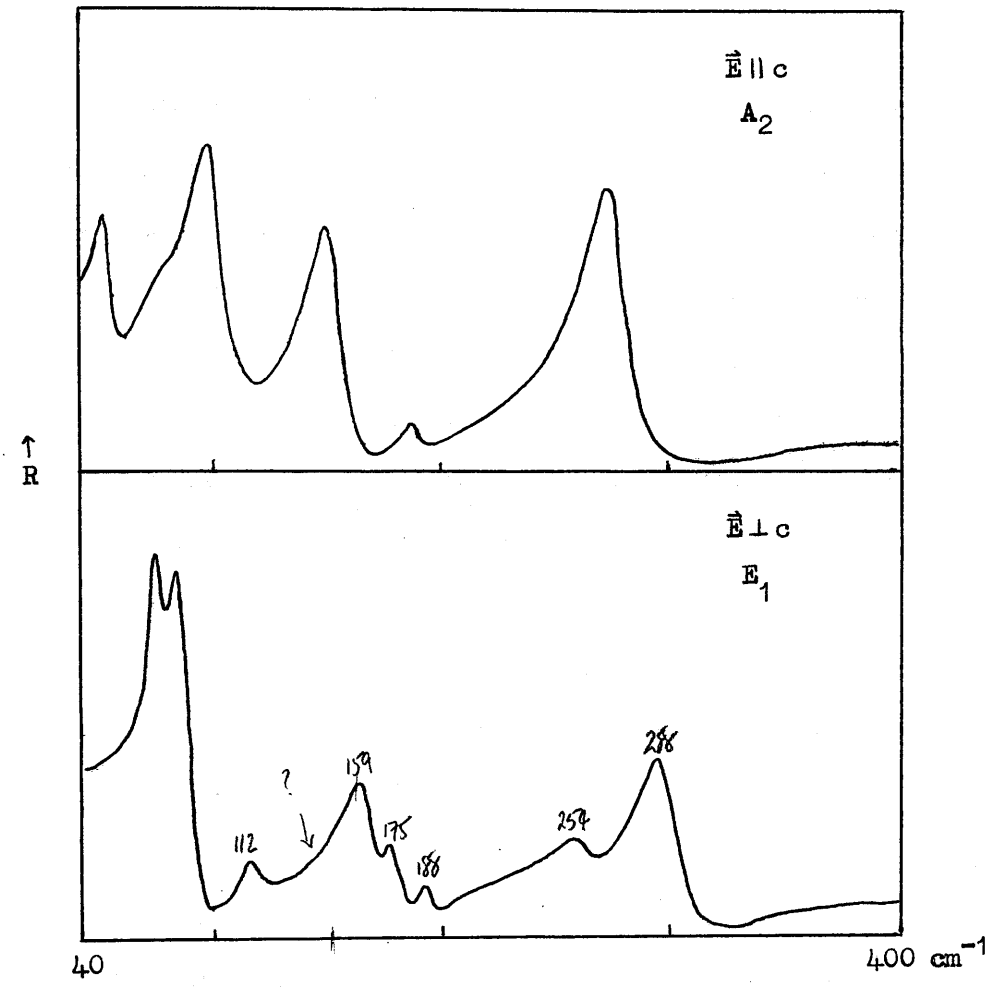

Figure 3.6: I.r. reflectance spectra of $CsCuCl_3$ single crystals.

3.4: $AHgX_3$ Complexes

Although the known structures of the $AHgX_3$ complexes are related to the cubic perovskite structure, an important distinction arises from the presence in these complexes of molecular HgX_2 units. A number of structures, some of which are polymorphic modifications, have been reported[8,12,16,17] for $CsHgCl_3$. The most helpful description[17] is based on the ideal perovskite structure in which the mercury forms two short bonds to chlorine atoms, and the resulting linear $HgCl_2$ molecules are statistically oriented along the three possible directions in each pseudocell. The smearing out of the random arrangement by X-ray diffraction leads to a description of the structure in terms of a cubic pseudocell with a statistical distribution of chlorine atoms at or near the face centres. $CsHgBr_3$ is also described[12] as having a cubic structure, but, as for the chloride, a high degree of structural complexity would be expected.

NH_4HgCl_3 is the only reported example of a tetragonal structure, in which the $HgCl_2$ molecules are aligned with the c axis.[36] The distorted octahedral coordination of the mercury atom is completed by free chloride ions lying in the plane perpendicular to the c axis. The basis for the classification of this structure as a perovskite modification[37] is rather tenuous.

The present work is intended to extend and clarify the structural data available for the $AHgX_3$ complexes by X-ray powder diffraction methods and i.r. spectroscopy, and to investigate the effect of structure on the vibrations of the HgX_2 units present in the various condensed phases.

Results and Discussion

The X-ray diffraction patterns of samples of $CsHgCl_3$ prepared

under a variety of conditions were all identical and, with the exception of some weak lines, could be indexed on the basis of a cubic unit cell with a_o = 5.42Å. No evidence for polymorphism was found. $CsHgBr_3$ gave a more complex diffraction pattern than the chloride, with a number of lines in the vicinity of each expected "cubic" reflection. These could not be indexed according to any simple unit cell, suggesting that the size of the bromine atoms causes a greater distortion from the ideal perovskite structure than in the case of the chloride.

The frequencies of the bands observed in the spectra of $CsHgCl_3$ and $CsHgBr_3$, with assignments based on those reported for $HgCl_2$ and $HgBr_2$[38,39] are presented in Table 3.10. The two highest bands in the chloride have already been observed by Coates and Ridley.[40] The forms of the spectra, as shown in Fig. 3.7, are closely similar apart from the intensity of the ν_1 bands. In the chloride this has about one third of the intensity of ν_3, while in the bromide it is weaker and more diffuse.

In order to interpret the $CsHgX_3$ spectra in terms of the site symmetry of the HgX_2 molecules, the possibilities arising in a disordered or complex structure must be considered. The cubic pseudocell of these complex halides may be derived from the ideal perovskite unit cell by covalent bond formation between the mercury atom at the body centre and two halogens at the centres of opposite faces, causing these atoms to be drawn into the cell. Of the remaining four neighbouring halogen atoms, two form covalent bonds to mercury atoms in adjacent pseudocells, while the other two retain their positions at the face centres, and are largely ionic in character. There are thus two possible arrangements when only one molecular sub-cell is considered, i.e. one in which the halide ions occupy opposite faces, and another where these are on adjacent faces, with approximately D_{2h} and C_{2v} site symmetries of the HgX_2 molecules respectively. Although the true site symmetry may be formally reduced

Table 3.10: Observed i.r. frequencies and assignments for the $CsHgX_3$ complexes.

$CsHgCl_3$	$CsHgBr_3$	
320	228	ν_3 (HgX_2)
284	188	ν_1 (HgX_2)
198	134	lattice mode
96	68	ν_2 (HgX_2) and lattice mode
60		lattice mode

Table 3.11: Correlation diagram for the HgX_2 molecules in $CsHgX_3$.

Site group C_{2v}	Isolated molecule $D_{\infty h}$	Site group D_{2h}
A_1 [a]	$\Sigma_g^+(\nu_1)$	A_g
B_1 [a]	$\Sigma_u^+(\nu_3)$	B_{1u} [a]
B_2 [a]	$\pi_u(\nu_2)$	B_{2u} [a]
		B_{3u} [a]

[a] dipole active modes

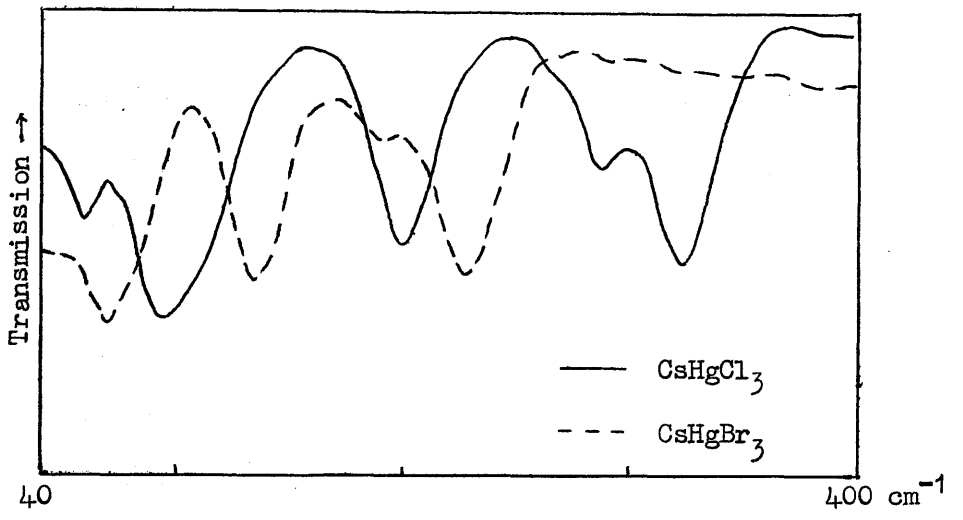

Figure 3.7: I.r. transmission spectra of the $CsHgX_3$ complexes.

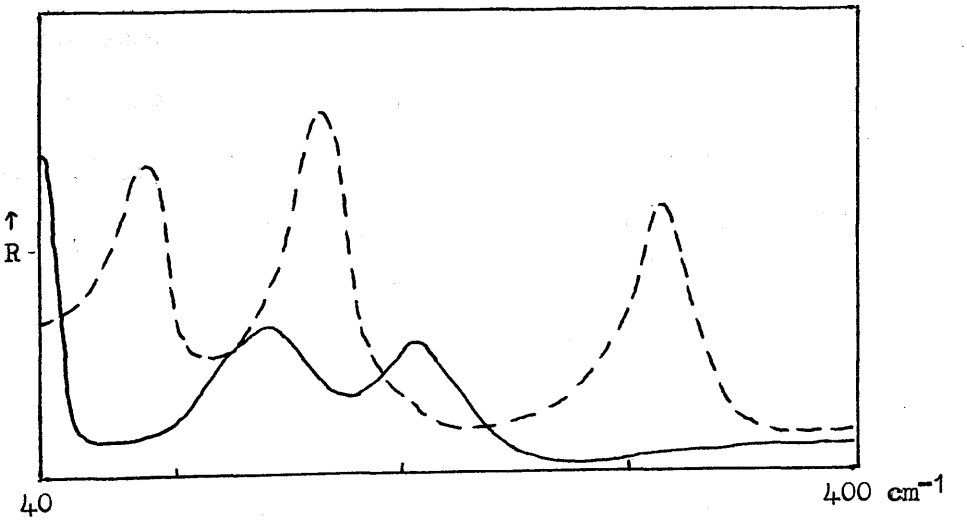

Figure 3.8: I.r. reflectance spectra of NH_4HgCl_3 (solid line- observed E_u bands; dashed line - inferred A_{2u} bands).

to C_1 when the molecular orientations throughout the entire crystal are considered, a discussion of the site group modes in terms of approximately D_{2h} or C_{2v} symmetry is still valid, since the strongest influence on the form of the vibrations of the molecular units will be exerted by the arrangement of the halogen atoms immediately surrounding them. The effect of the two possible site symmetries on the HgX_2 vibrations is illustrated by the correlation of the site group and molecular modes given in Table 3.11. The main difference between the two lies in the i.r. activity of ν_1. Correlation coupling can be ignored, so that the site group approximation is applicable.

The observed i.r. intensity of the ν_1 band in $CsHgCl_3$ is therefore compatible with the assumption that at least a major proportion of the $HgCl_2$ molecules occupy sites of approximately C_{2v} symmetry. In $CsHgBr_3$, the lower relative intensity of the ν_1 band would suggest that the $HgBr_2$ molecules are more evenly distributed between the two possible sites. On the other hand, the disposition of the lattice modes in the spectra of the two complexes is remarkably similar, and this would normally be expected to be sensitive to changes in structure.

NH_4HgCl_3 and $RbHgCl_3$: The X-ray powder diffraction pattern of $RbHgCl_3$ was almost identical to that of NH_4HgCl_3, and from the high order reflections unit cell dimensions of $a_o = 4.21$, $c_o = 8.01$Å were calculated (c.f. $a_o = 4.20$, $c_o = 7.94$Å for NH_4HgCl_3 [8]). It was concluded that $RbHgCl_3$ is isostructural with NH_4HgCl_3,[36] having space group $P4/mmm$ (D^1_{4h}) ($Z = 1$). A factor group analysis based on this structure (neglecting the H atoms in NH_4HgCl_3) predicts six i.r. active modes given by the representation 3.7. Of these, there are two internal

$$\Gamma = 3A_{2u} + 3E_u \qquad 3.7$$

modes of the $HgCl_2$ molecules, $\nu_3(A_{2u})$ and $\nu_2(E_u)$, while the remainder are lattice modes.

In the far i.r. transmission spectra of both $RbHgCl_3$ and NH_4HgCl_3, only four broad bands were observed, of which the highest frequency band was assigned to ν_3. Polarised single crystal i.r. reflectance spectra are therefore necessary for the assignment of ν_2, and also to resolve the unobserved bands. Although attempts to grow single crystals of $RbHgCl_3$ and NH_4HgCl_3 using the Stockbarger technique were not successful, a polycrystalline boule containing partially oriented domains of NH_4HgCl_3 was obtained. A polished face of this boule exhibited complete dichroism of the ν_3 band when the crystal was rotated with respect to the electric vector of the polarised incident radiation. Using the intensity of this band as a guide, and knowing the predicted number of modes and their symmetry, it was found that certain orientations gave exclusively E_u modes, while others gave a mixture of A_{2u} and E_u modes. Despite the anomalous effects which may arise in the reflectance spectra of uniaxial crystals when the electric vector of the incident radiation is not aligned with specific crystallographic axes (see Chapter 5.2) it was found possible, by subtraction of the E_u bands from the spectra containing bands of both symmetries, to make tentative assignments of the six i.r. active modes in NH_4HgCl_3. The A_{2u} bands shown schematically in Fig. 3.8 were identified in this way. The frequencies of the bands observed in both the reflectance and transmission spectra together with assignments are given in Table 3.12. Although some error in the frequencies of the A_{2u} modes is possible because of anomalous dispersion, the reflectance frequencies are in good agreement with those observed in the transmission spectrum. The polarised reflectance spectra allow the observation of the bending mode, ν_2, in NH_4HgCl_3, while in the transmission spectrum, this band is obscured by the broad overlapping lattice bands. The same is probably true for the rubidium complex, in which all of the lattice modes are of lower frequency because of the increased mass

Table 3.12: I.r. reflection and absorption frequencies (cm^{-1}) for NH_4HgCl_3 and $RbHgCl_3$.

Transmission		Reflection		Assignment
$RbHgCl_3$	NH_4HgCl_3	NH_4HgCl_3		
		E_u	A_{2u}	
312	308		310	ν_3
170	196	196		lattice mode
			154	" "
110	152			
		140		ν_2
72	96		94	lattice mode
		40		" "

of the cation.

Poulet and Mathieu[39] have noted the expected decrease in the frequency of ν_1 for the $HgCl_2$ molecules in a series of chloromercurates(II) with increasing HgCl bond length. A similar variation is observed in the asymmetric stretching mode ν_3 for the complexes $HgCl_2$, $CsHgCl_3$ and NH_4HgCl_3 as shown in Table 3.13. By interpolating the value of ν_3 for $RbHgCl_3$ in this trend, an Hg-Cl bond distance of about 2.33Å can be estimated for this complex.

A further general point which emerges from a consideration of the spectra of the complexes examined is the unusually high frequencies observed for some of the lattice modes, e.g. those at 198 and 134 cm^{-1} in $CsHgCl_3$ and $CsHgBr_3$ respectively. This phenomenon will be encountered again in connection with the spectra of Cs_3CoCl_5 (Chapter 4.5), and results from the presence of free halide ions as well as complex groups in these crystals.

Table 3.13: Variation of ν_3 with Hg-Cl bond length (d) in some $AHgCl_3$ complexes.

	$HgCl_2$	$CsHgCl_3$	NH_4HgCl_3
ν_3 (cm^{-1})	377	320	308
d (Å)	2.25	2.29	2.34

3.5: Experimental

Preparations: All of the AMX_3 complexes, except $CsCuCl_3$, NMe_4MnCl_3 and the cadmium complexes, were prepared by fusion of the appropriate halides. Where necessary, the anhydrous metal dichlorides were prepared by sublimation in an atmosphere of hydrogen chloride. The manganese, iron and cobalt complexes were grown as large single crystals by the Stockbarger method, with reference to published phase diagrams or melting points.[8,33,41] Attempts to grow $CsPbCl_3$ and NH_4HgCl_3 by the same method were only partially successful. As well as the fused samples, small crystals of $CsHgCl_3$ and $CsHgBr_3$ were prepared from aqueous and ethanolic solutions under a variety of conditions.

$CsCuCl_3$, NMe_4MnCl_3, $CsCdBr_3$ and $CsCdCl_3$ were also crystallised from aqueous solutions of the constituent halides. The first three of these gave mainly hexagonal rods, with some bipyramids in the case of $CsCuCl_3$. Only very small crystals of $CsCdCl_3$ were obtained from solution, mostly of the cubic modification. These were used in the growth of large hexagonal crystals from the melt.

The melt-grown 2L crystals all showed good $(1\bar{1}00)$ cleavage planes. For the 6L and 9L structures, the poor cleavage was useful only for orienting the samples, and the preparation of suitable faces had to be carried out by grinding and polishing. The directions of the

crystallographic axis in these hexagonal crystals were determined by birefringence.

Analysis of i.r. reflectance spectra: In a number of cases, the true oscillator frequencies were derived by a Kramers-Kronig analysis of the reflectance spectra, using the expressions 1.6-1.10. The necessary computations were carried out on a KDF 9 computer. The infinite integral 1.8 was evaluated in the range 20-400 cm^{-1} using the trapezoidal approximation, and outside this range constant values of R from 0-20 cm^{-1} and 400-∞ cm^{-1} were assumed. A correction term[42] taking account of the inaccuracy arising from this extrapolation produced no significant change in the frequencies (ν_j) of the maxima in ϵ''. Since the approximation $\gamma_j/\nu_j \ll 1$ holds (where γ_j is the half-width of the ϵ'' peak) the values of ν_j give the oscillator frequencies. The results of this analysis on the spectra of $CsCoCl_3$ are shown in Fig. 3.4.

References

1 V.M. Goldschmidt, Geochem. Vert. d. Elem., 1927, 7.

2 C.K. Møller, Nature, 1957, 180, 981; Kgl. Danske Videnskab. Selskab. Mat. Fys. Medd., 1959, 32, 1.

3 M. Kestigian, W.J. Croft and F.D. Leipziger, J. Chem. Eng. Data, 1967, 12, 97.

4 J.M. Longo and J.A. Kafalas, J. Solid State Chem., 1971, 3, 429.

5 A. Hardy, Acta Cryst., 1962, 15, 179.

6 H.J. Seifert and F.W. Koknat, Z. anorg. Chem., 1965, 341, 269.

7 H. Soling, Acta Chem. Scand., 1968, 22, 2793.

8 H.F. McMurdie, J. de Groot, M. Morris and H.E. Swanson, J. Res. Nat. Bur. Stand., Sect. A, 1969, 73, 621.

9 R.W.G. Wyckoff, "Crystal Structures", 2nd edn., Vol2, Interscience, New York, 1965.

10 G. Shirane, R. Pepinsky and B.C. Fraser, Acta Cryst., 1956, 9, 131.

11 J.M. Longo and J.A. Kafalas, J. Solid State Chem., 1969, 1, 103.

12 G. Natta and L. Passerini, Gazzetta, 1928, 58, 472.

13 Y. Syono, S. Akimoto and K. Kohn, J. Phys. Soc. Japan, 1969, 26, 993.

14 B. Morosin and E.J. Graeber, Acta Cryst., 1967, 23, 766.

15 A.W. Schuleter, R.A. Jacobsen and R.E. Rundle, Inorg. Chem., 1966, 5, 277.

16 I. Náray-Szabó, Publ. Univ. Techn. Budapest, 1947, 1, 30.

17 Z.V. Zvonkova, V.V. Samodurova and L.G. Vorontsova, Dokl. Akad. Nauk. SSSR, 1955, 102, 1115.

18 See refs. 5 and 6 of Chapter 2; see also W.G. Nilsen and J.G. Skinner, J. Chem. Phys., 1968, 48, 2240.

19 I. Nakagawa, A. Tsuchida and T. Shimanouchi, J. Chem. Phys., 1967, 47, 982.

20 J.M. Barraclough, D.H. Brown, A.P. Lane, D.A. Paterson and D.W.A. Sharp, Chem. Comm., 1969, 608; C.H. Perry, Japan, J. Appl. Phys., 1964, 4, 564; C.H. Perry and D.B. Hall, Phys. Rev. Letters, 1965, 15, 700.

21 G. Zanmarchi and P.F. Bongers, Solid State Comm., 1968, 6, 27.

22 P.A. Fleury, J.M. Worlock and H.J. Guggenheim, Phys. Rev., 1969, 185, 738.

23 J.T.R. Dunsmuir, I.W. Forrest and A.P. Lane, Mat. Res. Bull., 1972, 7, 525.

24 S.R. Chinn, Phys. Rev., 1971, B3, 121.

25 K. Kohn and I. Nakagawa, J. Chem. Soc. Japan, 1970, 43, 3780.

26 D.M. Adams and R.S. Smardzewski, Inorg. Chem., 1971, 10, 1127.

27 A. Ferrari and A. Baroni, Atti. Accad. Lincei, 1927, 6, 418.

28 F.W. Ainger, C.C. Clark, A. Marsh and P. Waterworth in "Proceedings of the International Meeting on Ferroelectricity", Prague, 1966, Vol. 1, p. 295.

29 C.A. Arguello, D.L. Rousseau and S.P.S. Porto, Phys. Rev., 1969, 181, 1351.

30 S. Siegel and E. Gebert, Acta Cryst., 1964, 17, 790.

31 P. Allamagny, Bull. Soc. Chim. France, 1960, 1960, 1099.

32 D. Babel, Z. Naturforsch., 1965, 20A, 165; R.W. Asmussen, T. Kindt-Larsen and H. Soling, Acta Chem. Scand., 1969, 23, 2055; A. Engberg and H. Soling, Acta Cryst., 1963, 16, A27.

33 H.J. Seifert and K. Klatyk, Z. anorg. Chem., 1966, 342, 1.

34 A.F. Wells, J. Chem. Soc., 1947, 1662.

35 D.M. Adams and D.C. Newton, J. Chem. Soc. (A), 1971, 3499.

36 E.J. Harmsen, Z. Krist., 1938, 100A, 208.

37 I. Náray-Szabó, "Inorganic Crystal Chemistry", Académiai Kiadó, Budapest, 1969.

38 Y. Mikawa, R.J. Jakobsen and J.W. Brasch, J. Chem. Phys., 1966, 45, 4529.

39 H. Poulet and J.-P. Mathieu, J. Chim. phys., 1963, 60, 442.

40 G.E. Coates and D. Ridley, J. Chem. Soc., 1964, 166.

41 H.J. Seifert, Z. anorg. Chem., 1961, 307, 137; P. Ehrlich, F.W. Koknat and H.J. Seifert, ibid., 1965, 341, 281; H.J. Seifert and F.W. Koknat, ibid., 1968, 357, 314.

42 P.N. Schatz, S. Maeda and K. Kozima, J. Chem. Phys., 1963, 38, 2658.

Chapter 4: Complexes Containing Discrete MCl_4^{2-} Ions

4.1: Introduction

The MCl_4^{2-} ion can adopt either a tetrahedral arrangement, as in the case of most of the first row transition metal complexes, or a square-planar configuration, typified by the K_2PtCl_4 structure. The present chapter will be concerned primarily with tetrahedral ions, both in the regular and distorted form.

Vibrational spectroscopy has proved useful in establishing the presence of tetrahedral anions in chlorometallates such as A_2MCl_4 and A_3MCl_5. Infra-red studies in particular have often been used to determine whether such ions existed as regular or distorted tetrahedra. The T_d ion has four fundamental modes of vibration: the symmetric stretching and bending modes ν_1 (A_1) and ν_2 (E), and the asymmetric stretch and bend ν_3 (F_2) and ν_4 (F_2). The last two are i.r. active, while all four are Raman active. In the distorted ion, the degeneracies may be removed, and the T_d fundamentals split. Various workers have carried out careful examinations of the i.r. mull spectra of a number of these complexes, mainly the alkylammonium and caesium salts, in attempts to resolve the crystal mode splittings and relate these to the degree of distortion of the anions.[1-3] These studies were hampered by the insensitivity of the method used, and real progress was made only with the introduction of single crystal i.r. and Raman[4,5] techniques.

Available Raman data include powder spectra of some alkylammonium and caesium complexes,[6-8] and the single crystal work of Beattie et al[4] on Cs_2CuCl_4 and Cs_2ZuCl_4, in which a large proportion of the predicted crystal modes were observed.

The present work sets out to examine the i.r. spectra, as single crystals where possible, of a range of chlorometallates of various structural types, containing tetrahedral and distorted tetrahedral anions. The origin and magnitude of the various effects contributing to solid-state splitting of the fundamental modes in these complexes, and the role of the distortion of the anion in determining the form of the spectra will be discussed. Examples of square-planar complexes will also be examined.

4.2: A_2MCl_4 Complexes (A = Cs, Rb, NMe_4)

The A_2MCl_4 complexes (A = Cs, M = Fe, Co, Cu, Zn; Rb_2CoCl_4; A = NMe_4, M = Co, Cu, Zn) form part of an extensive isostructural series containing isolated tetrahedral anions. The mull i.r. spectra of the caesium and tetramethylammonium salts of cobalt, copper and zinc have been reported.[1-3,6] In the case of the caesium salts, only the region of the metal-chlorine stretching vibrations was examined. This showed a single band corresponding to ν_3 of the tetrahedral MCl_4^{2-} ion except in the copper complexes, where this mode was split by 30 - 40 cm^{-1}, and Cs_2ZnCl_4, where the splitting was 7 cm^{-1}. The Raman spectra of single crystals of Cs_2CuCl_4 and Cs_2ZnCl_4,[4] and of powdered $(NMe_4)_2CuCl_4$[6] have also been reported.

Crystallographic studies have established that all of the alkali-metal complexes dealt with here are isostructural and crystallise in the orthorhombic system with space group Pnma (D_{2h}^{16}) (Z = 4).[9-13] The structures of $(NMe_4)_2CoCl_4$ and $(NMe_4)_2ZnCl_4$ can also be successfully refined in this space group,[14] although in both cases large anisotropic thermal parameters for certain atoms have been interpreted as evidence for orientational

disordering of both the anions and cations. $(NMe_4)_2CuCl_4$ has been shown[9] to have a similar structure apart from a tripling of the a_o axis, indicted by some faint reflections, which is thought to be due to small changes in the positions of nitrogen and carbon atoms in successive sub-cells. These complexes all contain MCl_4^{2-} tetrahedra, flattened to varying extents, on C_s sites, the extreme angles of the anions ranging from 108.4° and 112.1° in $(NMe_4)_2ZnCl_4$ to 99.6° and 129.8° in $(NMe_4)_2CuCl_4$.

The results of a factor group analysis of this structure are shown in Table 4.1. In the case of the $(NMe_4)_2MCl_4$ complexes, rotatory modes of the cation must be taken into account, but their internal vibrations are neglected, since these occur at higher frequencies than those of interest here. The internal modes of the MCl_4^{2-} ions on C_s sites can be correlated with the T_d modes of the isolated ion as shown in Table 4.2. The intermediate $T_d \rightarrow D_{2d}$ correlation applies to the $CuCl_4^{2-}$ ion, which has a large inherent Jahn - Teller distortion, reducing its symmetry to D_{2d}. In all, therefore, fifteen bands associated with the vibrations of the MCl_4^{2-} tetrahedra should be observed in the i.r. spectra of these complexes, seven of these occurring in the M-Cl stretching region, and eight in the bending region.

Results and Discussion

The i.r. absorption spectra of powdered samples of the alkali-metal tetrachlorometallates, except for that of Cs_2CuCl_4, show only three fairly broad, asymmetric bands in the region of the fundamental vibrations. The frequencies of these bands, which are in good agreement with those reported previously, are given in Table 4.3. In accordance with earlier work, the bands at around 300 cm^{-1} are

Table 4.1: Factor group analysis of A_2MCl_4 complexes with space group D_{2h}^{16}.

	A_g	B_{1g}	B_{2g}	B_{3g}	A_u	B_{1u}	B_{2u}	B_{3u}
N^a	13	8	13	8	8	13	8	13
T_a						1	1	1
T	6	3	6	3	3	5	2	5
R_-	1	2	1	2	2	1	2	1
N_i	6	3	6	3	3	6	3	6
R_+^b	3	3	3	3	3	3	3	3
I.r. activity						z	y	x

[a] for alkali-metal complexes

[b] cation rotatory modes - applies only to tetramethylammonium complexes

Table 4.2: Correlation diagram for the MCl_4^{2-} ions in the orthorhombic A_2MCl_4 complexes.

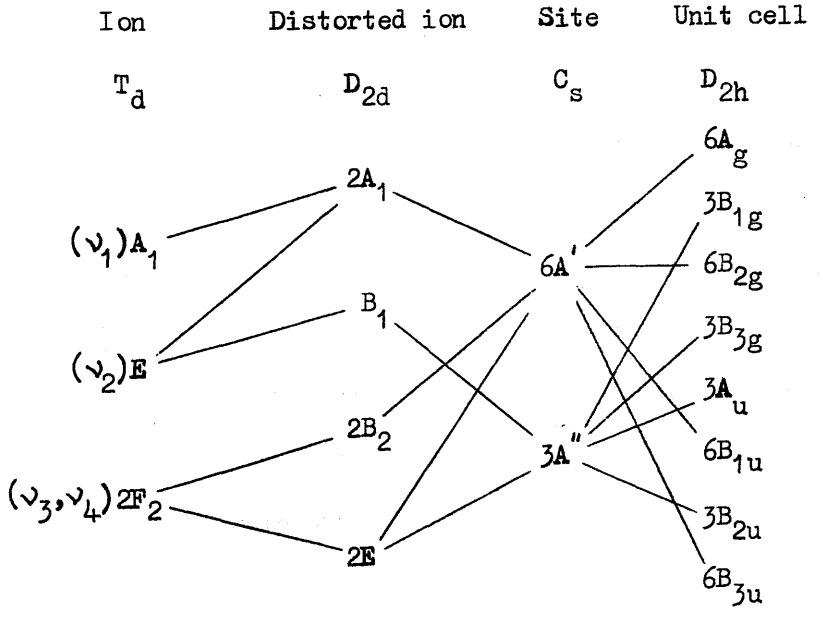

Table 4.3: I.r. absorption frequencies (cm^{-1}) of some A_2MCl_4 complexes.

	Lattice	ν_4	ν_3	ν_1 [a]
Cs_2FeCl_4	86	122	300	284
Cs_2CoCl_4	83	123	310	298
Rb_2CoCl_4	90	132	315	280
Cs_2CuCl_4	82	126, 149	260, 292	265
Cs_2ZnCl_4	84	132	294	279

[a] calculated from the combination band $\nu_1 + \nu_3$

assigned to ν_3 of the tetrahedral anions, and those at around 125 cm^{-1} to ν_4. For reasons which will become apparent later when the single crystal spectra are discussed, the suggestion[2] that the lowest bands below 100 cm^{-1} arise from i.r. active components of ν_2 has been rejected, and these have been confidently assigned to lattice vibrations. The spectra contain no resolved features which could be attributed to either ν_1 or ν_2. For Cs_2CuCl_4, both ν_3 and ν_4 are split into doublets separated by by about 25 cm^{-1}. With this exception, none of the expected crystal mode splitting is observed in the powder spectra of these complexes, which is not surprising in the light of previous results.

In order to overcome the insensitivity of the powder method and to obtain more detailed spectral data for this type of complex, the complete single crystal reflectance spectra of Cs_2ZnCl_4, $(NMe_4)_2CoCl_4$, $(NMe_4)_2CuCl_4$ and $(NMe_4)_2ZnCl_4$ were recorded, the B_{1u}, B_{2u} and B_{3u} modes being activated by incident radiation

polarised along the c, b and a crystallographic axes in turn. A less detailed examination of Cs_2CoCl_4 and Cs_2CuCl_4 was also made.

The frequencies of the bands observed in the spectra of the caesium complexes are given in Table 4.4. Fig. 4.1 shows the spectra of Cs_2ZnCl_4, in which all of the five crystal modes derived from ν_3 were observed, with distinct splitting of about 12 cm^{-1} between the B_{1u} and B_{3u} doublets. This splitting was less pronounced in the case of the ν_4 mode, and was observed only for the B_{3u} components, in the form of a shouler on the low frequency side of the main reflectance maximum. Further features to the low frequency side of the B_{2u} and B_{3u} components of $_4$ were observed; these were much weaker than the ν_4 bands and are therefore assigned

Table 4.4: Polarised i.r. reflectance data (cm^{-1}) for Cs_2MCl_4.

Cs_2ZnCl_4			Cs_2CuCl_4		Cs_2CoCl_4	T_d mode
B_{1u}	B_{2u}	B_{3u}	B_{2u}	B_{1u} or B_{3u}		
300	296	302	296	288	316	ν_3
288		288		258	314	
132	134	147	136	151	136	ν_4
		139		123	135	
					127	
	110	114				ν_2
87	77	90	79	83	98	lattice modes
67	60	75	61		82	
		67			75	
		55			70	
					60	

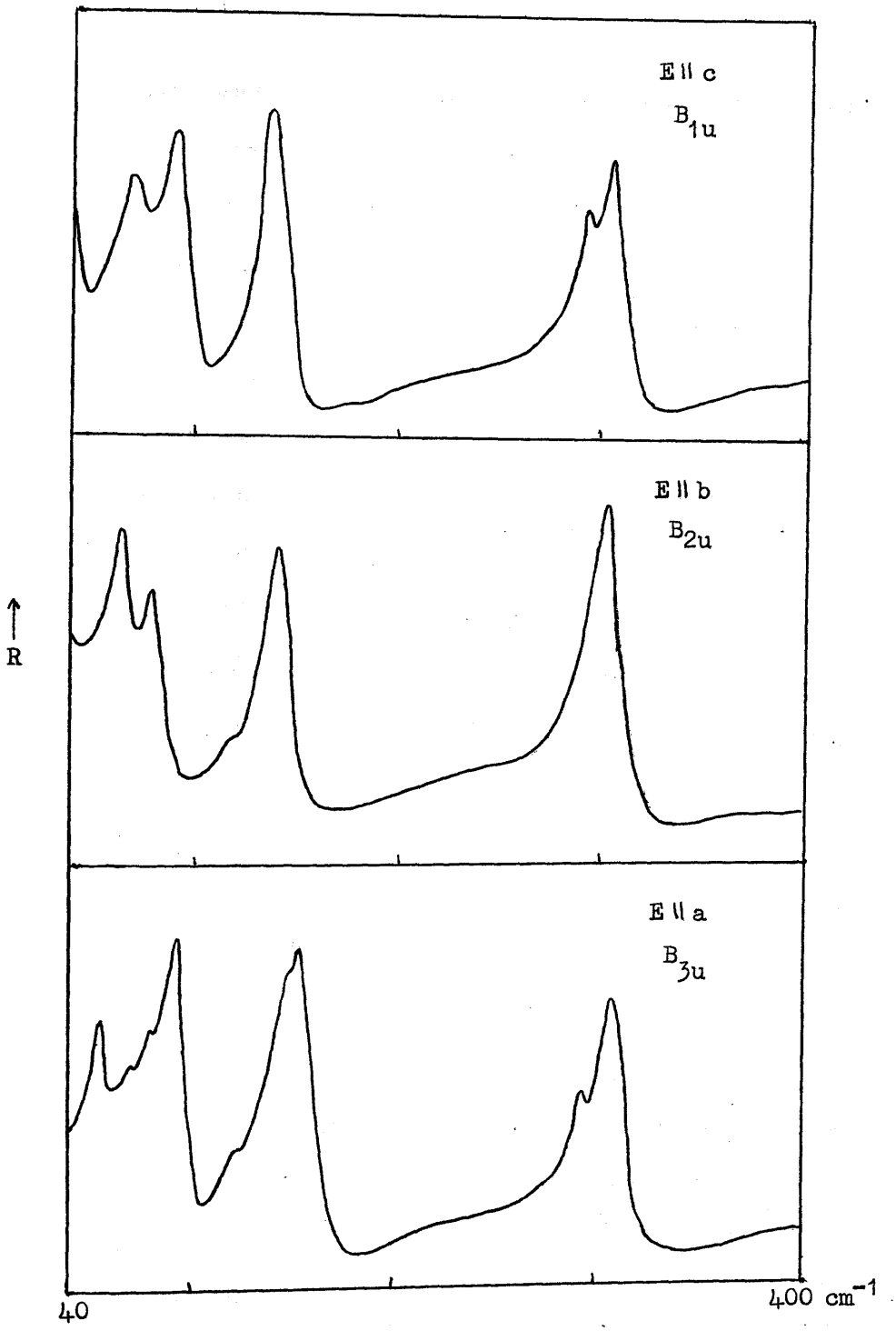

Figure 4.1: Single-crystal i.r. reflectance spectra of Cs_2ZnCl_4.

to the B_{2u} and B_{3u} components of ν_2. The low intensity is consistent with the expected weak dipole activity of bands derived from i.r. inactive modes of the isolated ion, and their frequencies are very close to those of the ν_2 modes in the Raman spectra[4] of Cs_2ZnCl_4. None of the predicted components of ν_1 was observed. From the Raman spectra, these should occur around 288 cm^{-1}, and it is therefore probable that the two i.r. active components of ν_1 are obscured by the more intense ν_3 bands. Below 100 cm^{-1} a total of eight bands was observed in the reflectance spectra of the three crystal orientations. These low-energy vibrations are assigned to lattice modes.

Complete polarised reflectance spectra could not be recorded for Cs_2CoCl_4 and Cs_2CuCl_4 owing to the poorer quality and smaller size of the crystalline samples obtained. In the case of Cs_2CuCl_4, the crystals were too narrow and fragile to permit the grinding of primitive (100) or (001) faces, so that the spectra were recorded from the natural (101) faces. This gave B_{2u} modes when the incident radiation was polarised along the crystallographic b axis, and a mixture of B_{1u} and B_{3u} modes when polarisation was perpendicular to the b axis.

The reflectance spectra of polished faces of a polycrystalline boule of Cs_2CoCl_4 were found to exhibit i.r. dichroism, due presumably to partial alignment of the crystallites. For reasons that will become evident in Chapter 5.2, little reliance can be placed on spectra obtained in this way, although they do demonstrate clearly the presence of solid state splitting which is unresolved in the powder spectrum.

The bands observed in the polarised spectra of the tetramethylammonium complexes at room temperature and 105K are listed in Table 4.5,

Table 4.5: Frequencies (cm^{-1}) of reflectance bands in the i.r. spectra of $(NMe_4)_2MCl_4$ single crystals.

	B_{1u}		B_{2u}		B_{3u}	
	l.t.	r.t.	l.t.	r.t.	l.t.	r.t.
$(NMe_4)_2CoCl_4$	310	298	301	297	315	306
	300				300	298
	133	134	135	132	140	132
					132	
$(NMe_4)_2CuCl_4$	288	272	300	278	292	285
	279		295		283	275
	238	234			239	234
	155	126	130	130	151	145
	134				136	127
	118					
$(NMe_4)_2ZnCl_4$	291	276	282	275	295	286
	282		277		278	278
	272					
	138	131	139	132	144	136
	130		134		132	129
	120					

l.t.- low temperature (105K); r.t.- room temperature

while these of the zinc complex are illustrated in Fig. 4.2. Below about 100 cm^{-1}, each of the spectra shows a broad band extending below 40 cm^{-1}. In the case of $(NMe_4)_2ZnCl_4$, spectra were recorded down to 10 cm^{-1} without revealing any distinct structure in these bands. Little change took place at low temperature apart from the appearance of some weak features near 100 cm^{-1}.

The room temperature spectra of the cobalt and zinc complexes show little evidence of the expected factor group splitting of the internal modes of the MCl_4^{2-} ions apart from very small differences in the frequencies of the B_{1u}, B_{2u} and B_{3u} bands, and the presence of two B_{3u} components of ν_3 and (in the zinc complex) ν_4. None of the predicted i.r. active components of ν_1 or ν_2 are observed. The spectra of $(NMe_4)_2CuCl_4$ agree more closely with factor group predictions, especially in the Cu-Cl stretching region.

When the spectra of these complexes are recorded at low temperature, some of the room temperature reflectance bands are split into a number of distinct maxima, which in most cases are very sharp. These low temperature spectra show all of the predicted B_{1u} and B_{3u} bands derived from ν_3 and ν_4 except for one B_{1u} component of ν_4 in $(NMe_4)_2CoCl_4$. A number of weakly allowed components of ν_1 and ν_2 are also observed. Contrary to expectations, the two B_{2u} bands of $(NMe_4)_2ZnCl_4$ are each split by 5 cm^{-1} to form doublets, with a similar splitting taking place for the ν_3 band of $(NMe_4)_2CuCl_4$ (the weak B_{2u} component of ν_4 in the latter can be resolved only with difficulty from the high-frequency tail of the broad lattice band).

In making these assignments, as well as those for the caesium complexes, consideration has been given to band intensities, group

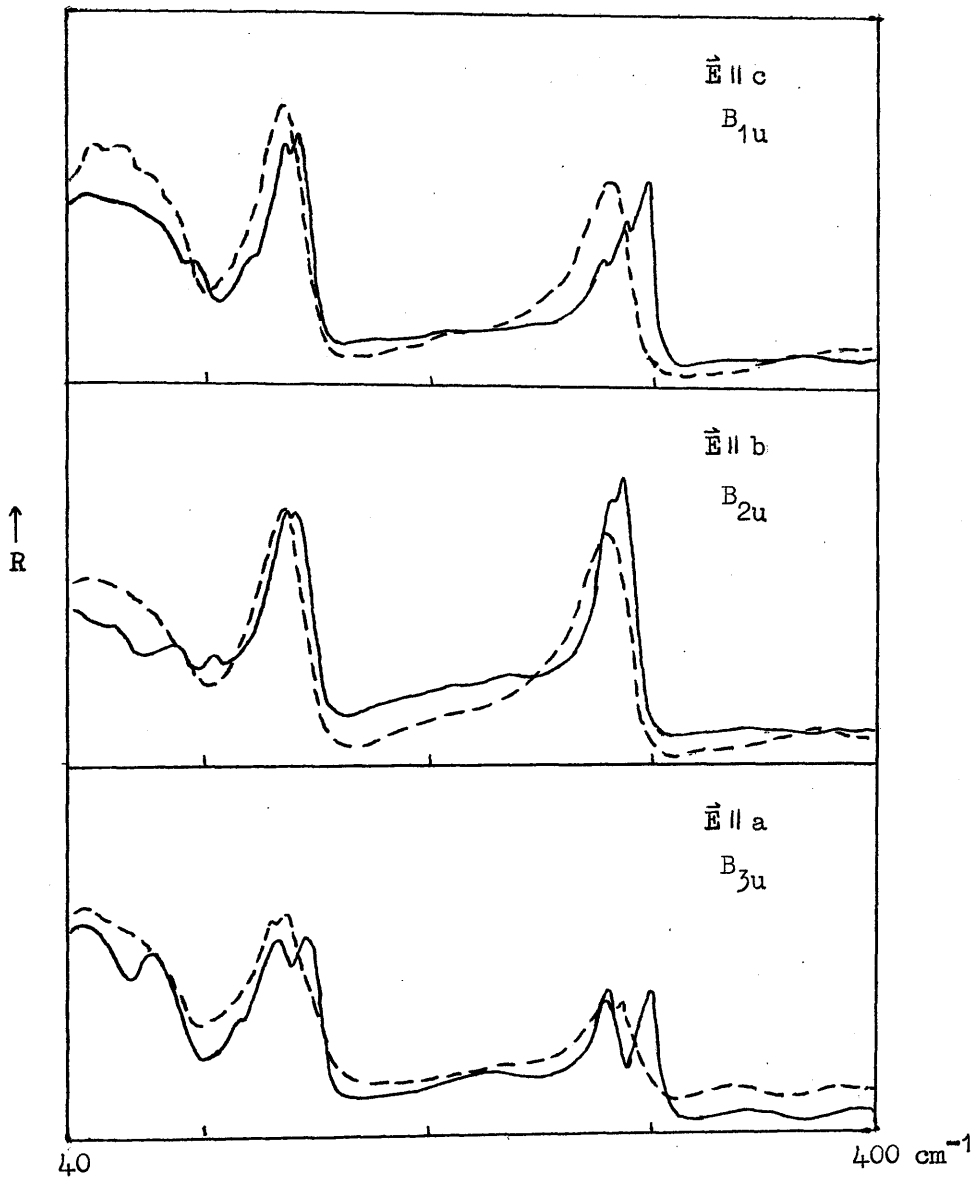

Figure 4.2: I.r. reflectance spectra of $(NMe_4)_2ZnCl_4$ crystals at room temperature (dashed line) and 105K (solid line).

theoretical predictions and the expected frequency ranges for the tetrahedral modes. Thus strong bands in the region of 300 and 130 cm^{-1} have been assigned initially to components of ν_3 and ν_4 respectively. Only weak bands of appropriate frequency have been attributed to ν_1 or ν_2, where all of the predicted ν_3 or ν_4 components of corresponding symmetry have already been accounted for . (In the case of the extra B_{2u} bands of the tetramethylammonium complexes, no ν_1 components are predicted.) It should be noted, however, that under the low site symmetry of the anions, mixing of the T_d modes may occur. The forms of the bending vibrations may be further complicated by mixing with lattice modes. Thus the description of the crystal modes in terms of the normal modes of the free ion must be regarded as approximate. The justification for the use of this approximation lies in the consistent interpretation it allows of the factors affecting the splitting of the crystal modes.

A further point which requires examination before proceeding to a discussion of correlation field effects is the reliability of the reflectance spectra in providing sufficiently accurate data. Examples given in Sections 4.3 and 5.2 will show that dispersion effects in a reflectance spectrum containing two neighbouring bands of the same symmetry (or active in the same ray) can cause the higher reflectance maximum to be displaced from its true frequency to one considerably higher, giving excessively large apparent splitting. In the low temperature polarised spectra of the tetramethylammonium complexes, and in the spectra of Cs_2ZnCl_4, there are a number of instances of two or three bands of the same symmetry occurring within a few wavenumbers of each other. If the frequencies of some of these bands are being influenced by dispersion effects, then this should show itself in unusually large differences

in frequency between Raman and i.r. active correlation components of a particular site group mode, since dispersion plays no part in Raman scattering in centrosymmetric systems. Comparison of the g and u mode frequencies of Cs_2ZnCl_4, listed in Table 4.6, reveals no major irregularities in the correlation splittings, and it may therefore be assumed that the i.r. frequencies are not significantly affected by dispersion.

Tables 4.6 - 4.8 show the correlation schemes for Cs_2ZnCl_4 and the $(NMe_4)_2MCl_4$ complexes. Although the symmetry of the site group mode from which each crystal mode is derived is determined by reference to the correlation diagram (Table 4.2), the identification of the correlation components of any particular site group mode is made possible in these cases only by the possibly fortuitous grouping of the crystal modes into distinct multiplets. The approximation involved in subsequent correlation with the T_d modes has already been mentioned.

Beattie et al[4] find evidence in the Raman spectra of Cs_2ZnCl_4 for mixing of the Raman active components of $A'(\nu_3)$ at 293 cm^{-1} and those of $A'(\nu_1)$ at 288 cm^{-1}. The proximity of all four bands (see Table 4.6) derived from the higher $A'(\nu_3)$ site group mode suggests that if appreciable mixing does take place, it is best regarded as involving the site group modes rather than individual symmetry pairs of correlation components. Examination of Table 4.6 shows that correlation splittings for Cs_2ZnCl_4 are about 6 cm^{-1} or less, with the exception of those for the lower $A'(\nu_4)$ modes.

In the case of the $(NMe_4)_2MCl_4$ complexes, information regarding correlation field effects must come from i.r. data alone, since no single crystal Raman data are available for these. Correlation schemes for the three complexes investigated are set out in Tables

Table 4,6: Assignments for the crystal modes[a] of Cs_2ZnCl_4

Frequency (cm^{-1})	Crystal mode	Site group mode	T_d mode
302	B_{3u}		
300	B_{1u}		
298	A_g	A'	
298	B_{2g}		
296	B_{2u}		
i.a.	A_u	A''	$F_2(\nu_3)$
-	B_{1g}		
-	B_{3g}		
288	B_{1u}		
288	B_{3u}	A'	
281	A_g		
-	B_{2g}		
288	A_g		
288	B_{2g}	A'	$A_1(\nu_1)$
-	B_{1u}		
-	B_{3u}		
147	B_{3u}		
141	A_g	A'	
-	B_{1u}		
-	B_{2g}		
139	B_{3u}		
132	B_{1u}	A'	$F_2(\nu_4)$
128	A_g		
-	B_{2g}		
134	B_{2u}		
i.a.	A_u	A''	
130	B_{1g}		
130	B_{3g}		
116	A_g		
116	B_{2g}	A'	
114	B_{3u}		$E(\nu_2)$
-	B_{1u}		
113	B_{1g}		
113	B_{3g}	A''	
110	B_{2u}		
i.a.	A_u		

[a] frequencies of g modes taken from ref. 4

i.a.- inactive

Table 4.7: Assignments of the bands in the low temperature spectra of $(NMe_4)_2CoCl_4$ and $(NMe_4)_2ZnCl_4$ (frequencies in cm^{-1}).

$(NMe_4)_2CoCl_4$	$(NMe_4)_2ZnCl_4$	Crystal mode	Site group mode	T_d mode
315	295	B_{3u}	A'	$F_2(\nu_3)$
310	291	B_{1u}		
300	282	B_{1u}	A'	
300	278	B_{3u}		
301	282	B_{2u}	A''	
	277	B_{2u}		
	272	B_{1u}	A'	$A_1(\nu_1)$
140	144	B_{3u}	A'	$F_2(\nu_4)$
	138	B_{1u}		
135	139	B_{2u}	A''	
	134	B_{2u}		
132	132	B_{3u}	A'	
133	130	B_{1u}		
	120	B_{1u}	A'	$E(\nu_2)$

Table 4.8: Assignments of the bands in the low temperature spectra of $(NMe_4)_2CuCl_4$.

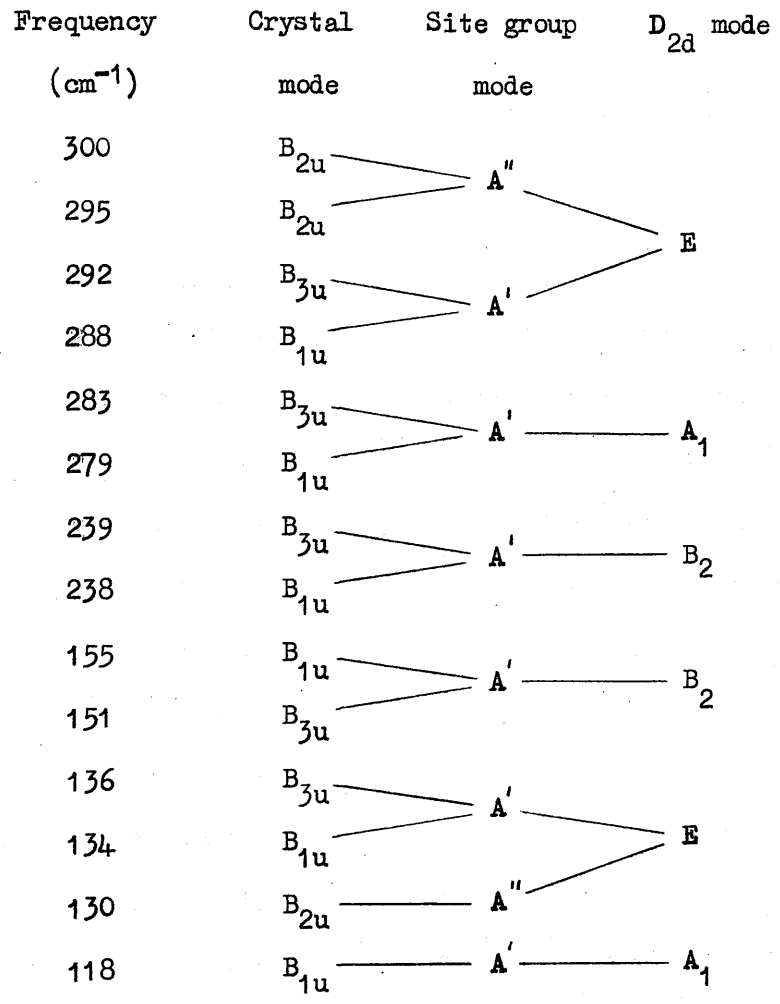

4.7 and 4.8. The splitting of some A'' modes into two B_{2u} components is not consistent with group theoretical predictions for the ordered D_{2n}^{16} structure, and will be discussed in Section 4.4.

For the cobalt and zinc salts, the relationship between crystal modes and free ion (T_d) modes is fairly straightforward, as in Cs_2ZnCl_4. These are shown in Table 4.7. In the case of $(NMe_4)_2CuCl_4$, because of the greater distortion, it is useful to take the free anion symmetry as D_{2d}. The question of the relative positions of the B_2 and E components then becomes important. This splitting of the T_d modes is thought to result from the inherent distortion of the $CuCl_4^{2-}$ ion, and appears in solution spectra. Forster[15] has observed the two components of ν_3 at 278 and 237 cm^{-1} in nitromethane. Corresponding groups of crystal modes are observed at around 290 and 238 cm^{-1} in $(NMe_4)_2CuCl_4$, the frequencies having been perturbed somewhat by the crystal field. The higher of these can be identified as being derived from the $E(D_{2d})$ mode because of the presence of B_{2u} components, which are absent in the case of the B mode, as can be seen from Table 4.2. The bending modes can be assigned using the same argument. The resulting assignments of Table 4.8 are consistent with the Raman bands of powdered $(NMe_4)_2CuCl_4$ reported at 276, 232, 133 and 114 cm^{-1}, which may now be assigned to $A_1(\nu_1)$, $B_2(\nu_3)$, $E(\nu_4)$ and A_1 or $B_1(\nu_2)$ modes of the D_{2d} anion. It should be noted from Table 4.4 that the same order of B_2 and $E(D_{2d})$ modes must also apply for Cs_2CuCl_4.

The correlation splittings in the $(NMe_4)_2MCl_4$ complexes are 6 cm^{-1} or less, about the same as were observed for Cs_2ZnCl_4. Bearing in mind that these are estimated from i.r. components only, this result is somewhat surprising, since the increase in unit cell volume and separation of the anions accompanying the substitution

of tetramethylammonium for caesium ions might be expected to weaken correlation field effects.

4.3: $(NEt_4)_2MCl_4$ Complexes.

The i.r. transmission spectra of $(NEt_4)_2MCl_4$ complexes have been investigated by a number of groups.[1,2,16] For the three examples dealt with here, the cobalt, nickel and copper complexes, the results of Adams et al[16] and Sabatini and Sacconi[2] are in reasonable agreement, while Clark and Dunn[1] observe a greater number of bands in the ν_3 region in the cobalt and copper complexes. The powder Raman spectra of $(NEt_4)_2NiCl_4$ and $(NEt_4)_2CuCl_4$ have also been reported, giving ν_1, ν_4 and ν_2 frequencies at 271, 100 and 88 cm^{-1} respectively in the former[17] and ν_1 at 277 cm^{-1} in the latter.[6]

$(NEt_4)_2CoCl_4$ and $(NEt_4)_2NiCl_4$ have been the subject of a detailed X-ray study[18] which has shown them to be isostructural in the tetragonal space group $P4_2/nmc$ (D_{4h}^{15}) (Z = 2). As in the case of the $(NMe_4)_2MCl_4$ complexes, there is evidence for orientational disordering of both anion and cation. However, whereas the distortion of the anions discussed in the previous section took the form of flattening of the tetrahedral anions, in the tetra-ethylammonium salts they are tetragonally elongated, giving in the case of $(NEt_4)_2NiCl_4$, for instance, two angles of 106.83° and four of 110.81° for the $NiCl_4^{2-}$ ion.

Because of the higher symmetry of this structure, the results of factor group analysis, summarised in Table 4.9, are simpler than for the D_{2h}^{16} structure. The internal modes of the tetraethylammonium ion are ignored, since these would not be expected below 400 cm^{-1}. A correlation diagram for the anions on D_{2d} sites is shown in

Table 4.9: Factor group analysis of $(NEt_4)_2MCl_4$ complexes with space group D_{4h}^{15}.

	A_{1g}	A_{2g}	B_{1g}	B_{2g}	E_g	A_{1u}	A_{2u}	B_{1u}	B_{2u}	E_u
N	3	2	4	2	8	2	4	2	3	8
T_a							1			1
T	1		2		3		1		1	2
R_+		1		1	2	1		1		2
R_-		1			1			1		1
N_i	2		2	1	2	1	2		2	2
I.r. activity							z			(x,y)

Table 4.10: Correlation diagram for the MCl_4^{2-} ions in the $(NEt_4)_2MCl_4$ complexes.

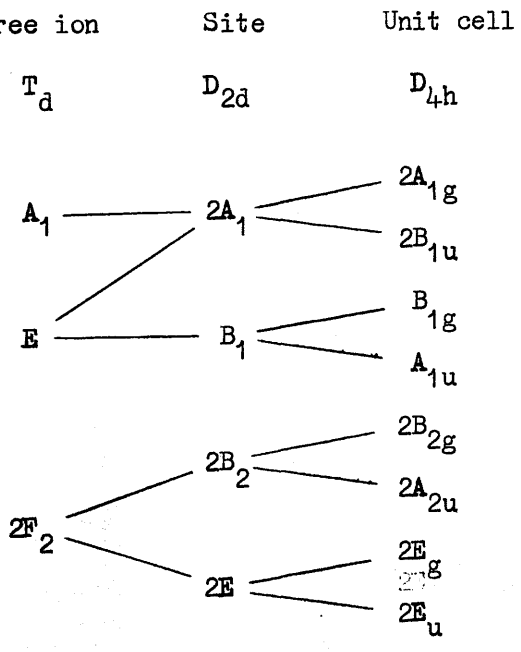

Table 4.10. It will be seen from this that one component of ν_3 and ν_4 should be present in each of the A_{2u} and E_u spectra, while none of either ν_1 or ν_2 will be observed.

No structural data are as yet available for $(NEt_4)_2CuCl_4$.

Results and Discussion

The reflectance spectra of $(NEt_4)_2CoCl_4$ and $(NEt_4)_2NiCl_4$ with the incident radiation polarised parallel and perpendicular to the crystallographic c axis (giving A_{2u} and E_u modes respectively) all showed one band in the M-Cl stretching region and one in the bending region, as expected, with a broad lattice band extending below 100 cm^{-1}. The frequencies and assignments of the bands observed are given in Table 4.11.

At room temperature, the spectra of these complexes are virtually independent of the direction of polarisation, while at 105K they exhibit the expected A_{2u}-E_u splitting, although this is

Table 4.11: Frequencies (cm^{-1}) and assignments of reflectance bands in the i.r. spectra of the $(NEt_4)_2MCl_4$ complexes.

$(NEt_4)_2NiCl_4$		$(NEt_4)_2CoCl_4$		Crystal	Site group	Free ion
l.t.	r.t.	l.t.	r.t.	mode	mode	mode
288	284	304	295	A_{2u}	B_2	ν_3
290	284	299	295	E_u	E	
104	100	133	128	A_{2u}	A_{2u}	ν_4
103	100	127	126	E_u	E	

l.t.- low temperature (105K); r.t.- room temperature.

still very small for the nickel complex. In the low temperature spectra of natural (101) faces of crystals of both complexes, with the incident radiation polarised parallel to the projection of the c-axis on the reflecting face two sharp peaks are observed in the M-Cl stretching region, separated by deep minima. These occur at 287 and 301 cm^{-1} for $(NEt_4)_2NiCl_4$ and 300 and 307 cm for $(NEt_4)_2CoCl_4$. Although the appearance of an A_{2u} and an E_u component of ν_3 in each of these spectra is not surprising, significant differences between these frequencies and those from the spectra of primitive (100) faces (Table 4.11) will be noted, and the latter must be regarded as accurate within the small error involved in the use of reflectance maxima. An explanation of this behaviour will be found in Chapter 5.2.

The powder i.r. spectrum of $(NEt_4)_2CuCl_4$ was recorded, and showed a peak at 269 with a shoulder at 248 cm^{-1} corresponding to ν_3 of the $CuCl_4^{2-}$ ion, two ν_4 bands at 141 and 120 cm^{-1}, and a lattice band at 77 cm^{-1}.

It is not possible to observe any correlation coupling in $(NEt_4)_2CoCl_4$ or $(NEt_4)_2NiCl_4$ from the i.r. spectra alone. The powder Raman spectrum of the nickel complex is reported[17] to have three bands at 271, 100 and 88 cm^{-1} assigned to ν_1, ν_4 and ν_2. The frequency of the ν_4 band, which could be due to the B_{2g} or E_g component, or both, coincides with the room temperature i.r. frequency, which is 12 cm^{-1} lower than that previously reported.[2] The determination of correlation field effects in these systems must therefore await low temperature polarised Raman data.

Although the frequency of the ν_2 band observed in the Raman spectrum of $(NEt_4)_2NiCl_4$ is close to that of the band in the i.r. spectrum tentatively assigned by Sabatini and Sacconi to the same mode, it is clear from Table 4.10 that group theory precludes the

possibility of any i.r. active components of ν_2.

In view of the results of the present single-crystal study, the splitting of the ν_3 mode of $(NEt_4)_2CoCl_4$ by 19 cm^{-1} reported by Clark and Dunn[1] must be regarded with reservations. It is interesting to note that the same authors observe three components of ν_3 in the powder spectrum of $(NEt_4)_2CuCl_4$, which would indicate a structure other than D_{4h}^{15}. The results of this work, together with those of other groups on this complex, however, are compatible with its being isostructural with the cobalt and nickel complexes.

In the fairly complex transmission spectrum of thin $(NEt_4)_2CoCl_4$ crystals above 400 cm^{-1}, a group of three sharp, weak bands at 593, 556 and 537 cm^{-1} can be assigned with some confidence to two-phonon combinations of Co-Cl stretching modes, these being $2\nu_3$, $\nu_1 + \nu_3$ and $2\nu_1$ respectively. This places ν_1 at 260 cm^{-1}. The sharpness of these bands indicates that the vibrations involved have relatively flat dispersion curves, which supports the distinction between internal and lattice modes in such systems, and suggests only weak coupling between the vibrations of neighbouring anions.

4.4: Effects of Orientational Disorder on the Spectra of the Tetra-alkylammonium Complexes

The marked absence at room temperature of factor group splitting of most of the internal modes in the tetra-alkylammonium complexes discussed in the preceeding sections has been noted. This may be attributed to the orientational disordering postulated in these systems.[14,18] The effect of such disorder on the vibrations of the anions would be to permit a continuous band of i.r. modes spanning the range of dispersion (dynamic as opposed to electromagnetic) of each of the fundamental vibrations.[19] The resultant broadening would appear to be sufficient to obliterate

most of the predicted splitting of the T_d modes of the anions, except for the grossly distorted $CuCl_4^{2-}$ ion.

The effect of disorder on the lattice mode spectra is even more marked. In contrast to the sharp lattice bands of the Cs_2MCl_4 complexes, the lattice spectrum of each of the tetra-alkylammonium salts shows a broad, almost featureless reflection band. This again probably corresponds to a "density of states" spectrum arising from the breakdown of the zone-centre (k = 0) approximation (i.e. all lattice modes within the Brillouin zone are allowed to interact with i.r. radiation).

While little change takes place in the low frequency region at low temperature, the bands above 100 cm^{-1} in all the spectra become considerably sharper, and in some cases are split into two or three components. For the tetragonal $(NEt_4)_2MCl_4$ complexes, the low temperature spectra are in accordance with the predictions made, but $(NMe_4)_2CuCl_4$ and $(NMe_4)_2ZnCl_4$ show additional splitting of B_{2u} bands, which is not expected from group theoretical considerations. These features are not compatible with the diffraction symmetry at the MCl_4^{2-} sites in these structures. In view of the similarity of the spectra of the three $(NMe_4)_2MCl_4$ complexes, it will be assumed in the following discussion that the copper complex is isostructural with the other two.

One possible reason for the extra B_{2u} bands is that the unit cells chosen are too small, as suggested[9] by the X-ray diffraction pattern of $(NMe_4)_2CuCl_4$. If this were the case, additional splitting of the B_{1u} and B_{3u} modes might also be expected. A more likely explanation involves the removal of mirror planes parallel to (010) caused by slight rotational displacements of the MCl_4^{2-} tetrahedra. This is supported by the shapes of the thermal ellipsoids obtained

from X-ray studies.[14] In principle this would give rise to nine i.r. active internal modes in each of the three crystal orientations by reducing the site symmetry of the anions to C_1. For small deviations from mirror symmetry, some of these modes would be very weakly dipole active, so that the spectra would show little change from those of the more symmetric structure. The extra B_{2u} bands may be regarded as the only observable features resulting from the relaxation of selection rules caused by the slight variations in the orientations of the MCl_4^{2-} ions relative to the mirror plane of D_{2h}^{16}. This variation could be random, producing pseudo-symmetry in the space group D_{2h}^{16}, or periodic in C_{2v}^{9}. Since the latter structure leads to the trivial result of all site group modes having a component of each symmetry, it is more meaningful to refer the crystal modes of the $(NMe_4)_2MCl_4$ complexes to the D_{2h} structure, bearing in mind the small orientational effects.

Recent heat capacity measurements[20] have revealed transitions in the range 125 - 300K in all of the tetra-alkylammonium complexes. These are thought to involve reorientation of the ions, although the exact structural changes proposed by the authors require rather drastic rearrangement of crystal packing in all cases, for which no evidence can be found in the present work. The fact that no transitions were observed below 125K does not rule out the possibility of residual disorder at 105K, since further transitions may be too diffuse to be observed.

4.5: A_3MX_5 Complexes

Although the stoicheiometry of the A_3MCl_5 (A = Cs, M = Fe, Co, Ni; and Rb_3CoCl_5) complexes might suggest a pentacoordinate anion, they in fact contain approximately tetrahedral MCl_4^{2-} ions, with an equal

number of free chloride ions. They are isostructural,[13,21-25] with space group Imcm (D_{4h}^{18}) (Z = 4). The only detailed X-ray study[22] to have been carried out, on Cs_3CoCl_5, shows that in this complex at least, the distortion of the $CoCl_4^{2-}$ ion takes the form of a slight tetragonal elongation, as in the case of the $(NEt_4)_2MCl_4$ complexes, giving angles of 106.0° and 111.2°. Layers of caesium and MCl_4^{2-} ions perpendicular to the tetragonal axis alternate with layers composed entirely of caesium and free chloride ions. Cs_3CoBr_5 has been shown to adopt the same structure.[25]

$(NMe_2H_2)_3CuCl_5$ also contains equal numbers of $CuCl_4^{2-}$ and chloride ions,[26] the structure in this case being the less symmetric Pnma (D_{2h}^{16}) (Z = 4). The $CuCl_4^{2-}$ ions occupy C_s sites, and are noteworthy in that they have the largest reported distortion from T_d symmetry of any of the chlorocuprates, with Cl-Cu-Cl angles of 97.7°, 98.6°, 135.5° and 136.1°.

The results of a factor group analysis on the Cs_3CoCl_5 structure are given in Table 4.12. The correlation of the crystal modes with

Table 4.12: Factor group analysis of the A_3MCl_5 complexes with space group D_{4h}^{18}.

	A_{1g}	A_{2g}	B_{1g}	B_{2g}	E_g	A_{1u}	A_{2u}	B_{1u}	B_{2u}	E_u
N	3	3	2	4	6	2	6	3	1	9
T_a							1			1
T	1	2	1	2	3	1	3	1		5
R		1			1				1	1
N_i	2		1	2	2	1	2	2		2
I.r. activity							z			(x,y)

the vibrations of the tetrahedral anions is identical to that shown in Table 4.10 for the tetragonal $(NEt_4)_2MCl_4$ complexes, since the site group is the same in both structures. Again, only ν_3 and ν_4 should be observed in the i.r., there being one component of each in the A_{2u} and E_u spectra. Only the spectrum of Cs_3CoCl_5 has previously been examined,[1] and one band observed at 309 cm^{-1}.

For $(NMe_2H_2)_3CuCl_5$, the correlation diagram of Table 4.2 is applicable. No discussion of lattice vibrations in this complex will be undertaken.

Results and Discussion

The frequencies and assignments of the bands observed in the i.r. absorption spectra of powdered samples of some A_3MCl_5 complexes are given in Table 4.13, together with approximate values of ν_1 calculated from the $\nu_1 + \nu_3$ combination bands. The spectra are very similar to those of the corresponding A_2MCl_4 complexes, and show little evidence for the predicted crystal splitting of the T_d modes, except in the copper complexes. The structure of Cs_3CuCl_5 is not known, but in view of the similarity of the spectrum to that of Cs_2CuCl_4, it is reasonable to assume that it contains distorted $CuCl_4^{2-}$ tetrahedra. It also seems likely that Cs_3ZnCl_5 is isostructural with the cobalt complex.

The blue compound Cs_3NiCl_5 decomposes below 417°C to give CsCl and red $CsNiCl_3$,[23] in which the nickel is octahedrally coordinated. Even in quenched samples, this decomposition was found to proceed fairly rapidly, so that the lower frequency bands of the pentachloro- were obscured by the absorptions of the decomposition products. As a result, only one band at 304 cm^{-1} could be attributed with certainty to Cs_3NiCl_5, since no band occurs above 290 cm^{-1} in the i.r. spectra

Table 4.13: I.r. absorption frequencies (cm^{-1}) of A_3MCl_5 complexes.

	Lattice	ν_4	ν_3	ν_1 [a]
Cs_3FeCl_5	83	124	300	312
Cs_3CoCl_5	82	128, 134[b]	312	306
Rb_3CoCl_5	93	137	315	300
Cs_3NiCl_5			304	
Cs_3CuCl_5	60, 71	120, 132	271, 288	225
Cs_3ZnCl_5	74, 85	132, 143	295	288
$(NMe_2H_2)_3CuCl_5$	-	115, 184	242, 304	-

[a] calculated from the combination band $\nu_1 + \nu_3$

[b] one of these bands is due predominately to ν_4, the other to a lattice mode (see text)

of $CsNiCl_3$ or CsCl.

The polarised i.r. spectra of single crystals of Cs_3CoCl_5 and Cs_3CoBr_5 were recorded with the incident radiation polarised parallel and perpendicular to the e axis, giving modes of A_{2u} and E_u symmetry respectively. The spectra of the chloride are shown in Fig. 4.3, while the frequencies and assignments for both are given in Table 4.14. The interpretation of these spectra is straightforward apart from the occurrence of two E_u bands in the M-X bending region, which requires comment. Only one E_u component of ν_4 is expected in this region, so that the extra band is undoubtedly due to a lattice mode of unusually high frequency. Consideration of the structure of these complexes suggests a reason for this behaviour. Since the lattice is composed of alternate (001) layers of composition Cs_2Cl and $Cs(CoX_4)$, it is

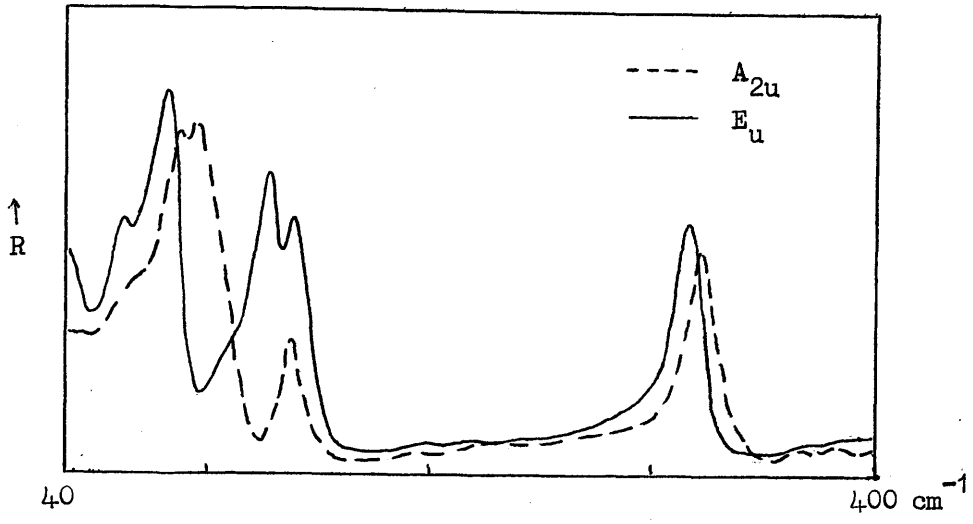

Figure 4.3: I.r. reflectance spectra of Cs_3CoCl_5 crystals.

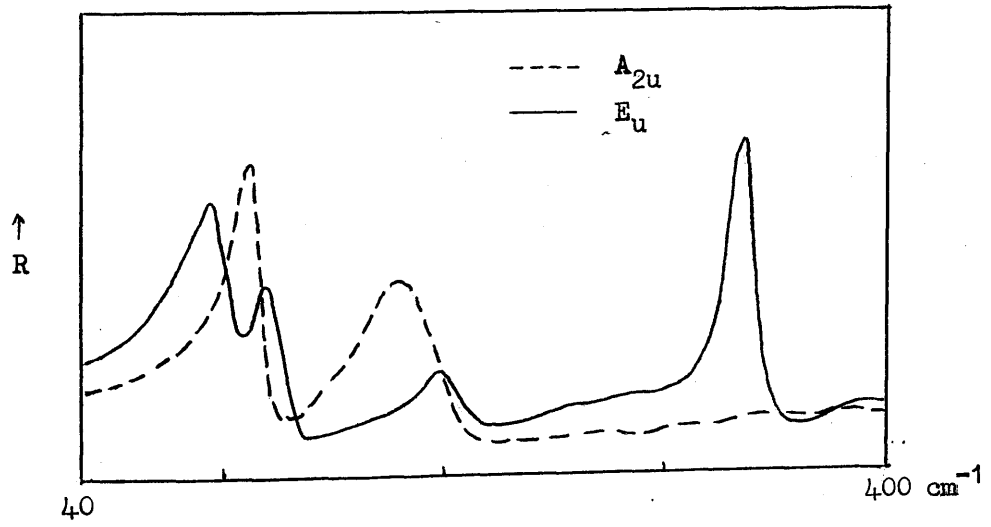

Figure 4.4: I.r. reflectance spectra of K_2PtCl_4 crystals.

Table 4.14: I.r. reflectance bands (cm^{-1}) of Cs_3CoX_5 single crystals.

Cs_3CoCl_5	Cs_3CoBr_5	Symmetry	T_d mode
317	247	A_{2u}	ν_3
312	239	E_u	
133	109	A_{2u}	ν_4
135	108	E_u	ν_4 +
124	104	E_u	lattice mode
89	68	A_{2u}	lattice
83		A_{2u}	modes
79	63	E_u	
59		E_u	

possible to envisage a lattice mode involving displacements normal to the c axis of atoms in the Cs_2Cl layers only. It is plausible that coupling of vibrations involving coplanar displacements of the CoX_4^{2-} ions with such a mode would be smaller than in the case of the A_{2u} modes in which displacements are normal to the layers. Thus one E_u mode might be expected in which anionic motion was confined almost entirely to the free halide ions, resulting in a higher frequency than when the more massive CoX_4^{2-} ions are involved. This effect of free halide ions on lattice mode frequencies has already been encountered in the $AHgX_3$ complexes discussed in Chapter 3.4.

Because of the similarity in frequency, appreciable mixing is likely between this lattice mode and the E_u component of ν_4 of the CoX_4^{2-} ion. Indeed, frequency shifts on going from the chloride to the bromide, and on lowering the temperature, when similar changes

are induced in both bands, reveal no difference in character between the two bands. It must be assumed that both are hybrid internal-lattice modes, so that there is no justification for assignment to one or other of the modes involved.

4.6: Influence of Crystal Field Effects and Distortion on the Vibrations of the MCl_4^{2-} Ions

The results of the foregoing sections now permit some discussion of the mechanisms governing splitting of the crystal modes. This discussion follows two main lines. The first of these is of general interest and relates to the behaviour of vibrations of isolated polyatomic groups in the solid state, while the second is of particular interest in systems containing tetrahedral species, and concerns the effects of distortion on the vibrations of the tetrahedra. This distinction is to some extent arbitrary, since all distortions are due at least partly to crystal packing forces.

One type of crystal field effect, that of correlation coupling in the caesium and tetramethylammonium tetrachlorometallates, has already been analysed in Section 4.2. Before proceeding to a discussion of static field effects, it is necessary to obtain frequencies for the site group modes corresponding to the sets of correlation multiplets. If the small effect of coupling between translationally equivalent ions is neglected, these may be calculated with reasonable accuracy from the weighted mean of the frequencies of their correlation components. However, in all cases except Cs_2ZnCl_4, detailed Raman data are lacking, so that these calculations must be based on the i.r. frequencies alone. That this procedure does not give rise to major discrepancies can be seen from the data for Cs_2ZnCl_4 in Table 4.6, where ignoring the Raman frequencies leads

to differences of less than 3 cm^{-1} from the values calculated from i.r. and Raman frequencies together.

Table 4.15 shows the shifts in the stretching frequency from those of the free ion in solution, and the removal of degeneracy due to the static crystal field in a number of systems. In general, there is an increase in frequency on going from solution to the solid state, this shift being greater for the smaller cations, as in the case of the copper complexes (where the ν_3 frequency of the undistorted ion would be the mean of the distorted ion vibrational frequencies, taking any possible degeneracies into account). These trends are not universally applicable, as can be seen from the tetra-alkylammonium tetrachlorozincates, which have lower stretching frequencies than the ion in solution.

Although such large splittings as are observed for the ν_3 mode of the copper complexes cannot be explained solely on the basis of the static field (unless this is interpreted loosely enough), it is possible at this stage to examine the spectra with a view to determining the principle coupling mechanism giving rise to solid state splitting. Since almost complete data are available for Cs_2ZnCl_4, this is obviously the most fruitful example to consider. The point of interest lies in a comparison of the splitting of the weakly and strongly dipole active modes, which should reveal the relative importance of dipolar and short range interactions.[28] Crystal modes derived from ν_1 and ν_2 of the tetrahedral anion would be expected to be only weakly i.r. active, and this is confirmed by the observed intensities. (A more accurate measure of strength would be given by the band widths, but a dispersion analysis would be required to determine these.) The most useful sets of crystal modes for comparison would seem to be those derived from ν_2 and ν_4, but

Table 4.15: Comparison of frequencies (cm^{-1}) of 'free ion' modes in solution and site-group modes[a] in the solid state.

M		MCl_4^{2-} (solution)	$(NEt_4)_2MCl_4$	$(NMe_4)_2MCl_4$	Cs_2MCl_4	Cs_3MCl_5
Co	ν_3	296[b]	304	313	316[f]	317
			299	301	314[f]	312
				300		
Cu	ν_3	278[b]	269[f]	298	296	288[f]
				290	285	
	ν_1	274[c]	277[c]	281	297[g]	-
	ν_3'	237[b]	248[f]	239	256	271[f]
Zn	ν_3	306[d]	277[e]	293	300	295[f]
				280	296	
				279	286	
	ν_1	275[d]	276[c]	272	288	-

[a] calculated from mean of correlation components; [b] ref. 15; [c] ref. 6; [d] ref. 27; [e] ref. 2; [f] from transmission or incomplete single-crystal data; [g] ref. 4.

it must be recognised that differences in the original degeneracies of these fundamentals, together with the distortion of the anion would make a direct comparison misleading. In anticipation of the conclusions of the discussion on the effects of distortion of the tetrahedral symmetry of the anion, it will be assumed that the components of the A'' and lower A' site group modes of ν_4 (i.e. excluding those above 140 cm^{-1}) are comparable to those of ν_2. Despite the fact that the correlation splitting of the A' (F_2) site group mode is the largest observed in this work, a comparison of the splitting of the ν_2 (E) and ν_4 (F_2) modes suggests that although it is larger for the strongly dipole active modes, the difference is not great enough for such splitting to be due to dipolar coupling alone, but that short range or steric interactions must play an appreciable part in the coupling mechanism.

In Section 4.2 it was established that for $(NMe_4)_2CuCl_4$ and Cs_2CuCl_4, in which the anions are subject to a large tetragonal flattening, the D_{2d} modes derived from ν_3 occur in the order E>B_2, while for ν_4 the order is reversed. The only assumption necessary was that the B_2 - E separation is greater than the site group splitting of the E component (for $(NMe_4)_2CuCl_4$ these are respectively 55 cm^{-1} and 8 cm^{-1}). These assignments are not in agreement with those of Beattie et al,[4] who propose the reverse order for both ν_3 and ν_4 in Cs_2CuCl_4 from Raman data. The adoption of alternative assignments of the crystal modes in the bending region in terms of the D_{2d} modes readily brings these into line with the i.r. data. In the stretching region, an extremely weak band at 253 cm^{-1} assigned to B_{1g} and B_{3g} components of E(ν_3) must be regarded as spurious, since the corresponding B_{2u} correlation component occurs at 296 cm^{-1} in the i.r. spectrum.

It should in principle be possible to determine the magnitude

of the B_2 - E splittings for the other orthorhombic A_2MCl_4 complexes in a similar manner, but in all except the copper complexes the small rhombic distortion superimposed on the tetragonal flattening of the tetrahedral anions becomes significant, so that the effective as well as formal site symmetry is C_s. This causes further site group splitting of the $E(D_{2d})$ modes to be of the same magnitude as B_2 - E splitting, and these two effects cannot be readily distinguished in all cases due to the ambiguity in the assignment of $A'(C_s)$ modes to either B_2 or E distorted ion modes. To avoid any arbitrary attempts at assignment, the $A'(F_2)$ - $A'(F_2)$ separation will be taken as a measure of the splitting accompanying the irregular distortion of the MCl_4^{2-} ions.

For the tetragonal Cs_3MCl_5 and $(NEt_4)_2MCl_4$ complexes, no such difficulties arise, since the site symmetry is the same as that of the tetragonally elongated ions, viz. D_{2d}. In these cases, since only one crystal mode corresponding to each of the B_2 and E site group modes is observed, it must be assumed that the A_{2u} - E_u crystal mode splitting offers a reasonable indication of the B_2 - E static field splitting, bearing in mind the small errors likely to attend this approximation.

Table 4.16 sets out the variation in the splitting of the asymmetric mode ν_3 with the degree of distortion of the MCl_4^{2-} tetrahedra in various complexes. The distortions are measured as the difference between the tetrahedral angle and the Cl-M-Cl angle bisected by the S_4 axis of D_{2d} (positive signs indicate flattening, and negative signs elongation of the tetrahedra). It can be seen from those cases which permit definite assignment of the B_2 and E modes that progressive flattening of the tetrahedra produces increasing splitting, the order in this case placing the E component above B_2, while for the elongated

Table 4.16: Tetragonal distortion of the MCl_4^{2-} ions in various complexes, and the observed splitting of ν_3.

	Distortion[a] (degrees)	Splitting of ν_3 (cm^{-1})
$(NMe_2H_2)_3CuCl_5$	26[b]	62
$(NMe_4)_2CuCl_4$	20[c]	55
Cs_2CuCl_4	15[c]	35
$(NMe_4)_2CoCl_4$	3.3[d]	13
$(NMe_4)_2ZnCl_4$	2.6[d]	13
$(NEt_4)_2NiCl_4$	-2.6[e]	2
$(NEt_4)_2CoCl_4$	-3.5[e]	5
Cs_3CoCl_5	-3.5[f]	5

[a] see text
[b] ref. 26
[c] ref. 9
[d] ref. 14
[e] ref. 18
[f] ref. 22

tetrahedra this order is reversed. $(NEt_4)_2NiCl_4$ is an apparent exception to this rule, but the splitting is small (2 cm^{-1}) and about the same as the anticipated errors in estimating the site group frequencies.

These findings are entirely in accord with the recently published theoretical calculations of Harvey and McQuaker on the spectra of distorted BH_4^- and NH_4^+ ions.[29] They also find that the order of splitting of the ν_4 bands is opposite to that of the stretching modes, as has been shown above in the case of $(NMe_4)_2CuCl_4$ and Cs_2CuCl_4. In the other MCl_4^{2-} systems, variations in the

splitting of ν_4 tend to be obscured by possible mixing with lattice modes.

Now that the magnitude of the variation in ν_3 splitting of MCl_4^{2-} ions, with angular distortion is established, it is interesting to re-examine the spectra of some of the $CuCl_4^{2-}$ species in Table 4.15 to see what light is shed on their shape. The $CuCl_4^{2-}$ ion itself exhibits a splitting of 41 cm^{-1} in solution, which would result from a distortion slightly greater than that of the ion in Cs_2CuCl_4. In $(NEt_4)_2CuCl_4$ and Cs_3CuCl_5, powder spectra reveal smaller splittings of approximately 21 and 17 cm^{-1} respectively. Since in other crystals of these series the anions are tetragonally elongated, the size of the splittings may indicate either competition of the inherent Jahn-Teller flattening with the crystal packing forces, leading to a smaller flattening than is found in other copper complexes, or alternatively, but less likely, the $CuCl_4^{2-}$ ions may adopt an elongated Jahn-Teller distortion.

4.7: Square-planar MCl_4^{2-} complexes: K_2PtCl_4 and K_2PdCl_4

The structures of these complexes make them particularly suitable for studying the vibrations of square-planar groups. They crystallise in the tetragonal space group $P4/mmm$ (D_{4h}) $(Z = 1)$ with the square-planar anions lying in the plane normal to the unique axis.[30] The i.r. active internal and lattice modes predicted by the previously published factor group analysis[31] are given by representations 4.1 and 4.2 respectively. Because of the simplicity

$$\Gamma = A_{2u} + 2E_u \qquad 4.1$$

$$\Gamma = A_{2u} + 2E_u \qquad 4.2$$

of the structure, the A_{2u} modes of the anion can be attributed to the out-of-plane M-Cl bend, and the E_u modes to the asymmetric stretch and in-plane bend.

The complete vibrational spectrum of K_2PtCl_4 has recently been elucidated by Adams and Newton,[31] using single-crystal transmission techniques in the case of the i.r. spectra. The present work, therefore, serves mainly to illustrate the usefulness of the experimentally more convenient reflectance technique in such cases.

Results and Discussion

The polarised reflectance spectra of K_2PtCl_4 crystals are shown in Fig. 4.4, and the frequencies and assignments for both K_2PtCl_4 and K_2PdCl_4 are given in Table 4.17, together with the relevant results of Adams and Newton for K_2PtCl_4. The reflectance spectra show none of the complications present in the form of fine structure and combination bands in the transmission spectra. It is also gratifying that the frequencies obtained by these two methods are in such good agreement. Since the vibrations of K_2PtCl_4 are likely to be of similar character to those observed in the spectra of complexes discussed previously in this chapter, this supports the idea that these spectra are not severely affected by dispersion.

It is interesting to speculate on the relationships connecting the T_d, D_{2d} and D_{4h} modes of the MCl_4^{2-} ion, since at the limit of tetragonal flattening, the D_{2d} ion would adopt a square-planar configuration. The behaviour of the B_2 modes of D_{2d} is of particular interest. These appear to converge as the tetrahedron is flattened, but in compliance with the non-crossing rule, a point of minimum B_2-B_2 separation must be reached at an intermediate configuration, after which the stretching and bending components move apart, to become eventually the B_{2g} stretching mode and the out-of plane A_{2u} bend respectively of the D_{4h} ion.

The explanation for this behaviour is not clear, although it

Table 4.17: I.r. reflectance bands (cm^{-1}) of oriented K_2PtCl_4 and K_2PdCl_4 crystals.

K_2PtCl_4 [a]	K_2PtCl_4	K_2PdCl_4	Symmetry	Description
323	328	328	E_u	ν(M-Cl)
194	194	193	E_u	δ(M-Cl)
170	172	172	A_{2u}	π(M-Cl)
112	116	117	E_u	lattice modes
98	105	105	A_{2u}	
87	91	92	E_u	

[a] single-crystal transmission frequencies from ref. 31

almost certainly involves mixing of the bond-oriented stretching and bending displacement coordinates in the D_{2d} ions. Reference to the symmetry coordinates of the T_d or D_{2d} configurations[32] shows that such mixing could be expected to lead to a decrease in the transition moment of the $\nu_3(B_2)$ vibration, which is in fact indicated by a lowering of the intensity of this mode relative to the $\nu_3(E)$ modes in the distorted $CuCl_4^{2-}$ ion.

4.8: Experimental

All alkali metal complexes except Cs_2ZnCl_4, Cs_2CuCl_4, Cs_3CoCl_5 and the platinum and palladium complexes were prepared by fusion of stoicheiometric amounts of the appropriate alkali metal chloride and anlydrous transition metal dichloride in an evacuated silica tube. Attempts to grow a large single crystal of Cs_2CoCl_4 from the melt by the Stockbarger technique resulted in the formation of a polycrystalline boule. Various sections of this boule were ground and polished, and

the polarised reflectance spectra recorded.

Crystals of Cs_2ZnCl_4, Cs_2CuCl_4 and the $(NMe_4)_2MCl_4$ complexes were grown by slow evaporation of saturated aqueous solutions containing the appropriate molar ratio of the constituent chlorides. Cs_2ZnCl_4 grew as large crystals with well developed (001) and smaller (100) faces (indexed according to space group Pnma, after transposition of the axes of Pnam given by Brehler[11]), while $(NMe_4)_2ZnCl_4$ took a variety of forms, generally with well-formed (100) and (010) faces. Crystals of $(NMe_4)_2CoCl_4$ grew as prisms bounded by (001), (011) and (010), and capped by (101) and (111). Both copper complexes grew as rods, of the form (011) terminated by (100) in the case of $(NMe_4)_2CuCl_4$, and (101) for Cs_2CuCl_4, which had no well defined terminating faces.

The $(NEt_4)_2MCl_4$ complexes were prepared by evaporation of nitromethane solutions. Crystals grew as distorted octahedra, all faces being of the form (101). In these cases, (100) faces were prepared artificially by grinding.

Crystals of Cs_3CoCl_5 were obtained from aqueous solution of the constituent chlorides by the method of Powell and Wells,[21] using a sixfold molar excess of CsCl. These grew as fairly regular rectangular prisms bounded by (110) and (001) faces. The axes were identified by the angles made by small (111) faces which occurred in some of the crystals, and verified by the birefringence of the various faces. For the unstable complex Cs_3NiCl_5, stoicheiometric amounts of CsCl and $NiCl_2$ were fused in a silica tube and then quenched rapidly. The i.r. spectrum of the complex was recorded immediately after quenching. $(NMe_2H_2)CuCl_5$ was prepared by the method of Shagisutanova et al.[33]

Recrystallisation of K_2PtCl_4 and K_2PdCl_4 gave long rods elongated along the c axis.

References

1 R.J.H. Clark and T.M. Dunn, J. Chem. Soc., 1963, 1198.

2 A. Sabatini and L. Sacconi, J. Amer. Chem. Soc., 1964, 86, 17.

3 D.M. Adams and P.J. Lock, J. Chem. Soc. (A), 1967, 620.

4 I.R. Beattie, T.R. Gilson and G.A. Ozin, J. Chem. Soc. (A), 1969, 534.

5 G.L. Cessac, R.K. Khanna, E.R. Lippincott and A.R. Bandy, Spectrochim. Acta, 1972, 28A, 917.

6 J.S. Avery, C.D. Burbridge and D.M. Goodgame, Spectrochim. Acta, 1968, 24A, 1721.

7 H.G.M. Edwards, L.A. Woodward, M.J. Gall and M.J. Ware, Spectrochim Acta, 1970, 26A, 287.

8 C.O. Quicksall and T.G. Spiro, Inorg. Chem., 1966, 5, 2232.

9 B. Morosin and E.C. Lingafelter, J. Phys. Chem., 1961, 65, 50.

10 L. Helmholz and R.F. Kruh, J. Amer. Chem. Soc., 1952, 74, 1176.

11 B. Brehler, Z. Krist., 1957, 109, 68.

12 M.A. Porai-Koshits, Kristallografiya, 1956, 1, 291.

13 H.J. Seifert, Z. anorg. Chem., 1961, 307, 137; H.J. Seifert and K. Klatyk, ibid., 1964, 334, 113.

14 J.R. Wiesner, R.C. Srivastava, C.H.L. Kennard, M. Di Vaira and E.C. Lingafelter, Acta Cryst., 1967, 23, 565.

15 D. Forster, Chem. Comm., 1967, 113.

16 D.M. Adams, J. Chatt, J.M. Davidson and J. Gerratt, J. Chem. Soc., 1963, 2189.

17 A. Mooney, R.H. Nuttall and W.E. Smith, J.C.S. Dalton, 1972, 1096.

18 G.D. Stucky, J.B. Folkers and T.J. Kistenmacher, Acta Cryst., 1967, 23, 1064.

19 E. Whalley and J.E. Bertie, J. Chem. Phys., 1967, 46, 1264.

20 T.P. Melia and R. Merrifield, J. Chem. Soc. (A), 1971, 1258.

21 H.M. Powell and A.F. Wells, J. Chem. Soc., 1935, 369.

22 B.N. Figgis, M. Gerloch and R. Mason, Acta Cryst., 1964, 17, 506.

23 E. Iberson, R. Gut and D.M. Gruen, J. Phys. Chem., 1962, 66, 65.

24 A. Engberg and H. Soling, Acta Chem. Scand., 1967, 21, 168.

25 R.P. van Stapele, H.G. Beljers, P.F. Bongers and H. Zijlstra, J. Chem. Phys., 1966, 44, 3719.

26 R.D. Willett and M.L. Larsen, Inorg. Chim. Acta, 1971, 5, 175.

27 D.F.C. Morris, E.L. Short and D.N. Waters, J. Inorg. Nuclear Chem., 1963, 25, 975.

28 J.C. Decius, J. Chem. Phys., 1955, 23, 1290; D.A. Dows, ibid., 1960, 32, 1342.

29 K.B. Harvey and N.R. McQuaker, J. Chem. Phys., 1971, 55, 4396.

30 R.G. Dickinson, J. Amer. Chem. Soc., 1922, 44, 2404.

31 D.M. Adams and D.C. Newton, J. Chem. Soc. (A), 1969, 2998.

32 G. Herzberg, "Infra-red and Raman Spectra of Polyatomic Molecules", D. Van Nostrand, New York, 1945, p. 100.

33 G.A. Shagisultanova, L.A. Il'yukevich and L.I. Burdyko, Russ. J. Inorg. Chem., 1965, 10, 229.

Chapter 5: Aquochlorometallates

5.1: Introduction

Water molecules present in crystalline inorganic complexes can be classified as either "free" water, held in position in the lattice by hydrogen bonding, or coordinated water, in which the oxygen forms an M-O bond. All of the examples dealt with in this chapter fall into the latter category.

Although the vibrations of the coordinated water molecules, especially the librational modes, are of considerable interest in themselves,[1,2] these will be ignored in the present work, since their study in the i.r. presents certain practical difficulties. Indeed, the water molecules will be treated as monatomic ligands, and attention concentrated on the M-O and M-Cl vibrations. In this manner, the vibrational spectra of a number of interesting chlorometallate moieties may be investigated, such as the distorted octahedral $CuCl_4(H_2O)_2^{2-}$ ion, with long and short Cu-Cl bonds, and $FeCl_5(H_2O)^{2-}$, in which the chlorines adopt a square-pyramidal arrangement about the iron atom. The aquochloromanganates also provide a variety of interesting structures, which have been more widely investigated than those of the other transition metals. Three examples of these will be discussed in Section 5.4.

5.2: $A_2CuCl_4.2H_2O$ Complexes (A = NH_4, K, Rb)

In a large number of copper (II) halide complexes, the preferred tetragonal environment of the copper ion takes the form of a distorted octahedron made up of four halide ions and two liganded species. In general, two of the halides form short bonds to the copper, while the remaining pair are at much greater distnaces from it. In chloride

complexes, 'short' and 'long' bonds are formed with Cu-Cl distances of about 2.3 Å and 3 Å respectively.[3] This has led to speculation and some confusion regarding the frequencies of the vibrations involving the long Cu-X bonds.[4-7] Interest has centred mainly on complexes of the type CuX_2L_2 (L = nitrogen donor ligand, H_2O; X = Cl, Br) many of which achieve pseudo-octahedral coordination of the copper by halogen bridging (where the steric requirements of the ligand permit). In the i.r. spectra of most of the chloride complexes, two bands are observed in the region 200-350 cm^{-1}. The higher of these is undoubtedly the short Cu-Cl stretching mode, but the assignment of the lower band to the long Cu-Cl stretch is open to question.[5,6] Beattie et al,[7] in a discussion of the single crystal Raman spectra of $CuCl_2.2H_2O$, have indicated the difficulties involved in forming any conclusions regarding the vibrational modes of long Cu-X bonds on the basis of their behaviour in halogen-bridged complexes. In such halogen-bridged systems, the vibrations of the long and short bonds are necessarily of mixed character, and this mixing would be expected to have a profound effect on the frequencies of these vibrations.

A detailed spectroscopic study of complexes containing non-bridging halogen atoms is therefore desirable in order that the assignement of 'long' Cu-X vibrations may be clarified. Hydrates of the type $A_2CuCl_4.2H_2O$ (A = NH_4, K, Rb) containing isolated pseudo-octahedral anions, meet this requirement. These complexes, which form an isomorphorous series whose structure has been elucidated in some detail,[8,9] should be particularly suitable for the study of the Cu-Cl vibrations. The presence of isolated $CuCl_4(H_2O)_2^{2-}$ anions removes the complications inherent in bridged systems, and the vibrations of the coordinated water molecules do not interfere

in the region of interest.[6] An additional advantage is that the bond directions of the complex anion are related in a simple manner to the crystal axes. This last point, together with the ease of preparation of crystals of suitable dimensions, facilitates their study by polarised i.r. reflectance techniques.

Complexes of the type $A_2CuCl_4.2H_2O$ crystallise with the tetragonal space group $P4/mnm$ (D_{4h}^{14}) with two molecules in the primitive unit cell.[8,9] The $CuCl_4(H_2O)_2^{2-}$ anions are oriented with the Cu-O bonds parallel to the c axis of the crystal and the Cu-Cl bonds (2.32 and 2.95 Å long in the potassium complex) lying in the ab plane. The results of a factor group analysis of this structure, neglecting the hydrogen atoms, are given in Table 5.1. It should be noted that the long Cu-Cl bonds are regarded as having some covalent character, so that vibrations of these bonds are arbitrarily classified as internal modes of the complex anion. An alternative but less helpful description in terms of free chloride ions would merely alter

Table 5.1: Factor group analysis of the $A_2CuCl_4.2H_2O$ complexes with space group D_{4h}^{14}.

	A_{1g}	A_{2g}	B_{1g}	B_{2g}	E_g	A_{1u}	A_{2u}	B_{1u}	B_{2u}	E_u
N	3	2	3	4	6	1	5	4		10
T_a							1			1
T			1	1	2	1	1	1		3
R		1	1		2					
N_i	3	1	1	3	2		3	3		6
I.r. activity:							z			(x,y)

the designation of these vibrations to that of translatory lattice modes. Of the possible modes listed in Table 5.1, only those of A_{2u} and E_u symmetry are i.r. active, and these interact with radiation whose electric vector is polarised parallel and perpendicular to the c axis respectively. Thus the total number of i.r. active modes (subject to the qualification mentioned earlier) is given by representation 5.1.

$$\Gamma = 4A_{2u} + 9E_u \qquad 5.1$$

Ignoring for the moment the possiblility of mixing between modes of the same symmetry, it can readily be established by correlating the modes of the isolated complex anion with the crystal modes that the four A_{2u} vibrations will consist of a Cu-O stretch, an in-plane bend of the short Cu-Cl bond, a long Cu-Cl bend and a lattice mode. Similarly, the nine E_u vibrations are made up of a long and a short Cu-Cl stretch, in-plane and out-of-plane Cu-O bending modes, an out-of-plane short Cu-Cl bend, a long Cu-Cl bend and three lattice modes. Adams and his coworkers have made a number of studies of the spectra the aquochlorocuprates,[2,6,10] the latest using single-crystal techniques.[10]

Results and Discussion

The polarised i.r. reflectance spectra from 40-400 cm^{-1} of a (100) face of a single crystal of $K_2CuCl_4.2H_2O$ are shown in Fig. 5.1a and b with the incident radiation polarised parallel and perpendicular to the c axis respectively. In Fig. 5.1a three of the predicted four A_{2u} bands can be seen; the fourth band, arising from the ν(Cu-O) mode, occurs[2] at 445 cm^{-1}. Of those observed below 400 cm^{-1}, the in-plane bend of the short Cu-Cl bonds would be expected to have the highest frequency, and the band observed at 178 cm^{-1} is therefore

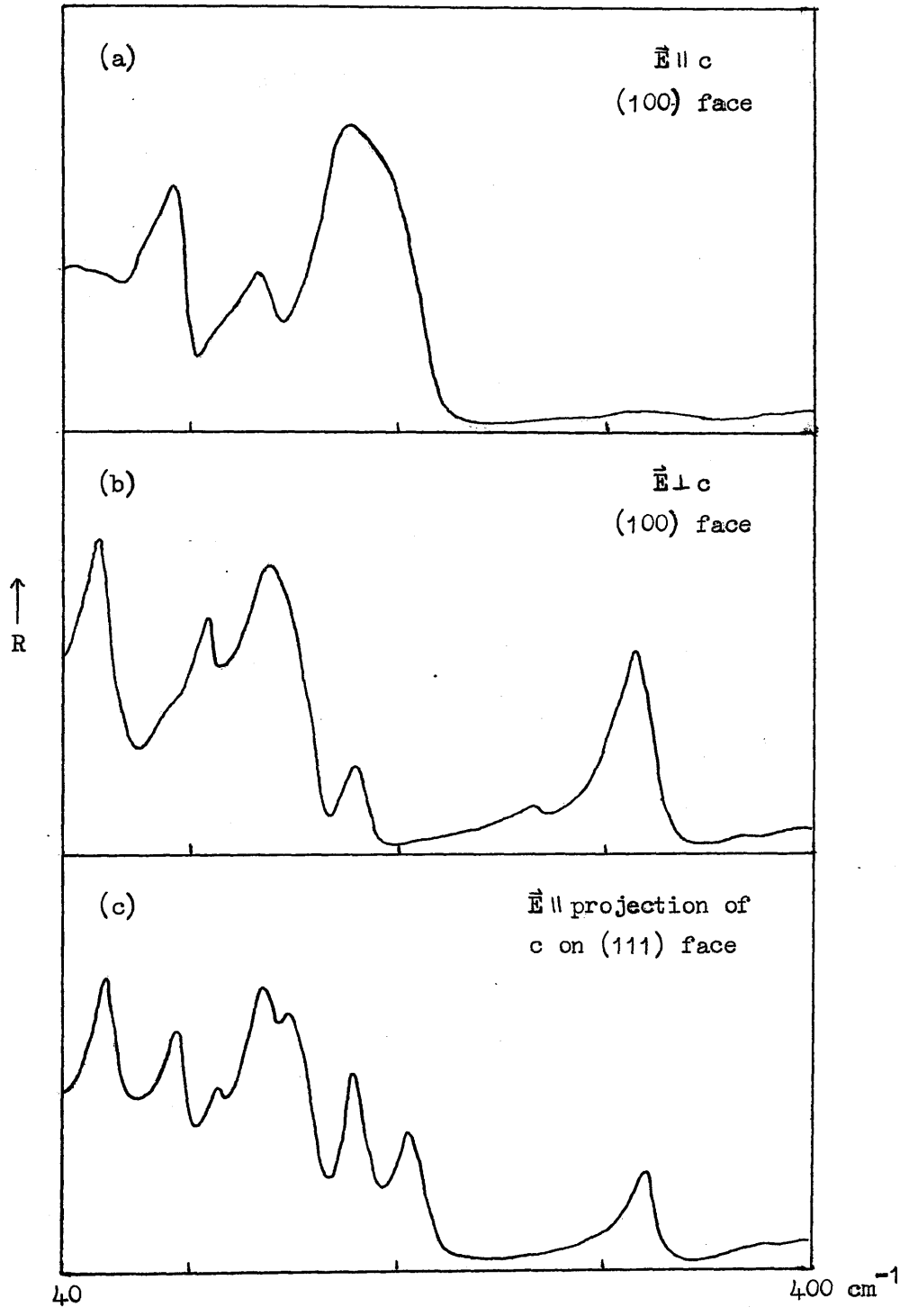

Figure 5.1: Far-i.r. reflectance spectra of $K_2CuCl_4.2H_2O$.

assigned to this vibration. This frequency lies in the range observed for δ(Cu-Cl) in $CuCl_2L_2$ complexes,[4] and is close to the value of 177 cm^{-1} reported for $Cupy_2Cl_2$, although such a comparison is not strictly valid. Nevertheless, the bending mode in $K_2CuCl_4.2H_2O$ would not be expected to be lower in frequency than that for the halogen-bridged $cupy_2Cl_2$ complex. The two lower frequency bands at 96 and 136 cm^{-1} are assigned to the lattice mode and the long Cu-Cl bending mode. The possibility of distinguishing between these will be discussed later.

The assignment of the E_u modes is less straightforward. Only six E_u bands are observed in the polarised reflectance spectra (Fig. 5.1b). The assignments of these bands are given in Table 5.2, and only those of the short Cu-Cl bend and the long Cu-Cl stretching mode require comment. The in-plane short Cu-Cl bend has already been assigned to the A_{2u} band at 178 cm^{-1}, and by analogy with square planar complexes such as K_2PtCl_4, (see Chapter 4.7) the out-of-plane bending mode would be expected to occur at lower frequency. There are two E_u bands in the expected range for δ(Cu-Cl), at 142 and 180 cm^{-1}. The short Cu-Cl bending mode is assigned to the lower of these, since it is unlikely that the in-plane and out-of-plane bending force constants are virtually identical, an assumption which is implicit in the alternative assignment. This then leaves the band at 180 cm^{-1} to be assigned to the long Cu-Cl stretching mode, as the occurrence of a lattice mode at such relatively high frequency is improbable unless vibrations of the long bonds are admitted into this category. The δ(Cu-O) band at 270 cm^{-1} is probably the out-of-plane vibration, the in-plane mode at higher frequency being obscured by the ν(Cu-Cl) band.

Also given in Table 5.2 are the frequencies and assignments of

Table 5.2: Reflectance maxima (cm^{-1}) in the polarised i.r. spectra of (100) faces of $A_2CuCl_4.2H_2O$ crystals.

A = NH_4	K	Rb	Assignment	
	445[a]		A_{2u}	ν(Cu-O)
317	317	322	E_u	ν(Cu-Cl) (short)
264	270	266	E_u	δ(Cu-O)
	180	176	E_u	ν(Cu-Cl) (long)
190	178	175	A_{2u}	δ(Cu-Cl) (short) i.p.
196	142	136	E_u	δ(Cu-Cl) (short) o.p.
145	136	135	A_{2u}	lattice mode or δ(Cu-Cl) (long)
96	112	100	E_u	
	96	83	A_{2u}	lattice modes
62	61	45	E_u	

[a] from ref. 2

the bands observed in the spectra of the isomorphous ammonium and rubidium complexes. The reflectance spectra of $Rb_2CuCl_4.2H_2O$ were closely similar to those of $K_2CuCl_4.2H_2O$ except for small changes in the frequencies due to the increased mass of the cation. Less detail was discernible in the spectra of the ammonium complex, which were characterised by broad bands with maxima at 190 and 196 cm^{-1} in the respective polarisations. The reasons for the difference in the form of these spectra compared with those of the other complexes is not entirely clear, since such marked changes in the internal frequencies cannot be accounted for by the comparatively small mass of the cation. Hydrogen bonding by the ammonium ion, which can produce

similar effects in other isomorphous series, may be involved (see Chapter 6).

The above assignments have been made fairly systematically on the assumption that little mixing of modes of the same symmetry takes place. While this is probably a reasonable approximation for the vibrations of the short Cu-Cl bonds, especially the stretches, it must be reconsidered in the case of those modes involving the long bonds. The possibility of mixing of these vibrations with the close-lying lattice modes and bends of the short Cu-Cl bonds must be recognised, and the question of the validity of the descriptions used for these modes examined. In this context, it is helpful to compare the conclusions of the present work with those of the more recent single-crystal study of the potassium salt by Adams and Newton.[10]

In general, the polarised i.r. data of these workers are in good agreement with those of Table 5.2, although they include an E_u band at 218 cm^{-1} assigned to the out-of-plane Cu-O bend which probably corresponds to the spurious feature in Fig. 5.1c observed by deliberate misalignment of the crystal. They prefer to assign the 180 and 142 cm^{-1} E_u bands to modes of mixed character, involving stretching of the long Cu-Cl bonds and bends of both long and short bonds. The most interesting features of the Raman spectra are the symmetric stretches of the short and long Cu-Cl bonds at 228 and 131 cm^{-1} respectively.

There is no definite evidence in these results for strong coupling of the stretching vibrations of the long Cu-Cl bonds with the bends or with vibrations of the potassium ions. Some cation dependence of the E_u stretch is evident from the spectrum of the rubidium complex, but this is no greater than for the other internal vibrations. The description of the 180 cm^{-1} band as predominantly an

asymmetric stretch of the long Cu-Cl bonds is therefore justifiable. It would nevertheless be hazardous to extend this qualitative treatment to the long Cu-Cl bending modes and accordingly no attempt is made to distinguish between these and lattice modes. Thus despite the fact that the symmetry coordinates forming the basis for the two lowest A_{2u} modes are known, their approximate normal coordinates cannot be inferred from the spectra.

One point which emerges from the results of the present work is that because of the overlapping ranges for δ(Cu-Cl) (short) and ν(Cu-Cl) (long), the separation of these bands will be difficult in the absence of polarised single crystal spectra. From the long Cu-Cl stretching frequencies reported here, and from what has been said regarding halogen-bridged systems, it seems unlikely that bands observed at about 220 cm^{-1} in the spectra of a number of $CuCl_2L_2$ complexes can properly be described as long Cu-Cl stretching modes as suggested by Campbell et al.[5] The alternative view of Adams and Lock, is to be preferred, viz. that these low frequency "stretching" bands are of obscure origin.[6]

In establishing the stretching frequency of the long Cu-Cl bonds in the aquochlorocuprates, this study has gone some way towards solving the spectroscopic problem posed by various copper complexes.[5-7] However, the underlying question of the mature of the interaction between copper and the long-bonded chlorine atoms remains to be answered, and in this respect, methods of study other than vibrational spectroscopy may prove to be more fruitful.

Fig. 5.1c shows the reflectance spectrum of a (111) face of a $K_2CuCl_4.2H_2O$ crystal when the incident radiation is polarised parallel to the projection of the c axis on the reflecting face. This arrangement would be expected to give both A_{2u} and E_u modes, but inspection

shows that the resulting spectrum is not simply a superposition of Fig. 5.1a and b. Certain of the bands have shifted perceptibly in frequency, e.g. the band at 317 cm^{-1} in Fig. 5.1b has a maximum at 320 cm^{-1} in Fig. 5.1c. A more striking change is the appearance of bands at 207 and 152 cm^{-1} which occur in neither of the original spectra. Similar effects are observable for $Rb_2CuCl_4.2H_2O$. While incorrect structural data or faulty alignment of the crystals might account for these changes, the first explanation is unlikely in view of the detailed work reported for these crystals, and the second could not satisfactorily explain the spectra shown in Fig. 5.1a and b. The anomalies observed are more likely to arise as a result of birefrigence of uniaxial crystals such as those dealt with here, and the dispersion of i.r. radiation by these crystals.

When radiation is incident normally on a (100) face, it will be split into extraordinary (E) and ordinary (O) rays polarised parallel and perpendicular to the c axis respectively. Each ray will have its own value of the refractive index or dielectric constant for any particular frequency, and dispersion of these rays by the crystal will be mutually independent. Fig. 5.1a and b show the A_{2u} and E_u modes of $K_2CuCl_4.2H_2O$ which are active in the E and O rays respectively. However when a (111) face is used, radiation of normal incidence makes an angle of about 55° with the c axis. When this is polarised parallel to the projection of the c axis on the reflecting face, only the E ray will be transmitted through the crystal. This is no longer polarised parallel to the c axis, but at an angle to it, so that it can interact with both A_{2u} and E_u modes of the crystal. Since the velocity of the E ray depends on its direction in the crystal, and will lie between the extreme value for the E ray and that for the O ray, the refractive index and dielectric constant of the crystal will

also have intermediate values in this arrangement. Since these determine the form of the reflectance spectrum,[11] slight changes in the frequencies of some bands might be expected and are in fact observed.

An important consequence of the i.r. activity of both A_{2u} and E_u modes in the E ray is that the dielectric response to this ray will be affected simultaneously by vibrations of both types. The effect of this is to produce a more complicated reflectance spectrum than would be obtained from a combination of the two sets of oscillators acting independently. Numerous cases are known for isotropic crystals of two oscillators of different strengths and similar frequencies giving rise to a confusing reflectance spectrum.[12] Thus features such as the maxima at 180 and 207 cm^{-1} in Fig. 5.1c can readily be accounted for by interaction of the A_{2u} mode at 178 cm^{-1} with the E_u mode at 180 cm^{-1}. This may result in an inversion in the broad A_{2u} band giving a reflectance minimum at 197 cm^{-1} and leaving the "tail" of the A_{2u} band at 207 cm^{-1}; alternatively, the higher frequency maximum may result from a more complicated variation induced in the dielectric response by the two neighbouring oscillators. The same considerations would apply to the features observed in the same region for $Rb_2CuCl_4.2H_2O$, and to the bands at 138 and 152 cm^{-1} in Fig. 5.1c. This shows that in the absence of a dispersion analysis, the interpretation of reflectance spectra must be approached with caution.

5.3: $K_2FeCl_5.H_2O$

Potassium aquopentachloroferrate (III) has the orthorhombic structure Pnma (D_{2h}^{16}),[13] with the four octahedral $FeCl_5(H_2O)^{2-}$ anions in each unit cell oriented so that all Fe-O and axial Fe-Cl bonds lie on mirror planes perpendicular to the b axis. Adams and his coworkers

have investigated the powder i.r.[2] and single-crystal Raman spectra.[14] Because of the complexity of the i.r. spectrum, specific assignments were difficult, but the Raman work permitted the identification of most of the internal modes of the anion. The present work completes the vibrational study of this complex with an examination of the single-crystal i.r. spectra.

The approximate forms of the internal vibrations of the $FeCl_5(H_2O)^{2-}$ ion and their correlation with the crystal modes given by Adams and Newton[14] are reproduced in Table 5.3. The presence of the (010) mirror planes in the crystal has the effect of allowing only B_{1u} and B_{3u} i.r. active factor group components of the A_1 and B_1 free anion

Table 5.3: Approximate forms and correlation of the vibrations of the anions in $K_2FeCl_5.H_2O$.

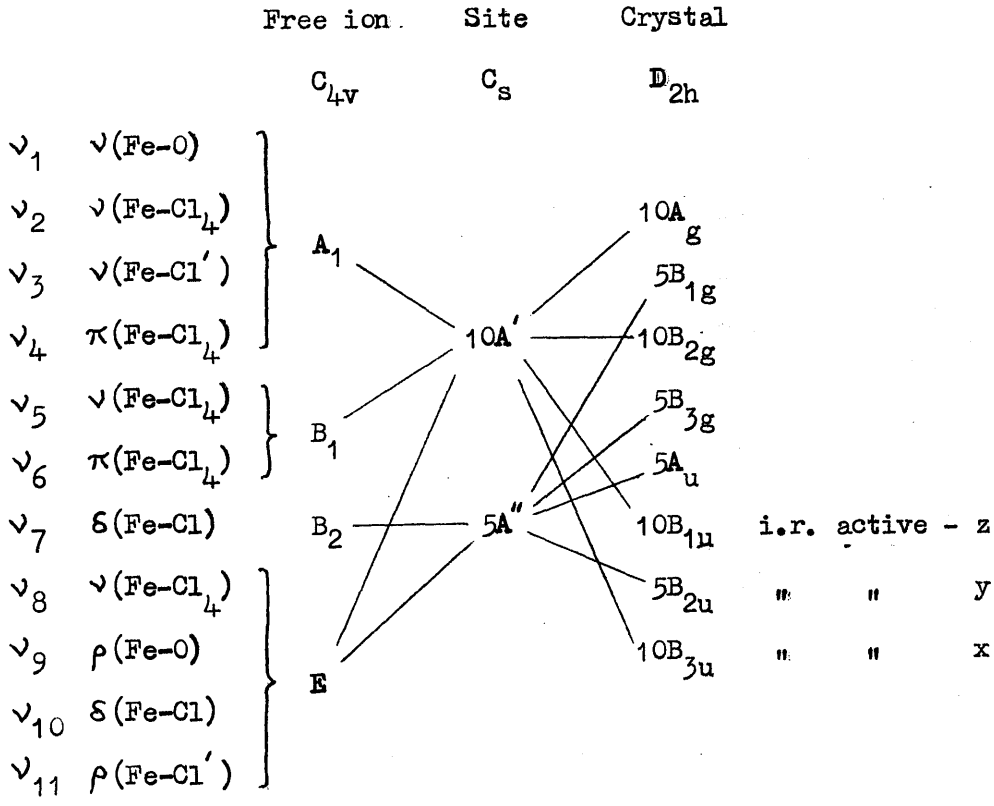

modes, and a B_{2u} component of the B_2 mode, while the E modes of the anion have a component of each symmetry. In addition, a number of i.r. active translatory and rotatory lattice modes are predicted by factor group analysis, and these are given by representations 5.2 and 5.3 respectively.

$$\Gamma_{\text{transl.}} = 4B_{1u} + 3B_{2u} + 4B_{3u} \qquad 5.2$$

$$\Gamma_{\text{rot.}} = B_{1u} + 2B_{2u} + B_{3u} \qquad 5.3$$

Results and Discussion

Table 5.4 lists the frequencies of the bands observed in the polarised reflectance spectra of $K_2FeCl_5.H_2O$, which are shown in Fig. 5.2. The bands below 120 cm^{-1} can be assigned to lattice modes, and those

Table 5.4: Reflectance bands (cm^{-1}) in the single-crystal i.r. spectra of $K_2FeCl_5.2H_2O$.

B_{1u}	B_{2u}	B_{3u}
	(372)[a]	
305	289	306
273	237	278
	196	218
180	176	171
		138
111	101	102
90		93
62	52	

[a] from powder transmission spectrum

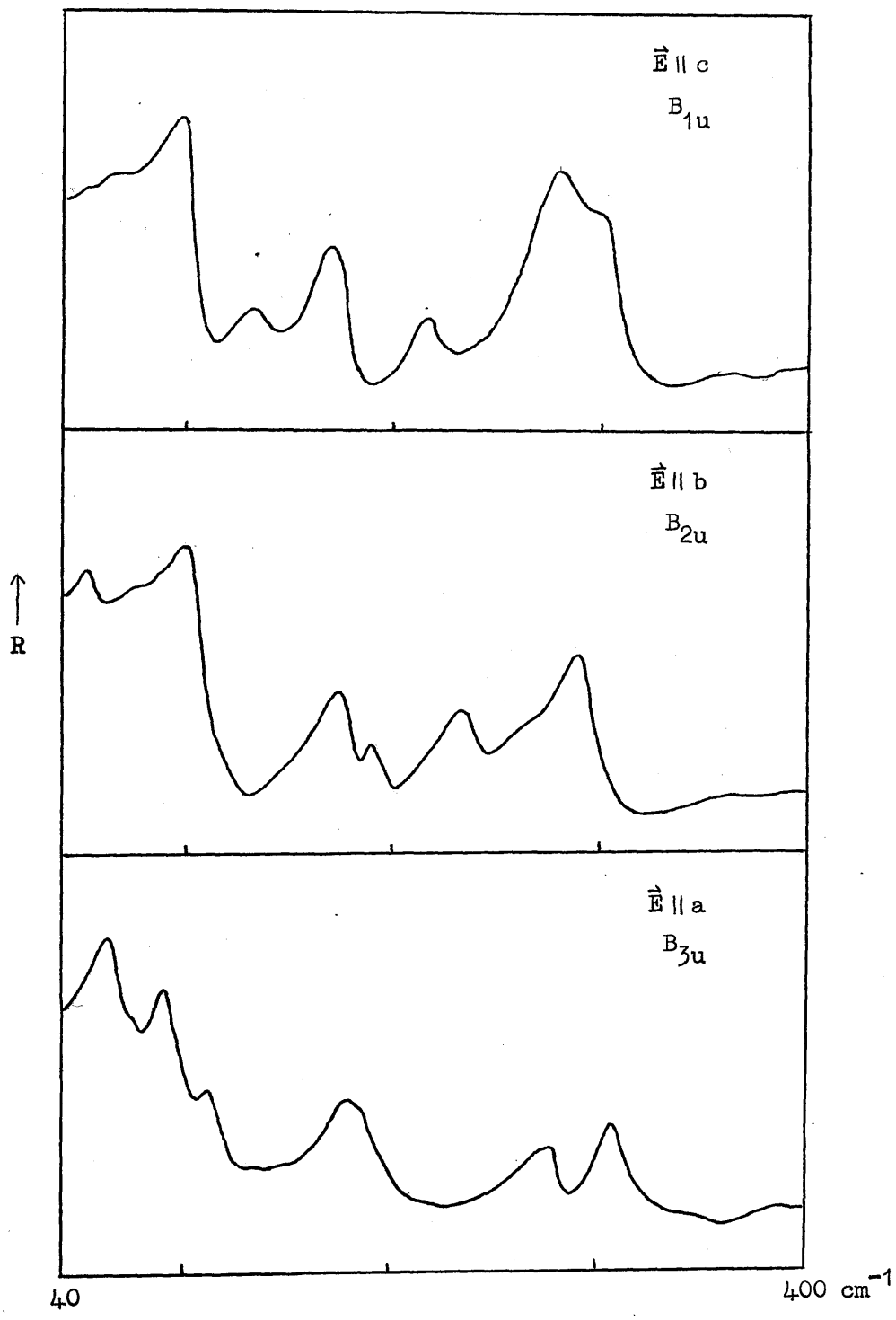

Figure 5.2: Far-i.r. reflectance spectra of $K_2FeCl_5.H_2O$ crystals.

above this frequency to predominantly internal vibrations of the anions.

Of the internal modes, the band at 372 cm^{-1} in the powder spectrum is clearly the stretch of the Fe-O bond, and the group around 300 cm^{-1} falls in the expected range for the ν(Fe-Cl) vibrations. The B_{2u} band at 289 cm^{-1} can be assigned unambiguously to the asymmetric $Fe-Cl_4$ stretch (ν_8). In the B_{1u} and B_{2u} spectra, two correlation doublets at 273/278 cm^{-1} and 303/307 cm^{-1} are observed. All four ν(Fe-Cl) modes are formally i.r. active in both of these orientations, but the axial and asymmetric equatorial stretching vibrations (ν_3 and ν_8) would be expected to have the greater intensities. By analogy with the isostructural indium complex,[14] the higher of the observed pairs is assigned to ν_3, and the lower to ν_8. However, the separation of the $A'(B_{1u} + B_{3u})$ and $A''(B_{2u})$ components of ν_8 may indicate appreciable mixing of the A' site group modes of each of the four Fe-Cl stretching vibrations, rather than true static field splitting resulting from a distortion from C_{4v} symmetry of the anion.

In the lower frequency region, the strong bands at 180, 176 and 171 cm^{-1} can be assigned to the $Fe-Cl_4$ bending mode, ν_{10}, and a B_{1u} component of the axial Fe-Cl wag (ν_{11}) is observed at 138 cm^{-1}. Deuteration studies [14] have shown the Raman bands at 222 cm^{-1} to be due to the wagging vibration of the Fe-O bond (ν_9), and the B_{2u} band at 237 cm^{-1} is accordingly assigned to this mode. This leaves a weak B_{2u} band at 196 cm^{-1}, which must be a component of the B_2 $Fe-Cl_4$ bend (ν_7) and a B_{3u} band at 218 cm^{-1}, which could be derived from either ν_4, ν_6 or ν_9. The former assignment is preferred, since the B_1 (ν_6) mode would be only weakly dipole active, and it would be difficult to explain a site group splitting of 19 cm^{-1} with the B_{2u} component of ν_9.

These assignments are summarised in Table 5.5, which also includes the Raman frequencies of Adams and Newton. Some minor changes in their assignments of the site group modes improve the consistency with the i.r. data. Thus since a B_{2u} component of $\nu_4(A')$ is found at 218 cm^{-1}, the assignment of the $\nu_4(A')$ and $\nu_6(A')$ Raman lines at 190 and 226 cm^{-1} is reversed, placing ν_6 above ν_4, contrary to what is observed for $Cs_2InCl_5.H_2O$. Similarly, interchanging the $\nu_7(A'')$ and $\nu_{10}(A'')$ modes produces a slightly better fit with the i.r. frequencies. Neither of these changes fundamentally affects the interpretation of the Raman spectra.

Even after these adjustments have been made, however, the fit of the Raman and i.r. frequencies can only be described as reasonable. Although the general pattern appears to be the same for both, a number of the g-u splittings are disturbingly large. It is reassuring in this respect to note that in one case at least, that of the $\nu_{10}(A')$ multiplet, the B_{3u} band, which is one of the stronger bands in the i.r. spectrum, lies well below the Raman component. It is therefore unlikely that the anomalies are caused by a general raising of the i.r. frequencies due to dispersion effects.

The complete vibrational spectrum of $K_2FeCl_5.H_2O$, in contrast to either of the sets of data on their own, would indicate that coupling of the vibrations of the four anions in each unit cell is very strong. No satisfactory explanation for this behaviour suggests itself. However, despite their fragmentary nature (only thirteen of the predicted twenty-five internal modes were observed), the i.r. spectra confirm the conclusion of Adams and Newton, that the forces acting in the crystal are such as to produce almost complete factor group splitting of the crystal modes.

Table 5.5: Vibrational assignments for $K_2FeCl_5.H_2O$.

Free anion mode	Site group mode	Crystal modes[a] correlating with A′(A″) $A_g(B_{1g})$	$B_{2g}(B_{3g})$	$B_{1u}(A_u)$[b]	$B_{3u}(B_{2u})$
ν_1	A′	384		(372)[c]	
ν_3	A′			303	306
ν_2	A′	300,			
ν_5	A′	276			
ν_8	A′			273	278
	A″	276			289
ν_9	A′				
	A″	222	222		237
ν_4	A′	226[d]	226[d]		218
ν_6	A′	190[d]			
ν_7	A″		180[e]		196
ν_{10}	A′	183		180	171
	A″	177[e]	174[e]		176
ν_{11}	A′	124			138
	A″	129	132		

[a] Raman frequencies from ref. 14

[b] inactive

[c] from i.r. powder spectrum (B_{1u} or B_{3u})

[d,e] assignments of ref. 13 interchanged

5.4: Aquochloromanganates

$A_2MnCl_4.2H_2O$ (A = Rb, Cs): These two complexes are isostructural,[15] with monomolecular triclinic unit cells of space group $P\bar{1}(C_i^1)$ containing approximately octahedral trans-$MnCl_4(H_2O)_2^{2-}$ anions on C_i sites. The two sets of Mn-Cl bonds are not equivalent, having lengths of 2.54 and 2.58Å in the rubidium complex, although no difference is detected in the caesium salt. Despite the low symmetry, the i.r. spectra of these systems should be fairly simple, containing a ν(Mn-O) mode and two δ(Mn-O), ν(Mn-Cl), δ(Mn-Cl) and π(Mn-Cl) modes, together with three translatory lattice modes, all of which are of A_u symmetry. Adams and Lock[2] have observed most of these in the powder i.r. spectra.

Results: Since all the i.r. active bands are of the same symmetry, the spectra were recorded by aligning the polarised radiation with three convenient orthogonal axes, in this case the optical extinction directions of the crystal between crossed polarisers. The spectra of the rubidium and caesium salts obtained in this manner were closely similar, and the bands observed in each are listed in Table 5.6. The possibility that some of the neighbouring pairs of bands are in fact due to one band whose frequency is orientation-dependent is discounted for two reasons. Firstly, most of these pairs can be observed simultaneously in one or other of the crystal orientations, and secondly, most of the bands have a corresponding feature in the powder spectrum. Excluding the lattice modes below 100 cm^{-1}, the only feature not previously observed in the transmission spectra is the splitting of the band at about 150 cm^{-1} in both complexes.

The assignments of the internal modes above 180 cm^{-1} follow those of Adams and Lock.[2] Of the four Mn-Cl bending modes, the lower two are attributed to π(Mn-Cl), although the reverse assignment of the middle two is possibly equally valid. All three of the lattice modes are

Table 5.6: Observed i.r. frequencies (cm^{-1}) for the triclinic $A_2MnCl_4.2H_2O$ complexes.

$Rb_2MnCl_4.2H_2O$	$Cs_2MnCl_4.2H_2O$	Assignment
340	300 ✓	ν(Mn-O)
246	236 ✓	ν(Mn-Cl)
212	212 ✓	
192	186	δ(Mn-O)
173	172	δ(Mn-Cl)
156	155 ✓	
148	147 ✓	π(Mn-Cl)
119	118 ✓	
92	84 ✓	lattice modes
80	70 ✓	
72		

Table 5.7: I.r. reflectance bands (cm^{-1}) of $MnCl_2.4H_2O$ crystals.

315	B_u	ν(Mn-O)
228	B_u	ν(Mn-Cl)
200	A_u	δ(Mn-O)
151	A_u	δ(Mn-Cl)
140	B_u	
121	A_u	ρ(Mn-Cl)
107	B_u	
60	B_u	lattice modes
54	A_u	

observed for the rubidium salt, and two for the caesium salt.

Thus all the internal modes except one Mn-O bend are observed for both complexes. The absence of this band could easily be due to near-coincidence of the two δ(Mn-O) modes. From the almost tetragonal symmetry of the $MCl_4(H_2O)_2^{2-}$ ions, the vibrations of the Mn-Cl bonds might also be expected to occur in fairly closely split pairs, but in fact the splitting is substantial in each case. Indeed, the pattern of frequencies bears some resemblance to that found for the $CuCl_4(H_2O)_2^{2-}$ ion. Differences in Mn-Cl bond lengths, however, are not sufficient to account for this splitting, and some other explanation, such as strong hydrogen bonding to one set of chlorines, must be invoked.

<u>$MnCl_2.4H_2O$</u>: The most recent structure determination[16] of this complex shows it to have space group $P2_1/n$ (C_{2n}^5). The four octahedral $MnCl_2(H_2O)_4$ molecules in each unit cell have the rather unusual cis configuration of the chlorines. Since all the atoms occupy general sites, each of the fifteen internal vibrations of the molecule will be formally i.r. active in both the A_u and B_u spectra. Five A_u and four B_u lattice modes are also predicted, three of each being molecular librations. The only vibrational study made of this hydrate was concerned solely with the vibrations of the water molecules.[1]

Results: Table 5.7 gives the frequencies observed in the single-crystal i.r. spectra of $MnCl_2.4H_2O$. The B_u modes are taken from two spectra employing perpendicular polarisation directions in the ac crystallographic plane. A wax coating had to be used to prevent dehydration of the crystal faces, and this had an adverse effect on the quality of the spectra, so that only the stronger features were reproducible. The spectra therefore show only a small proportion of the fifteen internal modes predicted for each symmetry species, although some of these would no doubt be coincident or vanishingly weak in any case.

The assignments of the observed bands are based on those for the $A_2MnCl_4.2H_2O$ complexes. An alternative description of the 200 cm^{-1} mode as the second stretching vibration of the cis-$MnCl_2$ moiety is possible but less likely, since this band is of similar low intensity to the M-O bending modes observed in other aquo-complexes.

$\underline{CsMnCl_3.2H_2O}$: This complex crystallises in the orthorhombic space group Pcca (D_{2h}^8) (Z = 4).[17] The structure consists of zig-zag Mn-Cl-Mn chains extending along the a axis, with the octahedral coordination of the manganese completed by two non-bridging chlorines and two water molecules in the cis configuration. There are two of these chains in each unit cell.

The single-crystal Raman and i.r. spectra of $CsMnCl_3.2H_2O$ have been reported by Adams and Newton.[18] Their group theoretical analysis of the vibrations of this complex shows that the isolated D_2 chain has the vibrations given by representation 5.4. The approximate descriptions

$$\Gamma = 8A + 8B_1 + 8B_2 + 8B_3 \qquad 5.4$$

of these modes is given in Table 5.8. Each of these modes is split into a g/u correlation doublet by interaction of the two chains, so that the B_{1u}, B_{2u} and B_{3u} spectra should each contain eight internal bands. The predicted i.r. active lattice modes are given by representation 5.5, and include one B_{3u} rotatory mode.

$$\Gamma_{ext} = B_{1u} + 2B_{2u} + 3B_{3u} \qquad 5.5$$

Results: Of the thirty predicted i.r. active crystal modes, twenty were observed in the present work, and are listed in Table 5.9. This is the same number as that previously reported,[18] and although certain of the bands are not common to both sets of data, there is excellent agreement between the two. Including the reported frequencies not observed in the present work, a total of eighteen internal vibrations can be identified, assuming that all lattice modes occur below 90 cm^{-1}.

Table 5.8: Approximate descriptions of the vibrations of the anionic chains in $CsMnCl_3.2H_2O$.

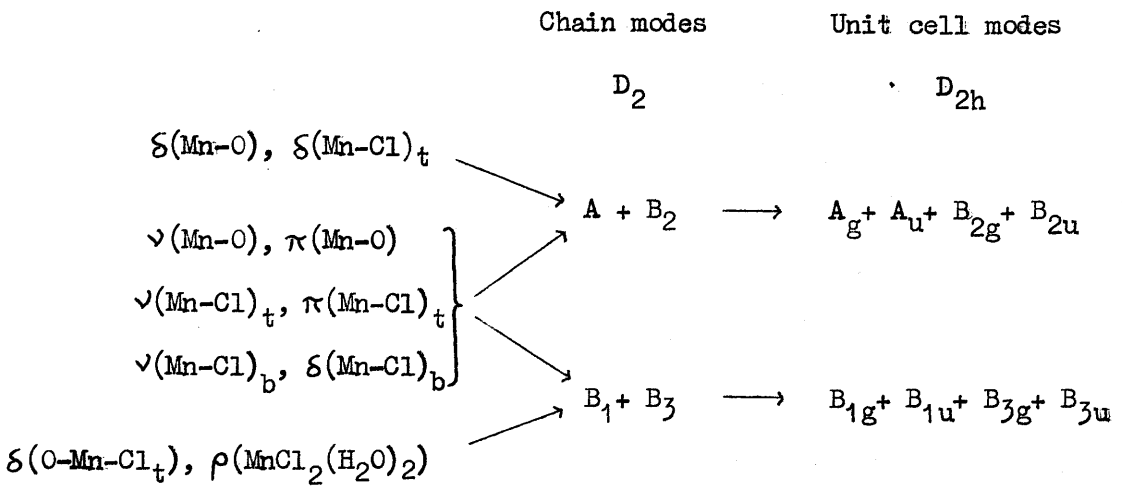

Table 5.9: Single-crystal i.r. frequencies (cm^{-1}) for $CsMnCl_3.2H_2O$.

B_{1u}	B_{2u}	B_{3u}	
310	320	(306)	ν(Mn-O)
(256)	231	241	$\nu(Mn\text{-}Cl)_t$
207			
183	180		
	168	170	
146	147	142	
127	128	129	
		106	
82	84		lattice modes
	44	60	

Frequencies in parentheses are taken from ref. 18

With this data, it is possible to deduce the complete pattern of the i.r. spectra.

There are four sets of bands comprising one component of each symmetry at about 310, 240, 145 and 128 cm^{-1}, which would seem to indicate that modes involving a particular internal coordinate occur over a narrow frequency range. This being the case, the bands around 180 and 170 cm^{-1} must form part of two more such groups, and the presence of missing B_{1u} and B_{3u} modes at these frequencies can be postulated. Similarly, the bands at 207 and 106 cm^{-1} must be members of B_{1u}/B_{3u} pairs at least. This leaves only two B_{2u} modes required to complete the internal modes. The positions of these cannot be inferred from the i.r. spectra, but the presence of A_{1g} bands in the Raman spectra at 213 and 110 cm^{-1} give some idea of the regions in which they might be expected, completing the two sets mentioned above. Thus the i.r. active internal vibrations of $CsMnCl_3.2H_2O$ can be grouped into eight sets consisting of one component of each symmetry. The reported Raman frequencies also fit this pattern.

This unexpected simplicity of the vibrational spectrum is of little help in assigning the observed bands. Although the two highest groups at about 310 and 245 cm^{-1} can be attributed with some confidence to the Mn-O and terminal Mn-Cl stretching modes respectively, it is difficult to make reasonably consistent assignments for the other groups, since the pattern observed requires that modes having only B_{2u} or B_{1u}/B_{3u} components should occur together to form complete sets. This is conceivable for the B_{2u} Mn-O and B_{1u}/B_{2u} O-Mn-Cl bending modes, but the twisting vibration of the $MnCl_2(H_2O)_2$ units about the chain axis is likely to be much lower in frequency than either the Mn-O or Mn-Cl B_{2u} bending modes. This difficulty suggests that the treatment of the low frequency vibrations in terms of symmetrised internal coordinates is

seriously affected by mixing of the modes concerned.

5.5: Experimental

All of the crystals were prepared by slow evaporation of aqueous solutions of the appropriate constituent chlorides.[8,14-17] The copper complexes grew as irregular octahedra of the (111) form, with a few (100) faces. Since the a and c unit cell dimensions do not differ greatly in these complexes, determination of the crystallographic axes by measurement of interfacial angles was verified by the i.r. dichroism of the faces. Crystals of the iron complex also took the form of distorted octahedra, with (101) and (110) faces together with some well-developed (001) faces.

$MnCl_2.4H_2O$ and $CsMnCl_3.2H_2O$ formed large, irregular prisms, with large (001) faces in the case of the former, while on crystals of the trichloro-complex all the primitive forms were well-developed. The $A_2MnCl_4.2H_2O$ complexes grew in a variety of prismatic habits.

It was found that $MnCl_2.4H_2O$ readily lost water during evacuation prior to recording the far-i.r. spectra. To prevent this, each face was coated with a thin layer of paraffin wax.

References

1 I. Nakagawa and T. Shimanouchi, Spectrochim. Acta, 1964, 20, 429.

2 D.M. Adams and P.J. Lock, J. Chem. Soc. (A), 1971, 2801.

3 A.F. Wells, "Structural Inorganic Chemistry", 3rd edn., Oxford, 1962.

4 M. Goldstein, E.F. Mooney, A. Anderson and H.A. Gebbie, Spectrochim. Acta, 1965, 21, 105; D.E. Billing, A.E. Underhill, D.M. Adams and D.M. Morris, J. Chem. Soc. (A), 1966, 902.

5 M.J. Campbell, M. Goldstein and R. Grzeskawiak, Chem. Comm., 1967, 778.

6 D.M. Adams and P.J. Lock, J. Chem. Soc. (A), 1967, 620.

7 I.R. Beattie, T.R. Gilson and G.A. Ozin, J. Chem. Soc. (A), 1969, 534.

8 S.B. Hendricks and R.G. Dickinson, J. Amer. Chem. Soc., 1927, 49, 2149.

9 R. Chidambaram, Q.O. Navarro, A. Garcia, K. Linggoatmodjo, Lin Shi-Chien, Li Hwan Suh, A. Sequeira and S. Srikanta, Acta Cryst., 1970, B26, 827.

10 D.M. Adams and D.C. Newton, J. Chem. Soc. (A), 1971, 3507.

11 F. Stern, "Solid State Physics", Academic Press Inc., New York, 1963, Vol. 15, p. 299; S.S. Mitra and P.J. Gielisse, Progress in Infra-red Spectroscopy", ed. H.A. Szymanski, Plenum Press, New York, 1964, Vol. 2, p. 47.

12 C.M. Phillippi, Technical report, 1969, AFML-TR-68-317; W.G. Spitzer, R.C. Miller, D.A. Kleinman and L.E. Howarth, Phys. Rev., 1962, 126, 1710.

13 A. Bellanca, Periodico Mineral. (Rome), 1948, 17, 59; R.W.G. Wyckoff, "Crystal Structures", 2nd edn., Interscience, New York, 1965, Vol. 3.

14 D.M. Adams and D.C. Newton, J.C.S. Dalton, 1972, 681.

15 S.J. Jensen, Acta Chem. Scand., 1964, 18, 2085.

16 A. Zalkin, J.D. Forrester and D.H. Templeton, Inorg. Chem., 1964, 3, 529.

17 S.J. Jensen, P. Anderson and S.E. Rasmussen, Acta Chem., Scand., 1962, 16, 1890.

18 D.M. Adams and D.C. Newton, J. Chem. Soc. (A), 1971, 3499.

Chapter 6: Effects of Hydrogen Bonding on the Infrared Spectra of Some Complex Ammonium Halides

Introduction

The ammonium ion has an ionic radius very similar to that of rubidium, and ammonium complexes are often members of isomorphous series containing the potassium, rubidium and, in some cases, caesium analogues. However, although ammonium behaves structurally as an alkali metal ion, it has been found in the course of the present work that its complexes are not in general suitable subjects for spectroscopic study in the far i.r. region, since the bands of interest tend to be more diffuse, if they are resolved at all, than in the corresponding alkali metal complexes. Such difficulties have been encountered in the $(NH_4)_2MF_4$, $(NH_4)_2MF_6$ and $(NH_4)_2CuCl_4.2H_2O$ systems. It has been suggested[1] that this is a result of hydrogen bonding by the ammonium ions in these complexes.

The effects of hydrogen bonding on both the structure of ammonium salts and the vibrational spectra of the cation in these salts have aroused considerable interest. The structural transformations and vibrational spectra of the simple ammonium halides have been the subject of thorough investigation,[2-5] and a number of spectroscopic studies of complex salts have been reported,[6,7] but no reliable and generally applicable rules for the detection of hydrogen bonding have emerged from this work.

The tetrahedral ammonium ion has the four fundamental modes of vibration, described in Chapter 4. In the crystalline state, the selection rules restricting the i.r. activity of ν_1 and ν_2 may be relaxed, depending on the site symmetry of the ammonium ion in the crystal. In addition, degeneracies of the T_d modes may be removed,

giving rise to splitting of these bands. No indications of correlation coupling have so far been observed. From the effects of hydrogen bonding on the i.r. spectra of a variety of other systems,[8] it would be expected that the formation of a hydrogen bond involving an ammonium ion should lower the frequency of the N-H stretching mode ν_3 and raise that of the bending mode ν_4. The stretching mode may also gain considerably in both intensity and breadth. However, these effects, with the possible exception of the variation in the frequency of ν_4, do not accurately reflect the strength of hydrogen bonding in the simple ammonium halides, since ν_3 for the iodide is lower than that for the more strongly hydrogen bonded bromide and chloride,[3,4] and at room temperature the band widths of ν_3 are almost identical.[2]

In the i.r. spectra of the ammonium halides an intense absorption is observed in the region 2800 - 3300 cm^{-1} which is resolvable into a number of broad overlapping bands. These have been assigned to ν_3 of the ammonium ion and various combination and overtone bands, the latter deriving their intensity from interaction by Fermi resonance with ν_3. In the N-H bending region ν_4 occurs as a fairly intense absorption at around 1400 cm^{-1}. Although ν_2 is not observed in the simple halides, it may be observed at about 1680 cm^{-1} in the spectra of complex salts in which the ion lies on a low symmetry site.[6] Other weak bands in the region 1400 - 2200 cm^{-1} can be assigned to combinations of the bending vibrations with lattice modes or with the torsional mode (ν_6) of the ammonium ion. Since this torsional mode results from restricted rotation of the ammonium ion caused by hydrogen bonding, the occurrence of the $\nu_4 + \nu_6$ band in the i.r. spectra of ammonium complexes has been proposed as a diagnostic feature of hydrogen bonding by Waddington,[9] from a general treatment of the i.r. spectra of a series of monobasic salts. The results of this study also support the idea that hydrogen bonded

ammonium salts are not in general isomorphous with their potassium or rubidium analogues.

The present work adopts a similar approach to that of Waddington, but in order to simplify the problem, investigations have been confined to complex ammonium halides. The i.r. spectra of a number of these complexes have been recorded in the region of the fundamental vibrations of the ammonium ion and the lattice modes. On the basis of the expected behaviour of the ammonium ion in these systems, the usefulness of spectral features such as band widths, variations in fundamental frequencies, crystal mode splitting and combination bands in determining the presence and strength of hydrogen bonding is assessed.

Results and Discussion

The frequencies and assignments of the bands observed in the i.r. spectra of some complex ammonium halides are given in Table 6.1. Assignments are based on those of Hornig et al[2-4] for the ammonium halides. Those given for the strong bands in the region 2800 - 3500 cm^{-1} seem to be reasonably consistent despite strong Fermi resonance in this region in the majority of complexes. In the region between 2800 cm^{-1} and 1400 cm^{-1}, a number of weak bands can be observed, and these fall into three groups. The two groups of higher frequency, at around 2000 cm^{-1} and 1800 cm^{-1}, can be assigned to combinations of the torsional mode ν_6 with ν_2 and ν_4 respectively. The third set of weak bands occur between 1580 cm^{-1} and 1720 cm^{-1}, and are probably combinations of ν_4 with a lattice mode, although it is possible that some of these bands at around 1700 cm^{-1} are i.r. active components of ν_2.

Table 6.1: Vibrational frequencies (cm^{-1}) for the ammonium ion in complex ammonium halides.

	ν_1 + lattice	ν_3	$\nu_2 + \nu_4$	$2\nu_4$	$\nu_2 + \nu_6$	$\nu_4 + \nu_6$	ν_2, ν_4 + lattice	ν_4
$(NH_4)_2MgF_4$	-	3230	3080	2900	2100	1840	1685	1485, 1420
$(NH_4)_2NiF_4$	-	3240	3100	2860	2170, 2070	1845	1716, 1675	1463, 1408
$(NH_4)_3InF_6$	-	3200	3045	2875	2110	1860	1715	1433
$(NH_4)_3ScF_6$	3450	3200	3050	2870	2100	1855	1695	1430
$(NH_4)_3GaF_6$	-	3220	3040	2870	2075	1830	1690	1425
NH_4BF_4	-	3320	3040	-	2070	1775	-	1432
$(NH_4)_2MnF_5$	-	3235	3100	2875	2140	1815	1680	1432, 1410
NH_4MnF_3	3420	3240	3090	2850	1970	1710	1630	1428
NH_4MgF_3	3430	3305	3120	2840	-	1720	-	1426
NH_4NiF_3	3420	3280	3100	2860	-	1700	1635	1420
$(NH_4)_2TiF_6$	-	3270	3100	2850	-	-	1655	1415
$(NH_4)_2SiF_6$[a]	3325	3145	3045	2810	2010	1735	-	1405
NH_4HF_2	3400	3130	3030	2805	b	b	b	1400
$(NH_4)_2SnCl_6$	3355	3240	3050	2820	-	-	1610	1400
$(NH_4)_2PdCl_6$	3330	3230	-	-	-	-	-	1398
$(NH_4)_2PtCl_6$	3330	3235	-	-	-	-	1585	1398
NH_4HgCl_3	-	3175	3040	-	-	-	-	1398
$(NH_4)_4CdCl_6$	-	3170	3030	2800	-	-	1635	1395
$(NH_4)_3ZnCl_5$	-	3130	3000	2800	1993	1755	-	1395
NH_4CdCl_3	-	3180	3050	2840	-	-	-	1393
$NH_4Pb_2Br_5$	-	3180	-	-	-	-	-	1390
$(NH_4)_2ReI_6$	-	3120	-	-	-	-	-	1388

[a] cubic form

[b] obscured by vibrations of bifluoride ion

Little of the predicted splitting of bands resulting from crystal symmetry was observed in the spectra recorded. Since ν_4 was the sharpest band in the spectra, this would be most likely to exhibit such splitting, but resolved components were observed only in the case of the $(NH_4)_2MF_4$ complexes and $(NH_4)_3MnF_5$. Crocket and Haendler[10] have suggested in connection with the $(NH_4)_2MF_4$ complexes that the two ν_4 bands might result from the vibration of ammonium ions in two non-equivalent sites, and not from true splitting of ν_4. However, this explanation was not supported by subsequent crystallographic work by Rüdorff et al[11] on $(NH_4)_2NiF_4$. Thus the room temperature mull spectra provide little information on the possible modification of the site symmetry of the ammonium ion by hydrogen bonding.

In order to establish trends in the frequencies of the fundamental vibrations of the ammonium ion, it must be assumed that in general hydrogen bonding will become progressively weaker on going from complex fluorides to iodides as is established for the simple halides. On the basis of this assumption, no definite trend in the frequencies of ν_3 for the various complexes is discernible. The frequencies of ν_4, however fall in distinct ranges depending on which halide is present in the complex; those of the complex fluorides occurring from 1485 cm^{-1} to 1400 cm^{-1}, the chlorides from 1400 cm^{-1} to 1393 cm^{-1} and the bromide and iodide at 1390 cm^{-1} and 1388 cm^{-1} respectively. This suggests that the frequency of ν_4 gives an indication of the degree of hydrogen bonding present in a complex. If the complexes examined are set out in order of decreasing frequency of ν_4 then the resulting arrangement could be taken as the order of decreasing hydrogen bonding. This can be rationalised

by considering three factors likely to influence hydrogen bonding in these complexes: (i) the halide ion present; hydrogen bonding will decrease in the order F > Cl > Br > I, (ii) the oxidation state of the metal - the higher the charge on the metal, the more polarised the M-X bond will be, thus reducing the capability of the halide ion to participate in hydrogen bonding, (iii) the coordination of the halide ion by metal ions - a halide ion on a bridging site would be expected to form hydrogen bonds less readily than a non-bridging ion coordinated to the same metal.

Although other factors such a nitrogen-halide separation and the geometric arrangement of the halide ions about the ammonium ion will obviously have an effect on the extent to which a complex is hydrogen bonded, these are much more difficult to assess and require a knowledge of accurate structural parameters which are not at present available in all cases. Nevertheless, it is possible to arrive at a satisfactory, if qualitative, understanding of the strength of hydrogen bonding in the complexes examined in terms of the three factors mentioned above. Thus complexes of the type $(NH_4)_2M^{II}F_4$, with equal numbers of bridging and non-bridging fluoride ions, would seem to be most strongly hydrogen bonded, while those of the type $NH_4M^{II}F_3$ in which all fluoride ions are bridging have lower frequencies for ν_4, occurring in the same region as those of the $(NH_4)_3M^{III}F_6$ complexes containing isolated MF_6^{3-} octahedral anions. Apart from the case of NH_4HF_2, in which the stronger hydrogen bonding takes place within the bifluoride ion, complexes of the type $(NH_4)_2M^{IV}F_6$ have the lowest values for ν_4 of the fluorides examined, as a result of the high oxidation state of the metal. The frequencies of ν_4 for the chloride complexes fall in

such a narrow range that variations cannot be considered meaningful.

The combination bands of ν_6 with ν_2 and ν_4, which have been used previously as indications of restricted rotation of the ammonium ion,[9,10] are observed in most of the complex fluorides and only one of the chlorides, implying stronger hydrogen bonding in the fluorides. It has been shown, however, that the absence of these bands does not necessarily indicate completely free rotation of the ammonium ion.[12]

It is difficult to draw any conclusions from the frequencies of ν_6 calculated from the combination bands. In the first place, anharmonicity of the vibrations and the possibility of Fermi resonance between $\nu_4 + \nu_6$ and ν_2 make these calculated frequencies somewhat unreliable. Secondly, interest in ν_6 arises from the information it provides on the barrier to free rotation imposed on the ammonium ion. Attempts to deduce barrier heights from torsional frequencies are hazardous, particularly when the form of the hindering potential is not known or even constant for the various structural types examined. However, it may be stated with reservations that the frequencies of ν_6 as calculated from the combination bands in Table 6.1. reflect the extent to which free rotation of the ammonium ion is restricted in those complexes where such bands are observed.

Another feature of hydrogen bonded systems which has received attention is the broadening of bands which is observed, particularly in the stretching region. The causes of this phenomenon have been treated from a theoretical point of view by various workers, notably Bratož and Hadži.[13] In the solid ammonium complexes there seems to be no obvious relationship between the breadth of the N-H

stretching vibrations and the degree of hydrogen bonding in these complexes, which is in agreement with the findings of Plumb and Hornig[2] for the ammonium halides. The breadth of the lattice modes may be more useful as an indication of hydrogen bonding. In all the complex fluorides examined, broad absorptions with half band widths of the order of 200 cm^{-1} were observed with maxima in the region 170 - 300 cm^{-1}. In comparison the lattice bands in other complex halides were generally much narrower and had approximately the same breadth as those of the potassium or rubidium isomorphs in those cases where a comparison was possible. Band widths and frequencies of these modes are listed in Table 6.2, while Fig. 6.1 contrasts the far i.r. spectra of typical fluoride and chloride complexes, and shows the potassium isomorph of the fluoride for comparison. The atypical behaviour of $(NH_4)_3ZnCl_5$ regarding the lattice and combination bands is probably due to the presence of free chloride ions in this complex.[14] Since, with this exception, the broadening of the lattice bands was observed only for the complex ammonium fluorides it cannot be attributed to a dispersion effect in the powdered samples. Therefore in accord with the prediction of Wagner and Hornig,[3] orientational disordering of the ammonium ions caused by hydrogen bonding is responsible for the breadth of the lattice modes. It should be pointed out that the mechanisms of broadening operating on the N-H stretching vibrations and the lattice modes are basically different. Although opinion is divided on the exact cause of the former, strong anharmonicity of the N-H bond probably plays an important part in the broadening process,[13] whereas it is the breakdown of selection rules

Table 6.2: Frequencies (cm^{-1}) and band widths of the lattice modes of complex ammonium halides.

$(NH_4)_2MgF_4$	200 (100), 280 (200)	$(NH_4)_2SiF_6$	190 (180)
$(NH_4)_2NiF_4$	250 (240)	NH_4HF_2	184 (100), 230 (160)
$(NH_4)_3InF_6$	240 (180)	$(NH_4)_2SnCl_6$	128 (28)
$(NH_4)_3ScF_6$	225 (160)	$(NH_4)_2PdCl_6$	145 (40)
$(NH_4)_3GaF_6$	210 (140)	$(NH_4)_2PtCl_6$	138 (34)
NH_4BF_4	186 (160)	NH_4HgCl_3	96 (35), 152 (60), 196 (70)
$(NH_4)_2MnF_5$	170 (140), 260 (200)	$(NH_4)_4CdCl_6$	a
NH_4MnF_3	230 (200)	$(NH_4)_3ZnCl_5$	180 (120)
NH_4MgF_3	290 (200)	NH_4CdCl_3	a
NH_4NiF_3	290 (200)	$NH_4Pb_2Br_5$	b
$(NH_4)_2TiF_6$	190 (200)	$(NH_4)_2ReI_6$	b

Figures in parenthesis give approximate half band widths (cm^{-1})

[a] complex spectrum of overlapping lattice and internal modes; similar to potassium isomorphs

[b] lattice modes occur below 40 cm^{-1}

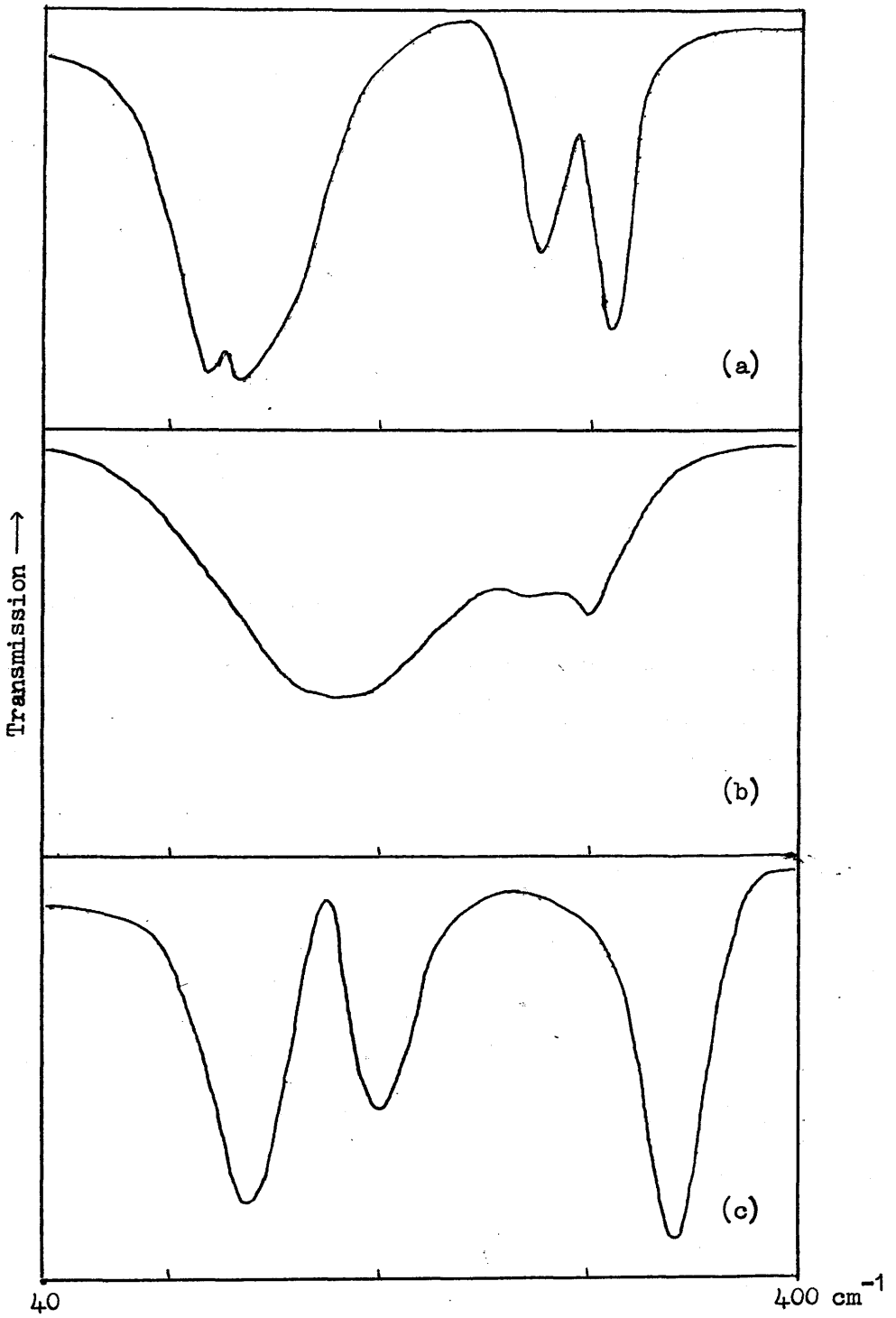

Figure 6.1: Far-i.r. transmission spectra of (a) K_2TiF_6, (b) $(NH_4)_2TiF_6$ and (c) $(NH_4)_2PtCl_6$.

resulting from disorder in the lattice induced by hydrogen bonding which is responsible for the broadening of the lattice bands.

The structural criteria used in the detection of hydrogen bonding require comment at this point. Waddington[9] put forward the idea that hydrogen bonding in ammonium complexes manifests itself in a structure differing from that of the potassium and rubidium analogues; while by implication it is likely to be weak or absent where these are isomorphous. The confirmation of hydrogen bonding in a number of complexes which have potassium or rubidium isomorphs, e.g. $(NH_4)_2SiF_6$[15] indicates the unreliability of this rule. If the presence of torsional combination bands in the i.r. spectra is accepted as evidence for hydrogen bonding, then the number of exceptions to the rule becomes so great as to limit its applicability to those complexes which are not isostructural with their alkali metal analogues, which do not form a large proportion of those studied. It has also been proposed[16] that hydrogen bonding is accompanied by a large decrease in the unit cell volume, as revealed by comparison of the unit cell dimensions of corresponding rubidium and ammonium complexes. However, large contractions are observed only in a few systems, and some in which little or no contraction is found have since been shown in this and other work[15] to be hydrogen bonded.

Conclusions

In summary, there are three ways in which hydrogen bonding in complex ammonium halides can be detected by i.r. spectroscopy.

These are:

(i) by the presence of bands arising from the combination of the librational mode ν_6 with the bending modes of the ammonium ion. Because of the possibility of confusion with ν_4 + lattice mode combination bands, identification of the torsional combinations is facilitated by the observation of both $\nu_4 + \nu_6$ and $\nu_2 + \nu_6$.

(ii) by the broadening of the lattice bands in the far i.r. region,

(iii) from the ν_4 frequency of the ammonium ion. In those complexes in which hydrogen bonding is detected using criteria (i) and (ii), the frequency of ν_4 is found to occur above 1400 cm^{-1}.

Experimental

Those complexes which were not commercially available were prepared by standard literature procedures. Spectra were recorded on samples dispersed in fluorolube and nujol mulls for the region 4000 - 400 cm^{-1}, and in polyethylene discs for the far i.r. region.

References

1 A.P. Lane and D.W.A. Sharp, J. Chem. Soc. (A), 1969, 2942.

2 R.C. Plumb and D.F. Hornig, J. Chem. Phys., 1955, 23, 947.

3 E.L. Wagner and D.F. Hornig, J. Chem. Phys., 1950, 18, 296.

4 E.L. Wagner and D.F. Hornig, J. Chem. Phys., 1950, 18, 305; 1953, 21, 366.

5 L.F.H. Bovey, J. Opt. Soc. Amer., 1951, 41, 836: J.R. Durig and D.J. Antion, J. Chem. Phys., 1969, 51, 3639; C.H. Perry and R.P. Lowndes, ibid., p. 3648; K.B. Harvey and N.R. Mcquaker, ibid., 1971, 55, 4390.

6 D.A. Dows, E. Whittle and G.C. Pimentel, J. Chem. Phys., 1955, 23, 1475; L.L. Oden and J.C. Decius, Spectrochim. Acta, 1964, 20, 667; C.J.H. Schutte and A.M. Heyns, J. Mol. Structure, 1970, 5, 37; J. Chem. Phys., 1970, 52, 864.

7 A.M. Heyns and C.J.H. Schutte, J. Mol. Structure, 1971, 8, 339; C.J.H. Schutte and D.J.J. van Rensburg, ibid., 1971, 9, 77; 1971, 10, 481; D.J.J. van Rensburg and C.J.H. Schutte, ibid., 1972, 11, 229.

8 W.C. Hamilton and J.A. Ibers, "hydrogen Bonding in Solids", Benjamin, New York, (1968).

9 T.C. Waddington, J. Chem. Soc., 1958, 4340.

10 D.S. Crocket and H.M. Haendler, J. Amer. Chem. Soc., 1960.

11 W. Rüdorff, J. Kändler and D. Babel, Z. anorg. Chem., 1962, 317, 261.

12 Y. Sato, J. Phys. Soc. Japan, 1965, 20, 2304.

13 S. Bratož and D. Hadži, J. Chem. Phys., 1957, 27, 991.

14 H.P. Klug and L. Alexander, J. Amer. Chem. Soc., 1944, 66, 1056.

15 E.O. Schlemper, W.C. Hamilton and J.J. Rush, J. Chem. Phys., 1966, 44, 2499.

16 B. Cox and A.G. Sharpe, J. Chem. Soc., 1953, 1783.

Chapter 7: Cyanide Complexes

7.1: Introduction

By virtue of the more complex electronic structure within the cyanide ligand as compared to chloride, for instance, the vibrational spectra of cyano-complexes are capable of revealing more chemically useful information regarding bond strengths, electronic distributions etc. than can usually be extracted from the spectra of halogenometallates. As in the case of the closely related carbonyls, a list of fairly simple rules governing the vibrational behaviour of cyano-complexes can be drawn up.[1] Gaps in the understanding of the spectra of these systems remain, however, as exemplified by the controversy surrounding the assignment of the M-C stretching and M-C-N bending modes in the octahedral hexacyanometallates. The application of far i.r. single crtstal techniques to this problem will be discussed in Section 7.3.

Some of the complexes dealt with here are of interest from a basically structural viewpoint. The molecular solid $Hg(CN)_2$ has a unique and interesting tetragonal structure,[2] while $K_2M(CN)_4$ complexes (M = Hg,Zn) provide examples among the cyanides of the spinel structure,[3] which is widely adopted by certain oxides, sulphides, etc.

In the past, assignment of the vibrations of species such as $M(CN)_6^{x-}$ was facilitated by isolating them for spectroscopic examination in a simple environment, e.g. as a dopant in an alkali-halide matrix.[4] Because of the sensitivity of C-N stretching vibrations to small changes of environment, and the improved understanding of the spectra of hexacyanometallates, this technique can also be employed to provide detailed information regarding the structure of the host lattice in the vicinity of the doped ions, as will be shown later.

7.2: $Hg(CN)_2$ and $K_2M(CN)_4$ (M = Hg, Zn)

$Hg(CN)_2$: This compound crystallises in the tetragonal space group $I\bar{4}2d$ (D_{2d}^{12}) with eight molecules in the crystallographic unit cell, or four per primitive unit cell.[2] It is made up of non-linear $Hg(CN)_2$ molecules of approximate C_{2v} symmetry, with Hg-C-N angles of 173° and a C-Hg-C angle of 171°. The isolated C_{2v} molecule would have nine fundamental modes of vibration: the symmetric (A_1) and asymmetric (B_1) stretching modes of the C-N and Hg-C bonds, A_1, A_2, B_1 and B_2 Hg-C-N bending modes and an A_1 C-Hg-C bend. These molecular modes are correlated with the molecular modes in Table 7.1, and a complete factor group analysis is given in Table 7.2.

The i.r. spectrum of the solid has been investigated by Jones,[5] who observed only three fundamentals of what he considered to be an approximately linear molecule, but was able to estimate the frequencies of the others from combination bands. Two bands at 2192 and 276 cm^{-1} have been observed in the Raman spectrum[6] of the solid, and four in that of an aqueous solution.[7]

The i.r. and Raman frequencies of $Hg(CN)_2$ observed in the present work are given in Table 7.3, together with approximate descriptions and the frequencies of Jones.[5] These represent unpolarised data, apart from the i.r. bands below 200 cm^{-1}. (Although polarised i.r. spectra were recorded up to 400 cm^{-1}, the bands at around 350 cm^{-1} were too weak to be observed by reflectance.) The reflectance spectrum with the incident radiation polarised parallel to the c axis of the crystals gave a strong, broad B_2 band at about 105 cm^{-1}. The E mode spectrum consisted of two sharp peaks at 112 and 62 cm^{-1}.

It can be seen from Table 7.3 that a number of coincidences of i.r. and Raman bands occur, as would be expected in a non-centrosymmetric system. Another effect of the absence of a centre of symmetry in

Table 7.1: Correlation diagram for solid $Hg(CN)_2$.

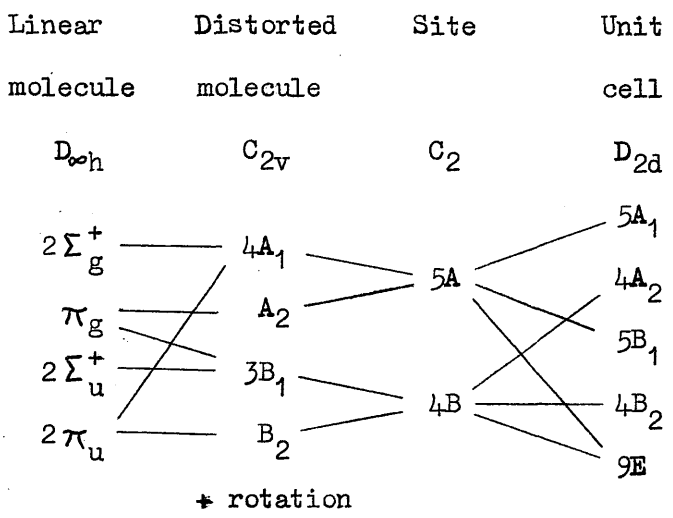

Table 7.2: Factor group analysis of $Hg(CN)_2$ (space group D_{2d}^{12}).

	A_1	A_2	B_1	B_2	E
N	7	8	7	8	15
T_a				1	1
T	1	2	1	2	3
R	1	2	1	2	3
N_i	5	4	5	4	9

Activity: Raman A_1, B_1, B_2, E

i.r. $B_2(z)$, E(x,y)

Table 7.3: Vibrational frequencies (cm^{-1}) of solid $Hg(CN)_2$.

Present work	Activity	Assignment	Jones[5]
2196	R		
2193	i.r.	ν(CN)	2193.5
2189	i.r.		2192
440	i.r.		
432	R	ν(HgC)	442
410	R & i.r.		415
398	R		
368	i.r.		
342	R		341
337	i.r.	δ(HgCN)	276
283	R		
271	R		
112	i.r.(E)	δ(CHgC)	100
105	R & i.r.(B_2)		
84	R	lattice modes	
62	R & i.r.(E)		
48	R		
33	R		

R - Raman

molecular crystals, where short-range anisotropic interactions are likely to be more important than long-range electrostatic forces in determining the behaviour of the vibrations, is that certain Raman bands (the B_2 and E modes) could have frequencies anywhere between those of their transverse and longitudinal components, depending on the scattering geometry.[8] This could lead to shifts in single-crystal bands, or broadening of powder bands, neither of which was observed in the spectra recorded, which could be accounted for by the weakness of the vibrations involved giving very small transverse-longitudinal splitting.

Of the three modes observed at around 2200 cm^{-1}, the band at 2196 cm^{-1} in the Raman spectrum can be assigned to the symmetric C-N stretching mode, while the two i.r. bands are probably both correlation components of the asymmetric stretch.

In the Hg-C stretching region a total of four bands are observed, while in the Hg-C-N bending region there are five. The ranges over which both of these sets of bands are spread are greater than would be expected for a linear dicyanide,[9] and must be due mainly to distortion from linearity of the $Hg(CN)_2$ molecules. The division between the two groups is not very definite, but it seems reasonable to include the 268 cm^{-1} band in the lower group. This being the case, group theory alone does not distinguish between the Hg-C stretching and Hg-C-N bending modes, since a total of five modes should be observed for former, and double that number for the latter.

The C-Hg-C bending modes and lattice vibrations together form a series of bands extending below 120 cm^{-1}. It is difficult to differentiate between the internal and lattice modes in the Raman spectrum, but the polarised i.r. data allow a tentative assignment to be made. It follows from the correlation diagram of Table 7.1

that the C-Hg-C bending mode should have one component of E symmetry and none of B_2. The E mode spectrum has only two bands, at 112 and 62 cm^{-1}. Since the higher of these is close to the calculated frequency of Jones,[5] it is likely that this is the bending mode. The other two low frequency i.r. bands may be either translatory lattice modes or librational modes of the $Hg(CN)_2$ molecules, which can have a high intensity in such systems.[10]

The above assignments offer only approximate descriptions of the modes involved, since considerable mixing must take place between the low frequency internal and lattice modes. The same will be true of the Hg-C stretching and Hg-C-N bending modes, some of which are close enough in frequency to interact significantly.

The number of bands observed in the spectra of solid $Hg(CN)_2$ cannot be adequately explained by the site group approximation, which is often applicable in molecular systems. Although by no means all of the predicted factor group splitting is evident, it is obvious that, for some of the modes at least, correlation coupling between molecules is fairly strong - for the Hg-C stretching modes it must amount to at least 12 cm^{-1}. This would appear to confirm Hvoslef's suggestion that there is some form of association between adjacent $Hg(CN)_2$ molecules.[2]

$\underline{K_2M(CN)_4\ (M = Hg,Zn)}$: These complexes adopt the spinel structure with the cubic space group $Fd\bar{3}m$ (O_h^7) (Z = 8) in which the tetrahedral $M(CN)_4^{2-}$ ions occupy T_d sites.[3] The only i.r. active crystal modes of the anion are of F_{1u} symmetry, and derive from the F_2 modes of the isolated ion. (These also produce a set of F_{2g} crystal modes by correlation splitting, each site group mode being split into two, not eight as stated by Jones, since the primitive unit cell is bi-molecular.) There are four F_2 vibrations of the T_d ion, these being

the asymmetric stretches and bends of the C-N and M-C bonds. In addition to these, two F_{1u} translatory lattice modes are predicted.

Jones has reported[11] the i.r. spectra of these complexes above 300 cm^{-1}, and the Raman spectra have also been recorded,[7,12] but the low frequency F_{1u} modes have not previously been observed directly.

The i.r. reflectance spectra of $K_2Hg(CN)_4$ and $K_2Zn(CN)_4$ were recorded from 20-400 cm^{-1}, and the powder transmission spectra in the mid-i.r. region. The observed frequencies are listed in Table 7.4. The two lattice bands in each were observed above 100 cm^{-1}, which is fairly high for modes involving displacements of the anions, as indicated by the anion-dependence of the frequencies. The C-M-C bending mode expected below 100 cm^{-1} could not be resolved in either complex.

Table 7.4: I.r. spectra of the cubic $K_2M(CN)_4$ complexes (frequencies in cm^{-1}).

$K_2Zn(CN)_4$	$K_2Hg(CN)_4$	Assignment
2155	2145	ν(CN) (ν_5)
359	328	ν(MC) (ν_6)
313	234	δ(MCN) (ν_7)
157	141	lattice
130	120	modes

7.3: $K_3M(CN)_6$ (M = Fe,Co)

The vibrational spectra of hexacyano-complexes of transition metals have aroused considerable interest, and the Raman and i.r. spectra of complexes such as $K_3M(CN)_6$ (M = Cr, Mn, Fe, Co, Rh, Re, Ir) and $K_4M(CN)_6 \cdot 3H_2O$ (M = Fe, Ru, Os, V) have been extensively studied.[13-19] Apart from the single-crystal i.r. transmission spectrum of $K_3Co(CN)_6$ (300-5000 cm^{-1})[17] and the single-crystal Raman studies of Chadwick,[18] and Devèze and Krauzman,[19] all spectra reported prior to the present work were recorded using solutions or powdered solids, which showed little of the predicted solid state splitting. More recently, a single-crystal Raman study of $K_3Fe(CN)_6$ has been carried out by Adams and Hooper.[20]

Opinion remains divided over the assignment of the M-C stretching and M-C-N bending modes in these complexes. Nakagawa and Shimanouchi recorded the powder i.r. spectra of some hexacyanometallates (III) at liquid nitrogen temperature, and, on the basis of the fifteen bands observed above 40 cm^{-1}, carried out a normal coordinate analysis which showed the M-C stretching frequency to be above that of the M-C-N bands.[16] This contradicts the earlier assignment of Jones.[17]

In this section, the i.r. spectra of $K_3Fe(CN)_6$ and $K_3Co(CN)_6$ in the region 40-400 cm^{-1} are examined using polarised single-crystal reflectance techniques. This allows the pattern of factor group splitting of the low frequency modes to be clearly established, and throws some light on the problem of the disputed assignments. Also discussed are the absorption spectra of the powdered solids and the single-crystal transmission spectrum of $K_3Fe(CN)_6$ in the region 400-3000 cm^{-1}.

$K_3Fe(CN)_6$: Barkhatov and Zhanov[21] have reported that $K_3Fe(CN)_6$ has a monoclinic unit cell with space group $P2_1/c$ (C_{2h}^5) and two molecules

per unit cell. The factor group analysis[16] based on this space group predicts a total of fifty-one modes corresponding to vibrations of the $Fe(CN)_6^{3-}$ anions in the crystal, which are given by the representation

$$\Gamma_{internal} = 18A_u + 18B_u \qquad 7.1$$

These internal modes of the $Fe(CN)_6^{3-}$ anions, where each iron atom is situated on a site of C_i symmetry, may be correlated with the normal modes of the isolated O_h anion as shown in Table 7.5a. The remaining modes of vibration are translatory lattice modes, given by the representation 7.2 and are vibrations of the potassium cations against the $Fe(CN)_6^{3-}$ anions.

$$\Gamma_{lattice} = 8A_u + 7B_u \qquad 7.2$$

Results: The i.r. reflectance spectra of single crystals $K_3Fe(CN)_6$ from 40-400 cm^{-1} are shown in Fig. 7.1. The observed frequencies and those calculated from a normal coordinate analysis by Nakagawa and Shimanouchi[16] are listed in Table 7.6, together with assignments, in which the conventional numbering of the modes[17] is used.

In a monoclinic unit cell, the vibrations of B_u symmetry are polarised in the ac crystallographic plane. The B_u modes were obtained by choosing orthogonal crystal directions in the ac plane which showed the greatest difference in spectral features on recording the reflectance spectra with the electric vector of the incident radiation parallel to these directions; these spectra are shown in Figs. 7.1a and b. Only one band at 169 cm^{-1} was common to both spectra, and no crystal direction in the ac plane could be found where this band was reduced to zero intensity. This indicates that there are two vibrations of B_u symmetry occurring at 169 cm^{-1}.

Vibrations of A_u symmetry are polarised along the crystallographic

Table 7.5: Correlation diagrams for the monoclinic and orthorhombic $K_3M(CN)_6$ structures.

(a) $K_3Fe(CN)_6$ - C_{2h}^5 (Z = 2)

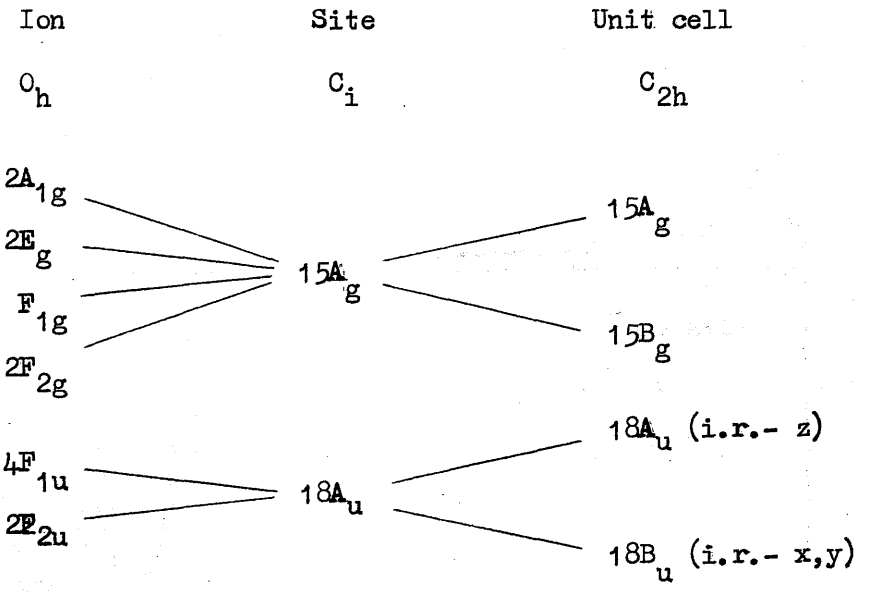

(b) $K_3Co(CN)_6$ (orthorhombic form) - D_{2h}^{14} (Z = 4)

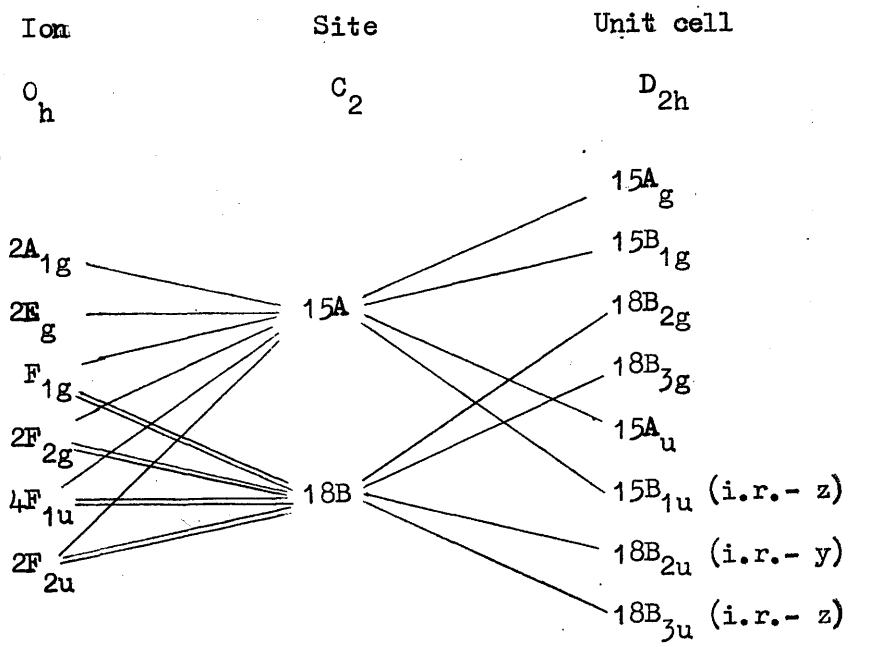

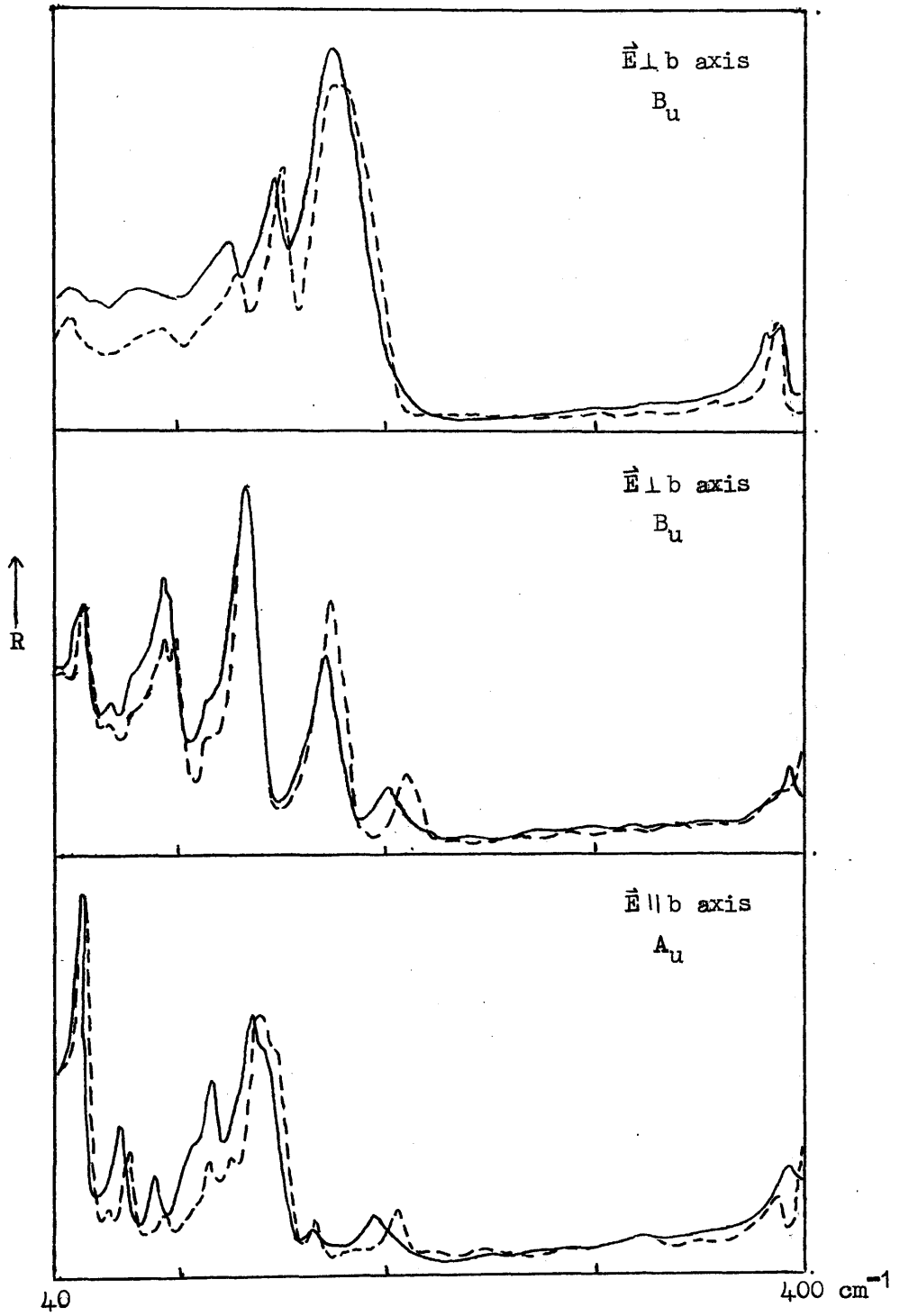

Figure 7.1: Reflectance spectra of $K_3Fe(CN)_6$ at room temperature (solid line) and 105K (dashed line).

Table 7.6: Observed and calculated i.r. frequencies (cm^{-1}) for $K_3Fe(CN)_6$.

A_u (calc)[a]	B_u (calc)[a]	A_u (obs) r.t.	B_u (obs) r.t.	A_u (obs) l.t.	B_u (obs) l.t.	Assignment
2126 2126	2126 2126	2119	2115	n.r.	n.r.	CN stretch
2125	2125					(ν_6)
523 522	523 522		512[b]	n.r.	n.r.	FeC sretch
520	520					(ν_7)
407 402	407 402		392 386			FeCN bend
400 388	400 388	388	378	384	384	(ν_8, ν_{12})
385 381	385 381					
206 193	206 194	196 190	203	206	212	lattice
165 143	164 143	162 141[c]	169 169 143	165 146[c]	172 172 147	CFeC bend
130 123	128 124	133 114	132 122	137 126	132 124	(ν_9, ν_{13})
117 95	112 103		114[c] 97[c]	114	116[c] 100	
86 79	89 74	88 71	93 70	94 75	95	lattice
62 49	68 50	49	56	56	56	modes

[a] ref. 16; [b] not assigned to symmetry species; [c] shoulder; r.t. room temperature; l.t. 105K; n.r. not recorded.

b axis of the monoclinic unit cell. The reflectance spectrum of the A_u modes shown in Fig. 7.1c was recorded by aligning the b axis parallel to the electric vector of the incident radiation.

The reflectance spectra of the three crystal orientations of $K_3Fe(CN)_6$ were recorded at 105 K, which resulted in the resolution of certain shoulders, and shifts of nearly all of the bands to higher frequency (3-12 cm^{-1}) relative to the room temperature spectra. This shift to higher frequency at low temperature has been noted previously[16] and results from a contraction of the unit cell causing stronger interaction between atoms and ions in the crystal.

Above 400 cm^{-1} fundamental frequencies were obtained from the absorption spectrum of powdered $K_3Fe(CN)_6$ dispersed in KBr, and hardly any splitting of bands was observed. However, splitting of the CN stretching mode (ν_6) did occur and the assignment of the two components was made on the basis of results obtained from single crystal transmission spectra. Although the crystasl used were too thick for the frequencies of the fundamental modes to be recorded, a number of combination and isotope bands were observed and their frequencies and assignments are geven in Table 7.7. Two isotope bands, each consisting of a doublet, corresponding to the $C^{13}N$ and CN^{15} stretching modes were observed when the direction of incident i.r. radiation was perpendicular to the crystallographic b-axis. However, when the direction of incident radiation was parallel to the b-axis, the high frequency component of each doublet was not observed, indicating that it has A_u symmetry. By analogy with these isotope bands the high and low frequency components of ν_6 are tentatively assigned to A_u and B_u modes respectively.

In all, twenty-five of the predicted thirty-two bands in the region 40-400 cm^{-1} were observed, indicating that interaction between

Table 7.7: Combination and isotope bands in the i.r. spectrum of $K_3Fe(CN)_6$.

Frequency (cm^{-1})	Assignment
2635	$\nu_1 + \nu_7$
2510[a]	$\nu_3 + \nu_8$; $\nu_1 + \nu_{12}$
2498	$\nu_3 + \nu_{12}$
2220	$\nu_6 + L_1$
2205	$\nu_6 + L_2$
2180	$\nu_6 + L_3$
2093	$\nu_{CN}15$
2089	$\nu_{CN}15$
2073	$\nu_{C}{}^{13}{}_{N}$
2068	$\nu_{C}{}^{13}{}_{N}$
1375	-
1225	-
1100	-
895	$\nu_2 + \nu_7$
795	$\nu_2 + \nu_8$

[a] shoulder; L = lattice mode

Table 7.8: observed i.r. frequencies (cm^{-1}) and assignments for $K_3Co(CN)_6$.

A_u (r.t.)	B_u (r.t.)	A_u (l.t.)	B_u (l.t.)	Assignment
2130	2128	n.r.	n.r.	CN stretch (ν_6)
2104	2101	n.r.	n.r.	CN^{15} stretch
2089	2086	n.r.	n.r.	$C^{13}N$ stretch
562[b]		n.r.	m.r.	CoC stretch (ν_7)
414[b]		n.r.	n.r.	CoCN bend (ν_8, ν_{12})
200 196	204	208	216 190	lattice modes
	176 173		176 174	
140 114	150 136	143 116	159 137	CCoC bend (ν_9, ν_{13})
	128 108		130 120 109	
96 76	94	98 78	98	lattice modes
54 44		56 46	58	

See Table 7.6 for explanation of symbols.

the two molecules in the unit cell is strong enough to cause almost complete factor group splitting in this region. In view of the closeness in frequency of many of the bands it is not surprising that previous studies using absorption techniques on powdered samples failed to show more than twelve bands in this region.

$K_3Co(CN)_6$: It has been established[22] that $K_3Co(CN)_6$ is polytypic, with monoclinic and orthorhombic modifications. The monoclinic form is isostructural with $K_3Fe(CN)_6$,[23] while the orthorhombic form has space group Pnca (D_{2h}^{14}) with four molecules per unit cell. Since it was impossible to distinguish between the monoclinic and orthorhombic structures using crystal morphology or birefringence, the structure of the crystals used in the present study was deduced from a consideration of the bands observed in the CN stretching region.

If an orthorhombic structure is adopted in which the $Co(CN)_6^{3-}$ anions occupy a site of C_2 symmetry, then each Raman active mode of the isolated octahedral $Co(CN)_6^{3-}$ anion will have an i.r. active component under the crystal symmetry as shown in Table 7.5b. Furthermore, since there are four molecules in the orthorhombic unit cell, eight bands should be observed in the CN stretching region (2160-2120 cm^{-1}) given by the representation 7.3 corresponding to the i.r.

$$\Gamma_{CN} = 4B_{1u} + 2B_{2u} + 2B_{3u} \qquad 7.3$$

active components of ν_1, ν_3 and ν_6.

Results: The i.r. absorption spectrum of a powdered crystal of $K_3Co(CN)_6$ in the CN stretching region was found to be identical, apart from frequencies of the observed bands, to that of $K_3Fe(CN)_6$. Since no additional bands or asymmetry of the main absorption bands were observed, it was assumed that the monoclinic form of $K_3Co(CN)_6$ had been isolated, and accordingly, Table 7.8 presents the recorded frequencies and assignments to A_u and B_u symmetry species. The

assignment of the observed bands is based on that already reported[16] for $K_3Fe(CN)_6$. Above 400 cm^{-1} only eight bands were observed, corresponding to the CN, $C^{13}N$, CN^{15} and CoC stretching and CoCN bending modes. The frequencies of these bands agree well with those obtained from single crystal transmission spectra reported by Jones.[17] As with $K_3Fe(CN)_6$ the only factor group splitting observed was in the CN stretching region. The polarised i.r. reflectance spectra in the region 40-400 cm^{-1} of three orthogonal crystal orientations (these were the same as for $K_3Fe(CN)_6$) were very similar to those of $K_3Fe(CN)_6$, which gave further justification for the assumption that the crystals used had the monoclinic structure. In general the frequencies obtained for $K_3Co(CN)_6$ were some 3 cm^{-1} to 10 cm^{-1} higher than those for $K_3Fe(CN)_6$ except in the case of the MCN bending mode where the difference was 25 cm^{-1}.

On recording the spectra (40-400 cm^{-1}) at 105 K the frequencies of the observed bands showed the expected shifts to higher frequency.

Discussion

Comparison of the observed frequencies in Table 7.6 with those calculated by Nakagawa and Shimanouchi[16] shows excellent agreement between the two, especially in the region 40-400 cm^{-1}. On the other hand, there is poor agreement with those calculated on the basis of the alternative assignment of the M-C stretching and M-C-N bending modes proposed by Jones.[17] The present work therefore strongly favours the assignment of these modes suggested by Nakagawa and Shimanouchi. The extension of the single-crystal study of $K_3Fe(CN)_6$ to the Raman spectra by Adams and Hooper[20] lends further support to this view, and Hancock and Thornton[24] regard this assignment as being more compatible with the observed transition metal dependence

of the frequencies. However, in recent work on hexacyanocobaltate systems, Jones has reaffirmed his earlier assignment,[25] although his calculated normal coordinates confirm that the two modes are thoroughly mixed, with only a slight preponderance of M-C stretching or M-C-N bending character. It may be, then, that the two views are not in fact as far removed from each other as they might seem although the balance appears to be in favour of the description proposed by Nakagawa and Shimanouchi.

7.4: Hexacyanometallate Ions in a KCl Lattice

Octahedral hexacyanometallate ions such as $Fe(CN)_6^{4-}$ and $Co(CN)_6^{3-}$ are readily incorporated in KCl matrices, replacing a potassium ion and its six surrounding chloride ions. The resultant charge imbalance is cancelled by vacancies at potassium ion sites, which will be close to the centre of excess positive charge in order to minimise electrostatic interactions. The proximity of these lattice vacancies will in general reduce the effective symmetry of the doped hexacyano-anion, which should be reflected in the complexity of the i.r. spectrum in the C-N stretching region. The spectra of $Co(CN)_6^{3-}$ and $Fe(CN)_6^{4-}$ substitutionally doped in KCl have been examined using this method by Jones,[4] and Root and Symons.[26] This work is now repeated for $Fe(CN)_6^{4-}$, $Fe(CN)_6^{3-}$ and $Co(CN)_6^{3-}$ present to the extent of 0.1-0.001% in a KCl matrix.

$Fe(CN)_6^{4-}$: The i.r. spectra of doped crystals show a complex pattern of bands in the C-N stretching region, the frequencies of which are listed in Table 7.9. A total of seventeen bands was observed, compared to ten reported by Root and Symons, although not all of these were present in any one spectrum. Observation of the weaker bands depended to some extent on the conditions of preparation

Table 7.9: ν(CN) bands of $Fe(CN)_6^{4-}$ doped in KCl.

Frequency (cm^{-1})	Relative intensity	Environment	O_h mode
2085.0	0-1	C_s	ν_1
2078.5	6	$C_{2v}(1)$	
2064.4	2-3	C_s	ν_3
2061.1	0-3	$C_{2v}(2)$	
2058.1	34	$C_{2v}(1)$	
2052.9	2-4	C_s	
2050.5	0-4	$C_{2v}(2)$	
2047.5	20	$C_{2v}(1)$	
2041.5	0-3	C_{3v} or C_{4v}	?
2033.4	sh	C_s	ν_6
2032.3	85	$C_{2v}(1)$	
2029.2	sh	C_s	
2028,2	100	$C_{2v}(1)$	
2011.6	1-2	-	$\nu(CN^{15})$
2005.5	1-2	-	
1992.5	1-2	-	$\nu(C^{13}N)$
1990.4	1-2	-	

sh - shoulder

of the matrix, and some variations in the relative intensities of the bands took place, aiding the identification of groups of bands arising from the $Fe(CN)_6^{4-}$ ion in a particular environment. Since a maximum of six C-N stretching modes would be expected for the complex ion, with all degeneracies removed and every mode i.r. active, it is obvious that the ions incorporated in the lattice must occupy a number of different types of site.

The $Fe(CN)_6^{4-}$ ion, having replaced a KCl_6^{5-} unit, requires the formation of one vacancy at a potassium ion site to neutralise its excess charge. As has been mentioned, electrostatic forces dictate that this vacancy should be close to the hexacyano-ion. The closest possible position is one adjacent to the iron atom, between neighbouring cyanide groups. This would reduce the symmetry of the O_h ion to C_{2v}. There are twelve such positions, at the edges of the cube containing the hexacyano-ion. If the layer of ions immediately outside this cube is considered, there are four more possible sets of sites for the potassium ion vacancy, the one at the corners of the enlarged cube, for instance, giving a local symmetry of C_{3v} for the complex ion. There is also a set of C_{2v} sites among this group, which will be designated $C_{2v}(2)$ to distinguish them from those already described. The various possible symmetries, with the number of each type and the selection rules governing the C-N stretching modes are given in Table 7.10.

The general features of the spectra of the doped lattices bear a striking resemblance to that of $K_4Fe(CN)_6.3H_2O$. The bands observed in the spectrum of this complex, recorded as a KBr disc, are listed in Table 7.11. It should be noted that most of these bands are in fact due to a dehydrated form of the complex,[14] whose formation during sample preparation is very difficult to avoid. This was not

Table 7.10: Possible sites for $Fe(CN)_6^{4-}$ ions doped in KCl.

Site symmetry	No. of equivalent sites	ν(CN) modes		
O_h	(free ion)	$A_{1g}(\nu_1)$	$E_g(\nu_3)$	$F_{1u}(\nu_6)$
$C_{2v}(1)$	12	A_1	$A_1 + B_1$	$A_1 + B_1 + B_2$
C_s	24	A'	$A' + A''$	$2A' + A''$
$C_{2v}(2)$	12	A_1	$A_1 + B_1$	$A_1 + B_1 + B_2$
C_{3v}	8	A_1	E	$A_1 + E$
C_{4v}	6	A_1	$A_1 + B_1$ [a]	$A_1 + E$

[a] i.r. inactive

recognised in previous i.r. studies.[15] In wet discs, or nujol mulls, the three lower frequency ν_6 bands become more intense than the others, so these may be due to the trihydrate.

By comparison with the spectrum of $K_4Fe(CN)_6.xH_2O$, those of the doped KCL lattices can be divided into four regions. The ν_1 and ν_3 modes of the $Fe(CN)_6^{4-}$ ions fall in the ranges above 2070 cm^{-1} and 2070-2040 cm^{-1} respectively, while the strong ν_6 bands are found from 2035-2025 cm^{-1}. The band at 2041.5 cm^{-1} cannot be confidently assigned to either ν_3 or ν_6. Below 2025 cm^{-1}, a number of C-N isotope bands are observed. It is reasonable to assign the strongest bands in each of the three main groups to the $C_{2v}(1)$ ion. All of the predicted vibrations of this ion are observed, except for one component of ν_6. Two other sets can be identified from variations in relative intensity, both having two bands in the ν_3 region. These must

therefore indicate $C_{2v}(2)$ and C_s environments. Table 7.10 shows that, statistically C_s sites should be twice as numerous as $C_{2v}(2)$, so the stronger set of bands is probably due to the former. This leaves one unassigned band at 2041.5 cm^{-1}, which could be a vibration of either the C_{3v} or C_{4v} hexacyano-ions.

In preparing the doped crystals for this study, every effort was made to remove water incorporated in the lattice during crystallisation, but traces of hydroxyl ions and water remained. Progressive removal of the water at first caused some small intensity changes in

Table 7.11: ν(CN) bands in the i.r. spectrum of $K_4Fe(CN)_6.xH_2O$ (frequencies in cm^{-1}).

2092	m	$\nu_1(A_{1g})$
2072	ms	$\nu_3(E_g)$
2061	ms	
2048.5	vs	$\nu_6(F_{1u})$
2042.5	sh	
2041	vs	
2030.5[a]	sh	
2029[a]	s	
2020[a]	s	
2019	w	$\nu(CN^{15})$
2014	w	
2004	w	$\nu(C^{13}N)$
2001	w	

[a] these bands are probably due to the trihydrate

the spectra, particularly in the ν_6 region, while the later stages of dehydration appeared to have little effect. If impurities remain in the vicinity of the hexacyano-ions, it would seem that the replacement of chloride by hydroxyl or the occupation of vacated potassium ion sites by water molecules does not appreciably affect the potential field.

The present work therefore interprets the 13 non-isotopic C-N stretching bands observed in the i.r. spectra of doped KCl crystals as evidence for at least four distinct environments of the $Fe(CN)_6^{4-}$ ions in the lattice. The most common of these is of C_{2v} symmetry, with a lattice vacancy immediately adjacent to the hexacyano-ion. Arrangements in which the vacancy occupies a site in the next nearest zone to the complex anion also occur to a lesser extent.

Co(CN)$_6^{3-}$ and Fe(CN)$_6^{3-}$: The i.r. spectra of KCl crystals doped with $Co(CN)_6^{3-}$ at various dilutions consistently show six C-N stretching bands, three of which have been observed previously by Jones.[4] After preparation of crystals containing $Fe(CN)_6^{3-}$, it was found that most of this had been reduced to $Fe(CN)_6^{4-}$, a process which could be accelerated by u.v. irradiation of the crystals. The resulting spectra were of poorer quality than for the cobaltate ion. The frequencies and relative intensities of the bands observed in both systems are given in Table 7.12.

Neutralisation of the excess charge on the hexacyanometallate (III) ions requires two vacancies in the lattice. Assuming these to be as close to the complex ion as possible, the local symmetry can be either D_{2h}, C_{2v}, C_2 or C_s, depending on the exact arrangement of the vacancies. The first of these would give three i.r. active components of ν_6, while the others would allow all six non-degenerate C-N stretching mode to become i.r. active. Jones regards the D_{2d}

Table 7.12: $\nu(CN)$ bands of $M(CN)_6^{3-}$ ions doped in KCl.

$Fe(CN)_6^{3-}$		$Co(CN)_6^{3-}$	
Frequency (cm^{-1})	Relative intensity	Frequency (cm^{-1})	Relative intensity
2025	5	2131.3	7
2017	10	2127.2	15
2109.8	65	2119.4	100
		2112.0	50
2102.6	100	2110.6	75
2098.8	60	2109.2	90

environment as most probable on electrostatic grounds, and bases his assignments on this arrangement.

The true situation is evidently rather more complex. From their intensities, the four bands below 2120 cm^{-1} in the cobaltate must be components of ν_6. Three of these are probably D_{2d} modes, while the fourth forms part of a set from one of the other environments. The bands at 2127.2 and 2131.3 cm^{-1}, one of which was assigned to ν_6 by Jones, are probably the ν_3 components of this set. The spectrum of $Fe(CN)_6^{3-}$ shows a similar pattern.

7.5: Experimental

Crystals of $Hg(CN)_2$ and the cyanometallates were grown by slow evaporation of aqueous solutions of the pure material, or of the constituent cyanides in the case of the tetracyano-complexes. The crystals of $Hg(CN)_2$ were prisms elongated along the c axis, and those of the $K_2M(CN)_4$ complexes were irregular octahedra.

$K_3Fe(CN)_6$ grew from solution as rather irregular crystals which

frequently displayed well developed diamond-shaped faces with an acute apical angle of 78°. These large faces were therefore (100) planes. This established the axes of the crystal, apart from the ambiguity concerning the direction of the a axis, which lies along one of two possible directions, although this is unimportant for the purposes of the present work. From the interfacial angles, the b axis lies along the bisector of the acute apical angle of the (100) face, as verified by the extinction positions of the crystals in plane polarised light. Although some crystals did have small (010) faces, it was usually necessary to prepare these faces by grinding and polishing in order to observe all the vibrations polarised in the ac plane.

The crystals of $K_3Co(CN)_6$ grew as thin diamond-shaped plates. Again the acute apical angle of the large faces was 78°. However, crystal morphology does not distinguish between the reported monoclinic and orthorhombic fors of $K_3Co(CN)_6$, since the observed interfacial angles agree, within the limits of accuracy, with those predicted from either structure. If the crystals are monoclinic, then the directions of the crystallographic axis will be identical to those of $K_3Fe(CN)_6$. However, if the crystals are orthorhombic, the large faces could be either (100) or (001) planes, so that although the directions of the crystallographic axis can be determined, they cannot be identified as the a, b, or c axes. The preparation of a ground face, as for $K_3Fe(CN)_6$, was necessary to obtain all the bands in the spectrum.

Crystals of KCl doped with hexacyanometallate ions were prepared from aqueous solutions with KCl:$M(CN)_6^{x-}$ molar ratios of 1:1,000 to 1:100,000. Some of these were large enough to permit direct transmission measurements, but the crystals could be ground up for drying

and pressed into a disc without affecting the spectra. The crystals were dried by evacuating for long periods at a temperature of about 100°C.

References

1 D.M. Adams, "Metal-Ligand and Related Vibrations", Arnold, London, 1967; K. Nakmoto, "Infrared Spectra of Inorganic and Coordination Compounds", Wiley, New York, 1963.

2 J. Hvoslef, Acta Chem. Scand., 1958, 12, 1568.

3 R.G. Dickinson, J. Amer. Chem. Soc., 1922, 44, 774.

4 L.H. Jones, J. Chem. Phys., 1962, 36, 1400.

5 L.H. Jones, J. Chem. Phys., 1957, 27, 665.

6 P. Krishmamurti, Indian J. Phys., 1930, 5, 651; M. Wolkenstein, Acta Physicochim. U.R.S.S., 1937, 7, 315.

7 H. Poulet and J.-P. Mathieu, Compt. rend., 1959, 248, 2079.

8 C.A. Arguello, D.L. Rousseau and S.P.S. Porto, Phys. Rev., 1969, 181, 1351.

9 L.H. Jones, J. Chem. Phys., 1957, 26, 1578; 27, 468.

10 G. Glocker, Rev. Mod. Phys., 1943, 15, 111.

11 L.H. Jones, Spectrochim. Acta, 1961, 17, 188.

12 L. Couture and J.-P. Mathieu, Ann. Physique, 1948, 3, 521.

13 I. Nakagawa and T. Shimanouchi, Spectrochim. Acta, 1962, 18, 101; V. Lorenzelli and P. Delorme ibid., 1963, 19, 2033; J.-P. Mathieu and H. Poulet, ibid., p. 1966; L.H. Jones, Inorg. Chem., 1963, 2, 777; D. Bloor, J. Chem. Phys., 1964, 41, 2573; W.A. McAllister, ibid., 1970, 52, 2786.

14 W.P. Griffith and J.T. Turner, J. Chem. Soc. (A), 1970, 858.

15 O. Salvetti, Ricerca sci., 1959, 29, 1128.

16 I. Nakagawa and T. Shimanouchi, Spectrochim. Acta, 1970, 26A, 131.

17 L.H. Jones, J. Chem. Phys., 1962, 36, 1209.

18 B.M. Chadwick, personal communication.

19 M. Krauzman, Compt. rend., 1966, 262B, 765; J. Deveze and M. Krauzman, ibid., 263B, 864.

20 D.M. Adams and M.A. Hooper, J.C.S. Dalton, 1972, 160.

21 V. Barkhatov and H. Zhdanov, Acta Phyicochim. U.R.S.S., 1942, 16.

22 J.A. Kohn and W.D. Townes, Acta Cryst., 1961, 14, 617.

23 N.A. Curry and W.A. Runciman, Acta Cryst., 1959, 12, 674.

24 R.D. Hancock and D.A. Thornton, J. Mol. Structure, 1970, 6, 441.

25 L.H. Jones, M.N. Memering and B.I. Swanson, J. Chem. Phys., 1971, 54, 4666; B.I. Swanson and L.H. Jones, ibid., 55, 4174.

26 K.D.J. Root and M.C.R. Symons, J. Chem. Soc. (A), 1968, 2366.

Chapter 8: General Experimental Methods

8.1: Crystal Growth

The single crystals used in the present work were prepared either from melts or from solutions. Melt growth techniques offered the only means of preparing some of the complex halides, while conversely, certain salts did not exist in the molten phase, and crystallised only from solution. In general, melt growth had the advantage of producing large crystals of very high purity, but required elaborate preparations, while crystallisation from solution provided an easier method for the majority of complexes.

Melt growth techniques: A number of congruently melting complex halides were grown by the Stockbarger method[1] from fused stoicheiometric mixtures of the anhydrous constituent halides. This, in essence, involves lowering a crucible containing the molten material slowly through a steep temperature gradient, from the hot into the cool zone. Provided that the melting point of the compound lies within the temperature differential, this induces gradual crystallisation upwards through the melt.

The type of furnace used in this method consisted of a silica tube about 60 cm long and 7 cm inside diameter, wound with resistance wire and thermally insulated by an efficient lagging material contained in an asbestos casing. The windings of the silica core were divided into two halves, connected in series, which gave a higher temperature in the upper section. The thicknesses of resistance wire used, and the spacing of the windings were such that at typical operating temperatures, a vertical temperature gradient of about 2°/mm was generated over the central region of the core. The furnaces were capable of maintaining temperatures in excess of 1000°C for protracted periods.

Chloride melts were enclosed in silica or glass tubes, depending on the melting point, while for fluorides, graphite or platinum crucibles in sealed platinium tubes were used.

A number of obvious steps were necessary to achieve optimum results by this method. Firstly, the starting materials had to be of a high purity, since contaminants tended to interfere with uniform crystallisation, and also to avoid the build-up of explosive pressures within the sealed tubes at high temperature due to the presence of volatiles such as moisture. Purity was insured in the first instance by using "Optran" grade reagents or sublimed materials wherever possible, and volatiles were removed by prolonged evacuation of the crucibles at elevated temperatures prior to sealing. Where necessary, handling of the starting materials was carried out in a moisture-free inert atmosphere box. Other possible pitfalls in the method are multiple nucleation at the bottom of the crucible, and uneven growth caused by fluctuations in temperature. These were avoided by using crucibles with cone-shaped ends in which nucleation takes place at the apex, and by efficient temperature control. The power supply to the furnace was regulated by a Skil or West proportional temperature controller, which automatically monitored the temperature at the centre of the furnace through a Pt/Pt-Rh or chromel/alumel thermocouple. This achieved thermal stability within $\pm 1^{\circ}$.

Having sealed the starting materials in an evacuated crucible, the the general procedure ran as follows: the temperature of the furnace was set so that the upper and lower halves were above and below the melting point of the salt to be prepared (information on melting points, etc. was obtained from published phase diagrams). Starting at a point above the central zone, the crucible was lowered through temperature gradient at the rate of 2.5 mm/hr. Subsequent cooling to room temperature was carried out slowly to avoid straining the crystal. The whole operation

took 3-4 days.

The dimensions of typical crystals grown by this method were (2 x 2 x 3) cm^3, although a high proportion of successes was attained only with certain types of compound. Structures containing some form of cross-linked lattice appeared to be more amenable than those made up of discrete ions - $CsCoCl_3$ could be grown with comparative ease, while attempts to prepare crystals of Cs_2CoCl_4 and Cs_3CoCl_5 met with limited success.

Another means of obtaining crystals of certain materials is by the flux method, which was employed here only in the case of K_2CoF_4. This involved cooling a molten equimolar mixture of KCl and CoF_2 in a platinum crucible. A furnace of the type described above was used, but instead of lowering the crucible into the cool zone, this was kept stationary and the temperature lowered from 900°C to 500°C at the rate of 3°/hr, and then at 20°/hr to room temperature. By analogy with similar methods used to prepare AMF_3 complexes,[2] the formation of K_2CoF_4 is expected in the melt, according to the reaction:

$$2KCl + 2\ CoF_2 \rightarrow K_2CoF_4 + CoCl_2$$

This was in fact found to take place, and the crystals of K_2CoF_4 could be removed from the $CoCl_2$ flux either mechanically or by dissolving away the chloride matrix. Some small equidimensional crystals of $KCoF_3$ which were also present were easily distinguishable from the tetrafluoride plates. The latter had edge lengths of up to 3 mm.

Crystallisation from solution: A large number of crystals could be grown simply by dissolving the appropriate materials in water or some other solvent and allowing the solution to evaporate slowly in a dust-free atmosphere. Most complex halides formed congruently saturated solutions from stoicheiometric amounts of the appropriate alkali metal and transition metal halides. For incongruently saturating complexes,

the correct molar ratios were found in the literature or by trial and error. Slow cooling of saturated solutions in sealed containers offered an alternative method of crystallisation for some complexes. A slow, even rate of cooling was maintained by immersing the container in a large heated water bath, whose temperature was regulated by controlling the power supply to the heater. The quality, size and morphology of the crystals obtained by both these methods varied considerable. A major disadvantage was that the crystals were generally less homogeneous, due to the presence of occlusions and gross defects, than those grown by the Stockbarger method, which led to greatly increased background scattering in the Raman spectra. Despite these shortcomings of the bulk crystals, the faces were mostly of suitable quality, though not always of sufficient size, for i.r. reflectance measurements. A further difficulty was that some crystals developed preferentially along certain directions giving plates or rods so that even in relatively large specimens, one or two of the crystallographic axis were poorly represented. Alteration of the conditions of crystallisation sometimes induced a change of habit, but in most cases this situation had to be accepted.

8.2: Sample Preparation

Once crystals of suitable size had been grown, it was necessary to check the composition and structure, determine the directions of the crystallographic axes within the sample, and select or prepare convenient faces for spectroscopic examination.

In confirming the composition of the crystals, elemental analysis was employed only in a few special cases, such as the K_2CoF_4 prepared by the flux method. Checks on congruently melting samples grown by the Stockbarger method were not usually necessary, since their composition

was determined by that of the melt. For these and solution-grown crystals, confirmation of the anticipated structure was generally taken as adequate proof of composition. A rough estimate of the purity of the samples could often be gauged from their appearance and cohesion.

Measurement of the interfacial angles and observation of optical birefringence of solution-grown crystals using a rotating-stage polarising microscope was normally sufficient to establish their structure. Microscopic examination also served to determine whether samples were in fact monocrystalline. Crystals of unknown structure and those prepared from the melt were examined by X-ray diffraction methods. This was necessary in any case where the possibility of polymorphic modifications existed. Powder diffraction patterns were recorded in a 11.46 cm Debye-Scherrer X-ray camera using Ni-filtered CuK_{α} radiation. Structures were determined by comparison with the patterns of reference samples.

The directions of the crystallographic axes in the crystals were deduced from the angles between natural faces or intersecting cleavage planes, and the optical extinction positions between crossed polarisers. In some cases, dichroism in the i.r. spectra helped in fixing the axes. When these had been found, suitable faces could be selected for spectroscopic examination. A large proportion occurred as well developed natural faces or cleavage planes, and no further preparation was necessary, but some which were either too small or absent required grinding and polishing. This could be done manually or on a Logitech PM2 polishing machine using a solder lap and 1 diamond paste.

Crystal size was relatively unimportant for Raman spectroscopy, the emphasis being on well formed crystals of good optical quality. Three orthogonal faces normal to the principal crystallographic directions were necessary for a complete set of polarisation data in uniaxial and

biaxial systems using 90° scattering. For polarised i.r. spectra the requirement is that each of the non-equivalent crystallographic axes should lie in the plane of one of the faces, so that only one face was needed for uniaxial systems, and two for lower symmetry systems. The area of face required varied according to the strength of the bands to be observed. In general, although reasonable results could be obtained with crystals measuring as little as 2 mm across, noise-free spectra required faces at least 5 mm square, and preferably larger.

In the case of small crystals, or those with long, narrow faces, it was often possible to increase the effective sample area by mounting a number of crystals of the same compound side by side on a non-reflecting support, taking care that the orientation was the same for each. This technique was particularly useful for needle-like uniaxial crystals such as those of $Cs_3Tl_2Cl_9$ and K_2PtCl_4.

8.3: Spectroscopic Techniques and Instrumentation

Far-i.r. region: Spectra below 400 cm^{-1} were recorded on a Beckman-R.I.I.C. FS 720 Fourier spectrophotometer. The transform of the interferometric output from this was performed by an FTC 100 analogue-digital computer, and the spectra plotted on a recording wave analyser. The normal range of the instrument was 40-400 cm^{-1}, but this was extended as far as 10 cm^{-1} by insertion of the appropriate thickness of Mylar beam-splitter and suitable filter. Optimum resolution was 2.5 cm^{-1}, and spectra were calibrated by a stored test function giving a reference peak in each range. Incorporated in the spectrophotometer was an FS 7RF module for near-normal incidence reflectance measurements. The whole instrument was evacuated during operation to remove water vapour.

Polarisation of the reflectance spectra was achieved using an

A.I.M. wire grid polariser. Because of the partial polarisation of the beam by the beam-splitter, the best arrangement was found to be one with the electric vector axis of the polariser set vertically, and the crystal samples oriented accordingly. The sample holder could be replaced by a VTL 2 variable temperature cell for work at liquid nitrogen temperature. Heating of the sample was also possible. The temperature was monitored by a copper-constantan thermocouple close to the sample position.

For powder transmission spectra, 5-20 mg of the ground material was dispersed in a wedged polyethylene (Rigidex T50) disc, which was placed at a focal plane in the beam, with an aluminised mirror blank at the normal sample position in the reflectance module.

Mid-i.r. region: For this region, P.E. 225 and 457 grating spectrophotometers were used, giving ranges of 200-5000 cm^{-1} and 250-4000 cm^{-1} respectively. The spectra were calibrated using polystyrene films or, in the 2000 cm^{-1} region, by the rotation-vibration bands of carbon monoxide. For the PE 225, resolution was better than 0.4 cm^{-1}.

Samples were prepared as either alkali metal halide discs or mulls in a medium such as nujol or fluorolube. For reflectance measurements, Wilks model 12 double beam reflectance attachments, set in the specular reflectance configuration and a Perkin-Elmer gold wire grid polariser were used.

Raman spectra: These were recorded on a Cary 81 spectrophotometer with a Spectra Physice He-Ne laser or on Coderg PHI and PHO instruments, with a choice of either the He-Ne source or a Coherent Radiation Ltd Ar^{+} laser, giving excitations at 632.8 nm and 488.0 nm respectively. Wavenumber reproducibility and effective resolution were both about 1 cm^{-1}. A 90° scattering geometry was normally used.

Interpretation of i.r. reflectance spectra: Where crystals were of

sufficient size to allow accurate measurement of absolute reflectivity, the spectra could be analysed using the Kramers-Kronig relationship to give true oscillator frequencies (Chapter 3). For the smaller crystals, only relative values were obtained, and frequencies were taken directly from reflectance maxima, or from powder transmission spectra, using the reflectance bands for assignments. In a few specified exceptions, such as the highest frequency mode in the x-polarised spectrum of $Rb_3Cr_2Cl_9$ (Chapter 2.3), vibrations were obviously associated with inversions in the reflectivity, and the frequencies were taken from the resulting minima.

References

1 D.C. Stockbarger, Rev. Sci. Instr., 1939, 10, 205.

2 N.N. Nesterova, I.G. Sinii, R.V. Pisarov and P.P. Syrnikov, Fiz. Tverd. Tela., 1967, 9, 21; A.G. Tutov and P.P. Syrnikov, Kristallografiya, 1967, 12, 713.